

Statistically Inferring the Mechanisms of Phage-Host Interactions

by

Joy Yang

B.A., Statistics, University of California, Berkeley (2011)

Submitted to the Program in Computational and Systems Biology
in partial fulfillment of the requirements for the degree of

Doctor of Philosophy

at the

MASSACHUSETTS INSTITUTE OF TECHNOLOGY

June 2019

© Massachusetts Institute of Technology 2019. All rights reserved.

Author
Joy Yang
Program in Computational and Systems Biology
March 22, 2019

Certified by
Martin Polz
Professor, Civil & Environmental Engineering
Thesis Supervisor

Accepted by
Christopher Burge
Director, Computational and Systems Biology Graduate Program

Statistically Inferring the Mechanisms of Phage-Host Interactions

by

Joy Yang

Submitted to the Program in Computational and Systems Biology
on March 22, 2019, in partial fulfillment of the
requirements for the degree of
Doctor of Philosophy

Abstract

Bacteriophage and their hosts are locked in an age-old arms race. Successful bacteria are subject to predation, forcing the population to diversify, and phage are also quick to adapt tactics for infecting these potential hosts. Sampling of closely related bacterial strains that differ in phage infection profiles can further elucidate the mechanisms of infection. The Polz Lab maintains the Nahant Collection - 243 Vibrio strains challenged by 241 unique phage, all with sequenced genomes. This is the largest phylogenetically resolved host-range cross test available to date. Genetically mapping out the depths of this dataset requires carefully designed analysis techniques as well as further experimental exploration.

First, we narrow in on a specific phage in the Nahant Collection, 2.275.O, to *characterize the pressures that may select for phage that shuttle their own translational machinery*. While translation is generally considered a hallmark of cellular life, some phage carry abundant tRNA. 2.275.O carries 18 tRNA spanning 13 amino acids. We find that while encoding translation-related components requires shuttling a larger phage genome, it also reduces dependence on host translational machinery, allowing the phage to be more aggressive in degrading and recycling the host genome and other resources required for replication.

Next we *develop a systematic approach for uncovering genomic features that underlie phage-host interactions*. We find that correcting for phylogenetic relationships allows us to pick out relevant signals that would otherwise be drowned out by spurious correlations resulting from statistically oversampled blooms of microbes. Using these results, we wrote an interative javascript visualization to facilitate the process of developing testable hypotheses concerning the mechanisms of phage infection and host response. From the visualization, we are able to identify, in the hosts, mobile genetic elements containing restriction modification systems that may defend against infection, as well as membrane protein modifications that may serve as phage attachment sites.

Thesis Supervisor: Martin Polz

Title: Professor, Civil & Environmental Engineering

Table of Contents

Acknowledgements	9
Chapter 1: Introduction	15
1.1 Background on phage research, focusing on one-step growth	16
1.2 Phage research today, in the era of sequencing	22
1.3 Phylogenetic Confounding	24
1.4 Interpretability	28
1.5 Goals of this thesis	30
Chapter 2: Selective advantages of bacteriophage tRNA	33
2.1 Abstract	34
2.2 Significance	34
2.3 Introduction	35
2.4 Results	37
2.4.1 Genomic analysis of phage and host reveals differences in genomic codon usage patterns	37
2.4.2 tRNA sequencing suggests that phage tRNA actively participate in translation	39
2.4.3 Codon usage bias is present but not pronounced	41
2.4.4 Host genomic DNA and RNA transcripts are degraded	43
2.4.5 Prolonging the replication period amidst host cell shutdown	46
2.5 Discussion	47
2.6 Materials and Methods	50

2.6.1	Exploratory genome-based codon usage bias analysis	50
2.6.2	tRNA Sequencing Timecourse	51
2.6.3	RNA Sequencing Timecourse	51
2.6.4	Total RNA extraction	52
2.6.5	High-throughput sequencing of tRNAs	52
2.6.6	Full transcriptome RNA-seq	53
2.6.7	Calling modifications on tRNA sequencing data	54
2.6.8	Calculating phage RNA expression timing	54
2.6.9	Assessing Genome Degradation	55
2.6.10	Codon Usage Bias Analysis	55
2.6.11	Assessing statistical significance of codon usage bias	57
2.6.12	tRNA array diversity analysis	58
2.7	Acknowledgements	58

Chapter 3: Interactive visualization of high dimensional genomic data

	underlying bipartite graph structure in virus-host interactions	59
3.1	Abstract	60
3.2	Introduction	61
3.3	The biological context	62
3.4	A guided walkthrough of the visualization	63
3.4.1	Div 1: Selecting a phage for finding host proteins that may allow or protect against its infection	64
3.4.2	Div 2: Selecting a host genome for identifying candidate proteins that inhibit infection	64
3.4.3	Div 3: Exploring the Manhattan plot to find candidate proteins that may allow or inhibit infection	66
3.4.4	Backtracking to Div 2: Selecting a genome for identifying candidate proteins that permit infection	69
3.4.5	Designing experiments based on hypotheses suggested by this visualization	70

3.5	Methodological notes	71
3.5.1	Regression results depicted	71
3.5.2	Implementation details	72
3.6	Discussion and future analyses	74
Chapter 4:	Conclusion	75
Appendix A:	Predicting Phage-Host Interactions Using Alternating Minimization	81
A.1	Abstract	82
A.2	Introduction	83
A.3	Methodology	85
A.4	Implementation and tuning	87
A.4.1	Initialization	88
A.4.2	Scaling A and B	88
A.5	Performance engineering results	90
A.5.1	Memory	91
A.5.2	Runtime	91
A.5.3	Correspondence with the original model	92
A.6	Additional directions for exploration	93
Appendix B:	Reasoning Through Games of Chance - Statistics for Play	97
B.1	Abstract	98
B.2	Introduction	98
B.3	MIT HSSP	99
B.4	Class Setup	99
B.5	Reflection and Outlook	102
B.6	Acknowledgements	104
References		107

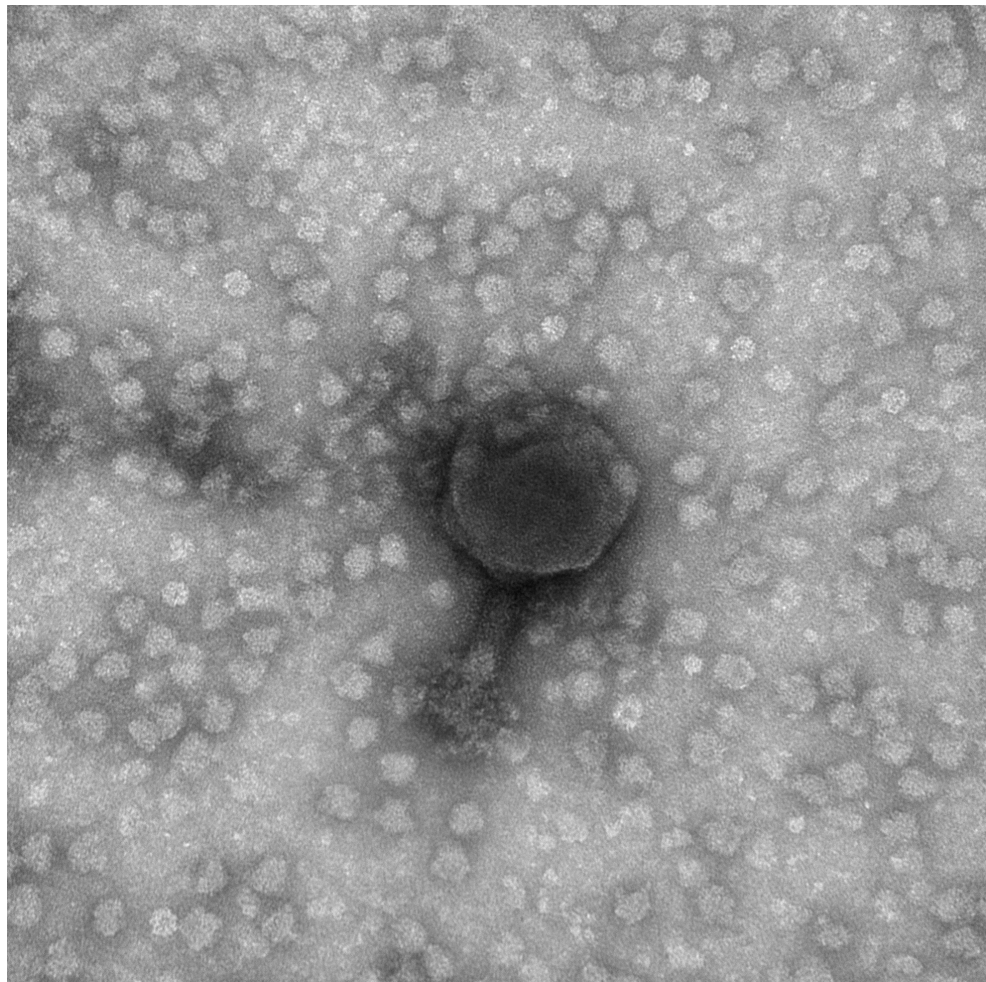
List of Figures

- 1-1 Emiliania huxleyi population collapse within a week of the bloom (bloom depicted here, image from NASA Earth Observatory) is largely attributed to predation by coccolithoviruses. 16
- 1-2 By synchronizing infection assaying phage concentration at short, approximately 10 minute, time intervals, Ellis was able to see that phage growth appears to occur in bursts. The y-axis shows P/P_0 in log-scale. P_0 is the initial concentration of plaque forming units, and P is the concentration at a particular time. This image is from their original paper, ©1939, by The Rockefeller Institute for Medical Research, adapted under CC BY-NC-SA 4.0 18
- 1-3 On the left is a picture of a phage plaque assay on a petri dish. The light hazy layer in the picture is a "lawn" of bacteria, and the spots scattered on top are "clearings" or "plaques." These plaques each can roughly be thought of as having grown out of one infection. The plaque count should then be proportional to the concentration of phage used for the plaque assay. On the right, a poisson distribution describes counts of an event in fixed intervals when there is a uniform probability for occurrence over the entire space. Phage dispersal on a plate is roughly uniform, and so plaque counts on equal areas should follow a Poisson distribution. The image analysis above was done with freshman miniUROPs Madelyn Focaracci and Jessica Wang. A timelapse plate read is also available online: <https://youtu.be/93p5phFAuo0>. 20

3-3	Div 2 gene summaries and zoom in. The working example of host host A is shown selected.	67
3-4	Div 3 and brush selection examples. The two zoomed-in views lie on region 3, the first shows the conjugative transfer element annotations, and the second shows the Type III restriction modification system genes.	68
3-5	Profiles of the top 100 phage proteins found to be associated with ability to infect a particular <i>Vibrio lentus</i> host. The columns represent phage genomes, and are ordered according to phylogeny, as depicted by the dendrogram. The black lines immediately below the dendrogram indicate the strains of phage that were able to infect the host of interest. On the heat map, red indicates absence of the protein in a particular phage, while off-white indicates presence of the protein. The color bars on the left indicate whether the effect is positive (blue), or negative (orange).	73
A-1	Depicted here are two representations of the infection data. One in matrix form, and the other as a bipartite graph. The hosts hail from ecologically differentiated populations; the phage are also genetically and morphologically diverse.	84
A-2	Initializing A and B randomly performs comparably to initializing with the SVD of M, indicating that random initialization could still be a reasonable strategy when working with the entire dataset.	89
A-3	When the rank of the coefficient matrices is set to 3, A and B project the phage and host genomes into a 3D space. The first dimension empirically always corresponds to the intercept. Proximity of phage and hosts in the second and third dimensions roughly corresponds to the success of infection. In this figure, the colorscheme is the same as that from before, and to emphasize the difference in organism type, phage are plotted as triangles while hosts are plotted as circles.	90

A-4 Blue points highlight operations performed in order to solve for A, the matrix of phage protein coefficients, and tan points highlight operations performed in order to solve for B, the matrix of host protein coefficients. Alternating grey and white backgrounds demarcate successive iterations. Snapshots at each step of the algorithm shows that memory usage increases every time the predictors for B are calculated, and memory usage drops when predictors for A are calculated, as they overwrite those for B.	92
A-5 Because parameter optimization involves searching in a high-dimensional space, the steps of solving for A and B are inevitably the rate-limiting steps of the method. Directly fitting the matrix M takes 1352 seconds (22 minutes) on the same machine.	93
A-6 In the first two plots here, the log likelihood and correlation with M (excluding the intercept term, the intercept term is so low in magnitude and so consistent with fitting that including it bumps up the correlation to around 0.97) are plotted for each iteration. Initial values are left off from these plots, since, because the parameters are randomly initialized, the log likelihood starts at -Inf and the correlation starts close to 0. The eigenvalues from singular value decomposition of the coefficient matrix M when solving for M directly is shown in the third plot. The first dimension is left off, since it is a value large in magnitude, corresponding to the intercept.	94
B-1 This map omits two students, one from Maine, another from Illinois.	100
B-2 When asked to summarize the sheep in their herd, one group responded with pictorial summaries.	102

Acknowledgements



“One Christmas Tukey gave his students books of crossword puzzles as presents. Upon examining the books the students found that Tukey had removed the puzzle answers and had replaced them with words of the sense: ‘Doing statistics is like doing crosswords except that one cannot know for sure whether one has found the solution.’” - David Brillinger [1]

At some point during our many meetings, my advisor Martin looked at me and said, “well, I suppose it takes a village.” This statement sums up my graduate experience very concisely, and I’ll now proceed to ramble on about the village that was kind enough to support me throughout graduate school.

First, as already mentioned, my advisor, Martin Polz, who has been incredibly patient with me, allowing me the freedom to learn anything I felt an impulse to learn. And while at first he very rarely discouraged going down new paths, he became quick to warn me against rabbit holes when he realized my inability to avoid them. His uncanny insights often lead me to wonder whether he had known and was hiding the answers all along.

My co-advisor Libusha Kelly is always willing to provide feedback on everything I write, however hopeless or trivial the draft may be. She has been thoughtful and dedicated in making trips from New York in order to attend my committee meetings in person. And I very much appreciate her ability to ask just the right questions whenever I lack the capacity for words.

The Computational Sciences Graduate Fellowship through the Department of Energy supported me financially during four years of my PhD, and provided me with funding for workstations, conferences, and professional development. I am incredibly grateful for their support. Their “requirements,” which I like to think of as perks held me to the promises I made to them and to myself upon first starting graduate school.

I have been incredibly lucky to have benefitted from starting my PhD following the heroic efforts of Kathryn Kauffman in carefully assembling and archiving the Nahant Collection. Working with this dataset and the organisms themselves has been an amazing avenue for me to synthesize and process what I’d studied in books and classes. I’m grateful to Fatima Hussain for having taught me to grow phage, Joseph Elshirbini for having introduced me to the joys and headaches of javascript, Javier Dubert for showing me how to transform *Vibrio*, Dave VanInsberghe for rescuing me from my NCBI submission woes, Annie Yu for being a partner in crime during all the late night experiments, Fabiola Miranda for allowing me to use her reagents whenever I’m unprepared myself, and Bruno Janeiro, Clovis Borges, Hannah Gavin, Manoshi Datta,

Nate Cermak, Phil Arevalo, Alison Takemura, Diana Chien, Christopher Corzett, plus anyone who I've failed to mention in the Polz lab for all the serious scientific discussions as well as the occasional banter.

My committee, all having students of their own to advise, has been generous in donating many hours of their time toward ensuring that I had all the resources I needed to proceed. After seeing that I had an interest in tRNA, and knowing of my utter incapacity for working with RNA at the bench, David Bartel introduced me to a post-doctoral fellow in his lab, Wenwen Fang. I am very grateful toward Wenwen, without whom the entirety of Chapter 2 would not have been possible. Despite having witnessed my denseness as a student in his class, Jeff Gore agreed to serve on my committee and has provided me with incredible scientific, career, and life advice. I learned through working with Philippe Rigolet that, even if I'm entirely intimidated, it's much better to ask questions in person when I don't understand than to spend many emails trying to type math into paragraphs while trying to implement the algorithm we'd discussed - which he was patient enough to bear with me through. I would also like to thank Philippe's students, especially JC Hütter, for help with brainstorming statistical methods and checking my calculations.

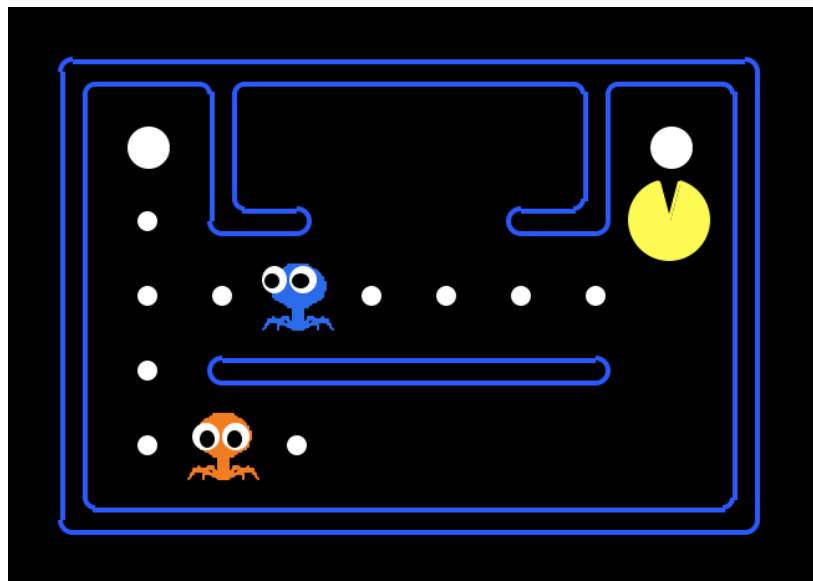
Additionally, Bruce Tidor suffered through not one, but two qualifying exams with me. Eric Alm provided me with a stimulating environment to work in during my first two years; I am lucky to have overlapped with many brilliant people there whose support and encouragement I deeply appreciate. Chris Burge has been a calm and collected voice of reason for our entire graduate program, and I am thankful for his guidance during the roughest moments of my PhD.

As teaching truly is the best way to learn, I'm very appreciative of Aviv Regev and Piyush Gupta's willingness to allow my co-TA Jonathan Teo and I to experiment with new homework problems and different ways of teaching recitation. I learned so much from Caroline Uhler and Stefanie Jegelka, as well as from my co-TAs Jennifer Tang, Abigail Katkoff, and Tahin Syed. I'm also very thankful to all of the students, who I've served as a TA to, for allowing me to learn with them.

While I won't rattle off all of my teachers since preschool, I am certainly grateful

to every one of my teachers since preschool. Thank you especially to the teachers who had the patience and ingenuity to teach each topic using three to five different approaches.

I would like to thank Yihui Xie for [bookdown](#), Chester Ismay for [thesisdown](#), and maintainers of all their dependencies (including R and latex) for making these tools freely available. If these thanks seem out of place, I assure you they are not, it has been exhilarating and of enormous convenience to have been able to integrate code into this thesis easily.



As for all of the social support I've been blessed with, I will mention the groups but refrain from listing individual names due to a preference for privacy. I hope it is nevertheless clear how much I appreciate everyone, and I hope this does not offend anyone who I do not list by name.

The Parsons Laboratory has been a great place for learning about environmental sciences, as well as for making what I feel will be life-long friends. I can't imagine going through graduate school without this wonderful community.

The Computational and Systems Biology graduate students is such a fun group of fascinated and fascinating individuals. I've enjoyed studying, joking about hypothetical science, and wandering the “back-alleys” of Kennebunkport together. Jacquie Carota is an incredible individual, thank you for making sure that we stay afloat.

Through the Computational Sciences Graduate Fellowship, I've met so many people from all over the US in various disciplines, all excited about computing. I feel very lucky to have been able to share science and shenanigans with everyone when we meet each year.

My amazingly generous classmates have spent many hours reviewing difficult concepts, entertaining philosophical discussions, and doing countless rounds of resume revisions with me. Thank you, I can only hope to send forward all the good karma.

For all of the roommates that I've lived with, thank you for tolerating me. My first year roommate fed me and dragged me home when I was still acclimating to graduate school and barely able to function. During my second and third years, I felt that I'd truly found a home in 22 Mag, and this is entirely due to the warmth and generosity of my roommates. I am amazed that we'd turned our pantry into a lab. And as for 77, where I landed after signing a roommate agreement littered with hidden white text, I still suspect that everyone is in on the long con. Beyond all the craziness of shoving trees out the window and throwing pumpkins off the roof, you're my people and I care about you.

I must also mention all my Bears who've supported me beyond college and has made an effort to keep in touch through assembling the most socially-conscious and depressing book club fathomable; a fantasy football league, where the only currency exchanged is embarrassment; and superbowl squares, when regardless of where everyone is living, we all participate in a gif exchange.

After quizzing one of his students, Tukey purportedly thought for a while and said "Well, what I think you need is folk dancing." I would like to thank everyone above for folk dancing with me. Without all of you, I would not feel human.

And finally, I would like to thank my family. My grandparents, Yang Su Hua, Yang Xiang Wu, Zhao Rui Fang, and Dai Yong Nian for their incredible strength and wisdom. And my parents, Aiping Dai and Dan Yang, for endless advice, asked and unasked for. I am grateful for their unconditional love and support, and for having placed me in an environment where I never needed to worry about basic needs or survival instincts, and so, had the freedom to develop a love for learning.

Chapter 1

Introduction

There are approximately 10 million viral particles per milliliter of sea water [2]. At such numbers, these tiny 30-100 nm particles can have an enormous impact on the ecosystem. To illustrate with a particularly stunning example, *Emiliania huxleyi* (a marine algae) can bloom to 1-100 thousand cells per mL over an area of 250,000 km^2 (in the upper 200 m of the ocean) [3]. After only a week, these blooms collapse, releasing calcite into the seabed and cloud-forming dimethyl sulfide into the atmosphere. This population collapse is largely attributed to predation by coccolithoviruses [4, 5].

The most common viruses are bacteriophage. These viruses' hosts (bacteria) are also abundant, at around 1 million cells per milliliter of sea water. This means "rare" events can happen frequently. For example, in order for a successful lytic infection to occur, a phage must encounter a bacterial host whose cell surface proteins it can bind to, protect itself from the host restriction modification systems, and replicate within its hosts cellular environment. All these road blocks make successful lytic infections rare [6]; however there are approximately 36 million km^3 of water in the top 100m of the sea. Therefore, rare events for a single cell do not equate to rare events for the whole population [7]. In fact, it has been estimated that new viruses are produced at rates of 1 million to 10 million particles per milliliter per hour [8]. From this, assuming an average burst size of 50 viruses per lytic event, the number of infections initiated by phage per second somewhere in the ocean can be very roughly approximated to be on the order of Avagadro's number [9].

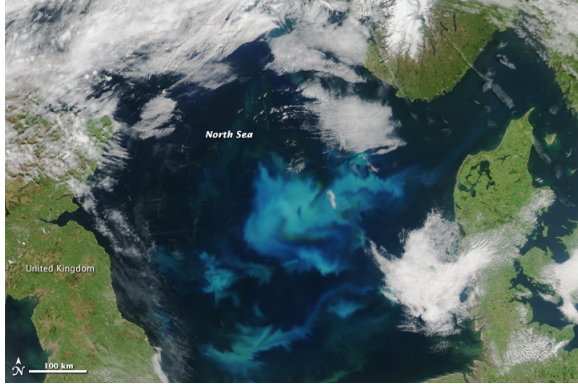


Figure 1-1: *Emiliania huxleyi* population collapse within a week of the bloom (bloom depicted here, image from NASA Earth Observatory) is largely attributed to predation by coccoviruses.

Lytic infections select for resistant hosts, forcing the population to diversify, and resistant hosts select for compatible phage variants. This rapid, recursive evolutionary arms race occurring at such a large scale leads to highly diverse phage. The recent explosion in bacteriophage genomes has revealed that phage genomes are highly mosaic in structure [10], suggesting frequent recombination; and contain hoards of uncharacterized proteins. On average, approximately 70% of open reading frames in a phage are unannotated hypothetical proteins [11]. While perplexing, this vast unknown may hold exciting prospects for future research.

1.1 Background on phage research, focusing on one-step growth

Bacteriophage were discovered in 1915 by Frederick Twort then independently again in 1917 by Felix d’Herelle. These “anti-microbes” were first studied for their potential to treat bacterial infections, but this interest declined in the 1930s due to the success of antibiotics. However, bacteriophage research quickly became foundational to molecular genetics [12, 13], as their small genomes, rapid growth rate, and low-maintenance nature make them particularly convenient for experimentation. In fact, many of the insights into the nature of DNA came out of “the phage group,” an informal network

of researchers centered around Max Delbrück, who, starting in 1945, taught an annual phage course in Cold Spring Harbor [14]. For example, in 1943, Salvador Luria and Max Delbrück showed using T1, the (lack of) Poisson distribution, and jackpotting that mutations occur spontaneously and can be selected for, as opposed to being induced by a selection event [15]. In 1952, using the T2 phage and a Waring blender, Alfred Hershey and Martha Chase showed that it is DNA, and not protein, that encoded the genetic material [16]. In 1957, Seymour Benzer showed using T4's rII gene that recombination occurs on the nucleotide level [17, 18]. In 1961, Crick, et al. showed, using Benzer's T4 rII system and various combinations of double and triple frameshift mutations, that the genetic code consists of triplet bases [19]. We will next outline in greater detail a particular study, the Ellis and Delbrück one-step growth experiment. As one of the earliest “phage group” studies, it laid out the experimental framework for others to come. Much of this framework is still widely used today; and in fact, for the purposes of this thesis, the following background may help clarify the methodological details presented in Chapter 2.

The Ellis-Delbrück study marks the introduction of Max Delbrück to bacteriophage research [20]. In the mid-1930s, Emory Ellis was an analytical chemist at Cal Tech working in cancer research. He had been drawn to cancers induced by viruses, such as the Rous sarcoma virus and the Shope rabbit papilloma virus; however, as so little was known about viruses at the time, he decided that a fundamental understanding of their biology was necessary in order to proceed. So he chose to start with bacterial viruses (as opposed to mammalian viruses or plant viruses) for the practical considerations of time, space, and cost. At the time, however, the most commonly accepted view, championed by Jules Bordet and John Northrop, was that the bacterial lysis witnessed by d'Herelle had been incorrectly interpreted as an infection by an exogenous body, when it was actually an endogenously catalyzed lytic event. Ellis's goal was therefore to replicate d'Herelle's studies by first isolating a virus for *E. coli* from sewage (as he had a culture of *E. coli* gifted to him by a colleague), then reproducing the stepwise pattern of phage growth.

Max Delbrück, on the other hand, had studied theoretical physics. And influenced

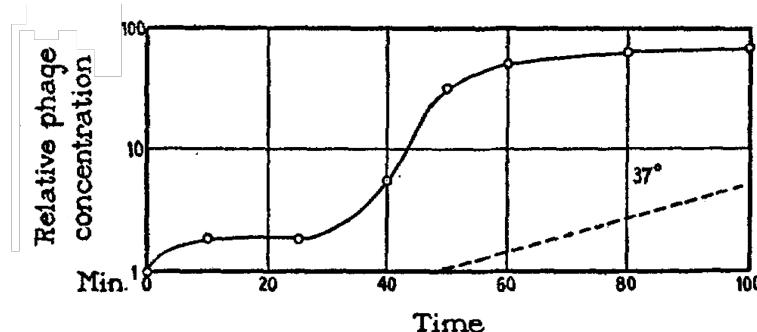


Figure 1-2: By synchronizing infection assaying phage concentration at short, approximately 10 minute, time intervals, Ellis was able to see that phage growth appears to occur in bursts. The y-axis shows P/P_0 in log-scale. P_0 is the initial concentration of plaque forming units, and P is the concentration at a particular time. This image is from their original paper, ©1939, by The Rockefeller Institute for Medical Research, adapted under CC BY-NC-SA 4.0

by Niels Bohr, he ventured into biophysics, where he became interested in characterizing the nature of the gene. Eventually, Delbrück arrived at Caltech to work on Drosophila genetics, but quickly became frustrated. Instead, he developed an interest in viruses and bacteriophage, thinking that “the growth of phage was essentially the same process as the growth of viruses and the reproduction of the gene.” So he sought out Ellis, and the two began to collaborate. The above biographical details of Ellis and Delbrück’s work together is summarized from William Summers’ *How Bacteriophage Came to Be Used by the Phage Group* [20]. The Ellis-Delbrück paper [21] combines the work that Ellis had been doing on phage growth curves with Delbrück’s characterization of the statistical nature of infections, which has, over time, evolved into the statistics of what is now known as the multiplicity of infection (MOI, or, the ratio of phage particles to bacterial cells).

The setup of Ellis’s one-step growth experiment was simple. Essentially, the idea was to synchronize at least the first round of infection in the following way:

1. Mix bacteria and viruses at a high concentration (on the order of 10^9 bacteria and viruses per mL), allow 5 minutes for the viruses to adsorb onto their hosts.
2. Dilute this mixture thoroughly using growth media (at a 1:12,500 ratio) so that

additional adsorption is unlikely to occur.

3. At approximately 5 minute intervals, plate samples of equal volume of this dilution on a background of concentrated bacteria in order to count how many viral particles had formed.

From this type of growth curve, it is possible to deduce the latent period, or the amount of time a phage spends replicating within a cell before the progeny lyse the cell; as well as the burst size, or the number of phage progeny that are produced from each infection.

Delbrück's statistical characterization of phage infections was equally intuitive. When there is a uniform probability for an event to occur in time or space, the number of events that occur in a given interval of time or section of space follows a Poisson distribution. A few concrete examples of events that can be modelled using a Poisson distribution include the number of yeast cells in each batch of Guinness beer (courtesy W.S. Gosset, or "Student," of the Student's T-test) [22], the number of phone calls arriving at a call center within a minute (A. K. Erlang), or the number bombs that fall in regions of London during World War II (R. D. Clarke) [23]. Analogous to these examples is the number of bacteriophage present in a given volume of liquid. In particular, the probability of seeing k phage in a milliliter is

$$P(X = k) = \frac{\lambda^k e^{-\lambda}}{k!}$$

where λ , the rate parameter, is the average number of phage present in each milliliter. One way to infer this parameter is to simply take the average - after making multiple plates of one milliliter aliquots of the same sample, count the number of plaques (or infection clearings) on each plate, and divide this by the number of plates. This is, in fact the maximum likelihood estimate, $\hat{\lambda}_{MLE} = \frac{1}{n} \sum_{i=1}^N k_i$.

Delbrück suggested another way to infer this parameter - according to the Poisson distribution, the fraction of plates without plaques is expected to be

$$P(X = 0) = \frac{\lambda^0 e^{-\lambda}}{0!} = e^{-\lambda}$$

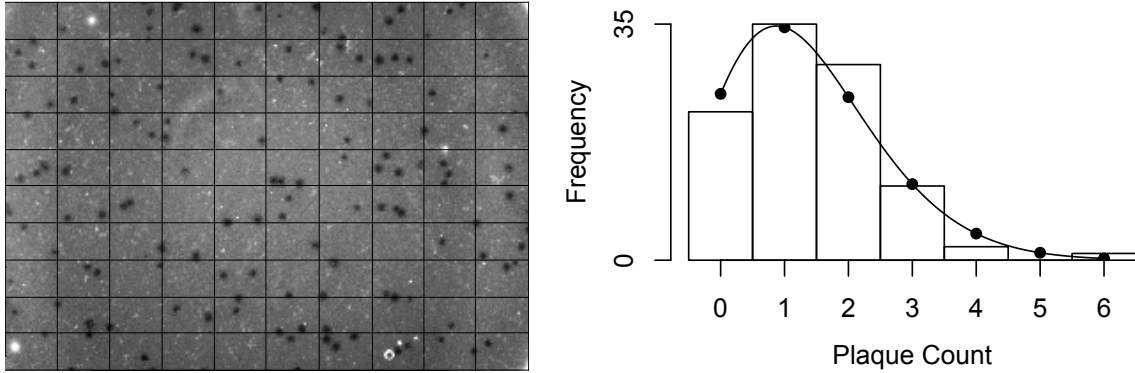


Figure 1-3: On the left is a picture of a phage plaque assay on a petri dish. The light hazy layer in the picture is a "lawn" of bacteria, and the spots scattered on top are "clearings" or "plaques." These plaques each can roughly be thought of as having grown out of one infection. The plaque count should then be proportional to the concentration of phage used for the plaque assay. On the right, a poisson distribution describes counts of an event in fixed intervals when there is a uniform probability for occurrence over the entire space. Phage dispersal on a plate is roughly uniform, and so plaque counts on equal areas should follow a Poisson distribution. The image analysis above was done with freshman miniUROPs Madelyn Focaracci and Jessica Wang. A timelapse plate read is also available online: <https://youtu.be/93p5phFAuo0>.

The rate parameter can then also be estimated as $\hat{\lambda}_0 = -\log(\frac{N_0}{N})$, where N_0 is the number of plates without any plaques.

Ellis and Delbrück observed, however, that there was consistently a discrepancy between the two estimates. The second was almost three times higher than the first (in their paper, $\hat{\lambda}_{MLE} = 0.22$, while $\hat{\lambda}_0 = 0.56$). This lead them to conclude that there may not always be a direct correspondence between phage particles and plaques¹. The comparison of these two estimates was termed the “efficiency of plating.”

The efficiency of plating is not a very commonly reported statistic today, perhaps because the biological meaning of this statistic is somewhat opaque. However, the

¹Because the title of this thesis includes the word “statistical,” there is some pressure to be statistically precise. So to be fair, the second estimate, $\hat{\lambda}_0 = -\log(\frac{N_0}{N})$ is a biased estimate of λ . $N_0 \sim \text{Binomial}(p_0, N)$, where $p_0 = e^{-\lambda}$. Using a Taylor expansion around p_0N , we see that $E(\log N_0) = \log(p_0N) - \frac{1-p_0}{2p_0N} + O(1/N^2)$. Therefore, $E(\hat{\lambda}_0) = \lambda + \frac{1-p_0}{2p_0N} + O(1/N^2)$. This calculation can be verified by plugging in values of N and λ and either running simulations or taking the sums. Given Ellis and Delbrück’s experimental setup, this bias is small. Forty plates were tested, and if we assume the true rate parameter was 0.22, the first order bias term is 0.003, which doesn’t come close to the discrepancy observed. Their conclusions are, therefore, still well-founded.

application of the Poisson distribution toward approximating phage infections has been adapted slightly and is now still commonly used to design experiments. To elaborate, if we assume that all plaque-forming phage are able to find a host, then the bacterial cells themselves are now analogous to the milliliter aliquots from the description above. The number of phage infecting each bacteria follows a Poisson distribution, with the rate parameter being the multiplicity of infection (MOI), or the ratio of phage particles to bacterial cells. The proportion of uninfected bacterial cells (infected by 0 phage) can be expected to be $P(Y = 0) = e^{-\lambda_{MOI}}$, the proportion of bacterial cells infected by just 1 phage can be expected to be $P(Y = 1) = \lambda_{MOI}e^{-\lambda_{MOI}}$, and the proportion of multiple infections, or bacterial cells infected by more than one phage, can be expected to be $P(Y > 1) = 1 - (1 + \lambda_{MOI})e^{-\lambda_{MOI}}$. For phage-host pairs where infection by more than one phage results in a different infection phenotype than infection by just one phage, it may be of interest to the experimenter to pick a low MOI, tuning $P(Y > 1)$ in order to control the number of multiple infections. For experiments where the goal is to observe a signal during infection, for example, RNA sequencing looking for changes in host gene expression during infection (as is the case in Chapter 2 of this thesis), it may be of interest to the experimenter to pick a high MOI, tuning $P(Y = 0)$ in order to reduce the background signal from uninfected cells.

Returning to the Ellis-Delbrück paper, the authors go on to describe many additional carefully executed experiments, which will not be further described here. However, to summarize a few highlights, they were able to conclude that plaque counts correlate incredibly well with phage concentration, and so each plaque likely grew from one instance of infection; during the growth experiment, phage concentration increases in a stepwise manner, indicating that phage are produced in bursts; and phage growth depends on bacterial growth. Recalling their original goal of assessing whether the bacterial death witnessed by d'Herelle was the result of endogenous enzymatic lysis or killing by an obligate intracellular parasite, they concluded that, while it is possible a different type of phage exists, theirs was an obligate intracellular parasite. This main conclusion is important as it laid the foundations for other studies based in phage. Additionally, their study also has lasting methodological impacts. In particular, Ellis's

one step growth curve continues to be the most accurate method for measuring the latent period and burst size for a phage-host pair, and Delbrück’s application of the Poisson distribution to infection frequencies is widely used for selecting an MOI during the design of experiments. Chapter 2 of this thesis, which explores the action of phage tRNAs during infection, extensively utilizes both of these methodological techniques.

1.2 Phage research today, in the era of sequencing

In 1944, Delbrück had drafted a “phage treaty,” in which he urged his colleagues to focus their attention on the T-phages (T_1, T_2, \dots, T_6). Because of this, the T-phages became incredibly well characterized model organisms. Bacteriophage research today, is often of a different flavor. While a concerted effort is valuable, studying model organisms comes with limitations, as our actual environment is much more diverse. And conveniently, sequencing costs have been declining, according to the National Human Genome Research Institute, even faster than Moore’s law [24]. Gone are the days of the “phage treaty.” In contrast to the elegant experiments and clever analytical calculations of the mid-1900s, phage research today often consists of large-scale sequencing efforts and a necessity for, what’s termed, “embarrassingly parallel” cluster computations. The explanation that this term comes from an “embarrassment of riches” is perhaps very appropriate for the data we face today.

To provide an example, the Tara Oceans survey [25] catalogues a 3 year expedition across “the world’s oceans,” with 35,000 samples of seawater spanning 10 size fractions. While only 43 of these samples have been sequenced for metagenomes of the $<0.22\text{ }\mu\text{m}$ fraction (the viral fraction), these samples are from 26 stations from the Mediterranean Sea, Red Sea, Indian Ocean, South Atlantic Ocean, and North Pacific Ocean [26]. From this data, the team has been able to identify 488,130 viral populations, only 19% of which were previously known. This type of large-scale metagenomic sequencing effort helps to illuminate the viral diversity in our environment, yet it is somewhat limited in its ability to provide information about what organisms these viruses may infect and how the uncharacterized viral genes may function.

As another example, the SEA-PHAGES program [27] combines discovery-based undergraduate education with citizen science. With the help of 20,000 students and 400 faculty instructors, the program has isolated 13,000 phage and amassed over 1,800 sequenced and annotated phage genomes. Many of the phage lysates are archived, and there is tremendous potential for further exploration of the data in order to gain mechanistic understandings of infections; however, the crowdsourced nature of the collection effort also has a drawback in that there does not appear to currently be an integrated cross-test of all hosts against all phage.

In this thesis, we wade into the Nahant Collection [28–30], which includes a cross-test consisting of 243 *Vibrio* strains challenged by 241 unique phage, all with sequenced genomes and archived cell glycerol stocks/phage lysates. This is the largest phylogenetically-resolved host range cross test available to date. These host strains match to 19 well-characterized populations that have been shown to be coexisting but ecologically differentiated. For example, *Enterovibrio norvegicus* are primarily free-living, *Vibrio cyclitrophicus* are large-particle specialists, *V. tasmaniensis* and *V. splendidus* are generalists, and *V. breoganii* are algal-degradation specialists and form biofilms [31, 32]. The phage fall into around 18 phylogenetically distinct groups; have diverse infection strategies, with both broad and narrow host-range phage; and have distinct morphologies, with representatives from nontailed (Tectiviridae), and tailed (Podoviridae, Myoviridae, and Siphoviridae) morphotypes.

These large-scale sequencing efforts hold much promise for better understanding the organismal and functional diversity of our environment; however, obtaining this understanding comes with a few statistical challenges. (1) Phylogenetic confounding: while the diverse population structure of phage and hosts is an interesting feature of the data, it means that statistical independence does not apply. (2) Interpretability: After conducting relevant analyses, with so much data and so many parameters tested, it may still be not clear what the results of these analyses mean. Chapter 3 of this thesis seeks to address these two challenges; however, as it may not, at first, be clear or intuitive what is meant by these challenges, the next sections are devoted toward providing some background.

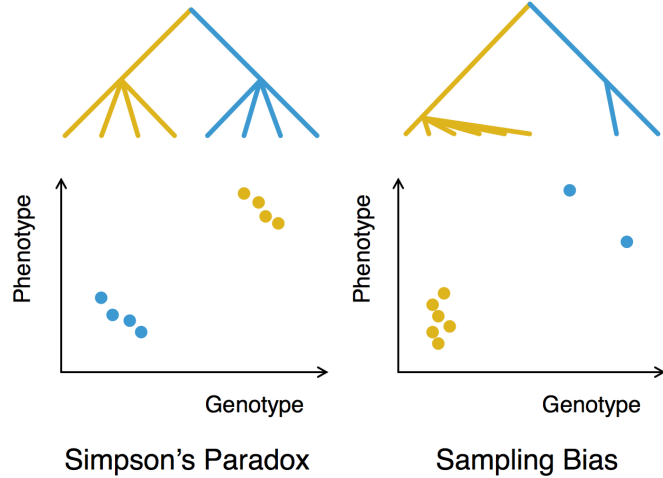


Figure 1-4: The figure above illustrates problems that can arise from confounding due to population structure. The scenario on the left is the classical Simpson’s Paradox, where conditioning on the population (yellow or blue) results in reversing the genotype’s effect. The scenario on the right is what we more typically observe in the Nahant Collection, where genotypes associated with an oversampled clade show up as strong effects when in reality, the effective sample size may be too low for there to be high confidence in the effect.

1.3 Phylogenetic Confounding

Geneticists have long been regressing phenotypes against genotypes as with genome wide association studies; however usually, the assumption behind these studies is that the individuals, or samples, are independent and identically distributed (iid). The polyclonal nature of the largescale sequencing studies means that this assumption is very much violated. For two closely related bacterial strains, knowing that one of them is immune to infection by a given virus should lead us believe that the other is likely also immune to the same virus. Likewise, knowing that one of these strains carries a particular gene should lead us to believe that its sister strain likely also carries a homolog of that gene. Therefore, assuming independence may lead us to the tempting conclusion that the gene protects against infection, but this may not be fair, as infection phenotype and genotype are both influenced by the underlying phylogenetic structure. This problem is referred to as “phylogenetic confounding.” One scenario that can arise is Simpson’s Paradox, where conditioning on the population

results in reversing the genotype's effect. To provide an illustrative example, let's suppose that the copy number of a particular gene is directly related to how well the bacteria can defend itself from phage infection. The more copies of this gene, the smaller the burst size we observe during phage infection. However, suppose we find two species of bacteria that carry this type of defense and can be infected by the same phage. One population carries less copies of this gene on average than the other population, however, it is also less susceptible to infection, perhaps because it also possesses another type of defense mechanism. In this example, if we treated bacteria from the two populations as being iid, we may have arrived at the conclusion that having more copies of this gene results in the bacteria being more susceptible to infection, which is the opposite of the setup of our example.

The above scenario is a very classical paradox; however, there is an additional scenario which is more representative of what we typically observe in the Nahant collection, in which genotypes associated with an oversampled clade show up as strong effects when in reality, the effective sample size may be too low for there to be high confidence in the effect. To illustrate, there is a group of 18 very closely related viruses in the Nahant Collection (this accounts for 8% of the viruses). Therefore, in taking a host and asking which phage genes may allow or prohibit a phage from infecting that particular host, if we treat the phage as iid, and pick a host that this group of 18 phage cannot infect, the 10 genes that these 18 phage all share in common almost always pops up as being negatively associated with the ability to infect. There is likely not a mechanistic link between these genes and infection capacity, however, we've simply oversampled these phage.

Through the years, a few techniques for addressing phylogenetic confounding have emerged, many reminiscent of models used in time series/longitudinal data analysis. The most popular of these models [33] include:

1. Independent Contrasts [34]: This method is similar to the differencing methods used in time series. Usually when building a phylogeny, the observed states are contained in the leaves of the tree, and the ancestral states in the internal nodes are not observed. Therefore, the first step is to infer the ancestral states,

then contrasts are taken between parent nodes and their children in order to, in essence, establish a sort of stationarity.

Drawbacks: Ancestral state reconstruction requires making assumptions about trait inheritance and taking contrasts requires making assumptions about the evolutionary difference between each parent and child pair. These steps introduce extra layers of bias in the model.

2. Phylogenetic Autocorrelation [35]: Traits are fit to an autoregression model $x = \rho Wx + \epsilon$, where W is a matrix of phylogenetic similarities and ρ is the phylogenetic autocorrelation coefficient. Each element of W is computed by $w_{ij} = 1/d_{ij}^\alpha$, where d_{ij} is the pairwise distance between species i and j , and α is a scaling factor to allow for further flexibility.

Drawbacks: This method relies heavily on the accuracy of W in specifying phylogenetic relationships. In addition, this formulation does not allow for regression against a non-phylogenetic component, although it may be possible to generalize this, for example, as a vector autoregressive method. Alternatively, the residuals can be treated as the new data, with phylogenetic components removed.

3. Stratifying on the principal components [36]: The Eigenstrat method first computes the principal components of the population based on the genotypes, then regresses phenotypes against principal components, and finally regresses the residuals against each genotype. This is equivalent to the population principal components as explanatory variables in a regression. This formulation of the model roughly corresponds to mixed models, described below in point 5.

Drawbacks: It can be unclear how many components should be used. And because this could require doing a high-dimensional regression, it is unclear what form of regularization should be used. (Applying some forms of regularization could yield equivalent solutions as choosing particular priors for the mixed model method described by point 5 below.)

4. Generalized Least Squares [37]: Acknowledging that the residuals of a linear model, $Y = X\beta + \epsilon$, would be correlated, the model is multiplied by the matrix square root of the inverse covariance matrix.

$$\Sigma^{-1/2}Y = \Sigma^{-1/2}X\beta + \Sigma^{-1/2}\epsilon$$

$$\tilde{Y} = \tilde{X}\beta + \tilde{\epsilon}$$

And now, $cov(\tilde{\epsilon}) = \Sigma^{-\frac{1}{2}}\epsilon\epsilon'\Sigma^{-\frac{1}{2}}' = \Sigma^{-\frac{1}{2}}\Sigma\Sigma^{-\frac{1}{2}}' = I$. In this context, the covariance matrix of the data is calculated by inverting the phylogenetic tree. We can alternatively consider using the covariance of the genomes themselves and skip the tree-building step altogether; however, enforcing a phylogenetic structure may keep this method more biologically intuitive.

Drawbacks: The covariance matrix is assumed to be fixed, so the estimates do not account for the uncertainty in the phylogenetic structure.

5. Generalized Linear Mixed Models [38–40]: The phylogeny is treated as a random effect, and other covariates can be included as either fixed or random effects. For example, a model may take the form $z_i = m + a_i + \epsilon_i$, where z_i represents the phenotype of a taxon, m is the phenotype at the root of the phylogeny, a_i is the phylogenetic random effect.

Drawbacks: Initially, phylogenetic random effects were simply based on factor variables, for example, five different species of birds, with each bird being treated as a different level, and categorizing the phage and bacteria imposes too large an assumption. However, it is possible for the random effect to directly assume a computed covariance structure; this would roughly correspond to regressing against principal components, described above in point 3. Taking this a step further, the uncertainty in the covariance structure can also be modeled by including a prior for the covariance matrix.

6. Multiple Regression: Regress the phenotype against all genotypes at once. The covariance correction methods above regresses a genotype on a phenotype

while/after correcting for population structure; however including all other genotypes would model the effect conditioned on the rest of the genome, which, in essence, accounts for population structure.

Drawbacks: Depending on the size of the genome and number of variants modeled, this can be an incredibly high-dimensional regression. It may then be necessary to regularize, however regularization can come with challenges in standard error approximation of the parameters. This may require bayesian estimates, which are often computationally costly, especially given the large number of samples and high dimensionality. Interpretation of high dimensional models can also be challenging.

In Chapter 3, we will utilize generalized least squares as it requires making relatively few assumptions compared to many of the other methods, performed well for simulated test cases, and is fast to compute. We believe that improvements upon this can definitely still be made; and in particular, an appropriate generalized linear mixed model may be more conceptually adherent.

1.4 Interpretability

Let's consider why interpretability is a difficult for analyses of the Nahant Collection. There are 241 phage and 243 hosts, approximately 1000 phage gene clusters and 10,000 host gene clusters. Taking the simplest possible approach of regressing each phage infection profile against each host gene (that's $241 \times 10,000$ regressions) or each host infection profile against each phage gene (that's 243×1000 regressions), how do we make sense of the results once we have them? (A less simple approach of using multiple regression to predict the infection matrix is presented in Appendix A.)

Genome wide association studies often make use of the “Manhattan plot,” which depicts either the log odds or the negative log of the regression coefficient p-values on the y-axis and the genome position on the x-axis. This helps identify the genetic locus of interest to a particular phenotype. There is a perfect analogy here, but one question is, what genome do we use? We cannot make a full genome alignment of

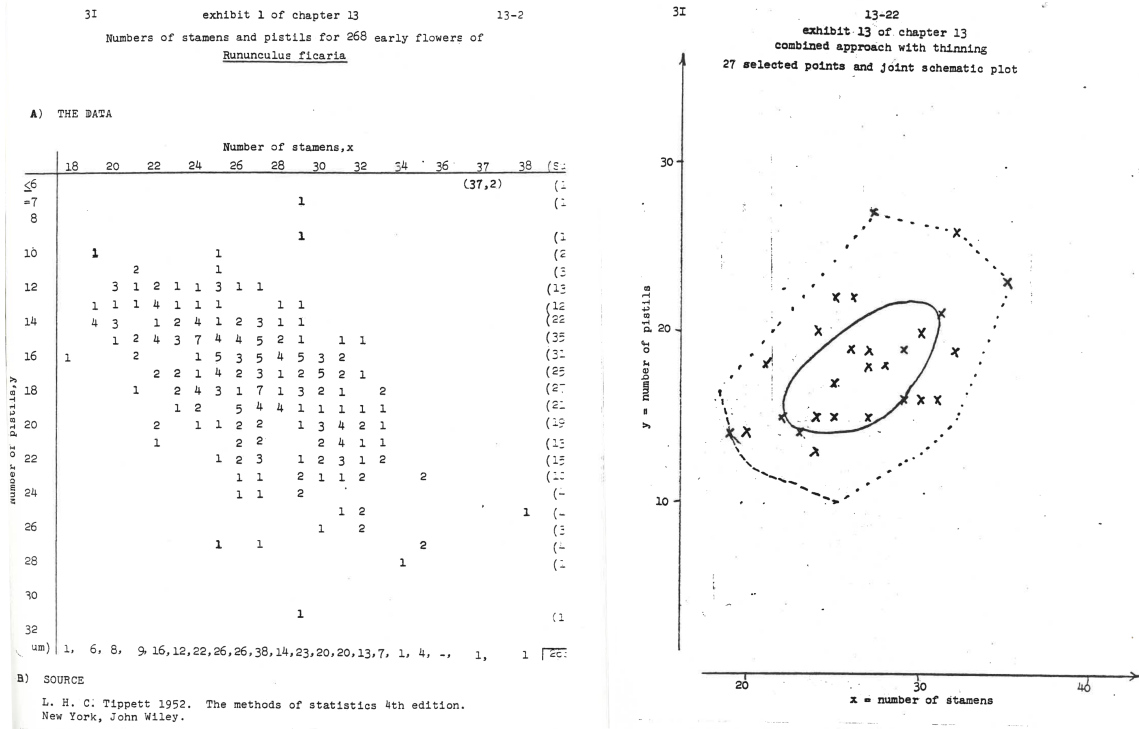


Figure 1-5: Tukey emphasizes the value of tracing paper in his original 1970 volumes of Exploratory Data Analysis. Here, he shows how a bagplot can be constructed for Fisher's Iris dataset. While tracing paper is perhaps less relevant for the large, high dimensional datasets we face today, his willingness to dive into the weeds and his emphasis on selecting the right medium are great guiding heuristics. Pages preceding Tukey, John W., Exploratory Data Analysis, 1st, ©1977. Reprinted by permission of Pearson Education, Inc., New York, New York.

either the bacteria or the viruses. And then if we make some type of full genome alignment, we would be left with 484 Manhattan plots to sift through. This challenge in interpretability is, in fact, a challenge in exploratory data analysis. The Nahant Collection is an observational dataset, and so while we can make associations between genes and infection phenotype, these associations must be validated with experiments. Therefore, the goal is really to facilitate intuitive exploration of various hypotheses in order to identify which of these hypotheses are most worth testing. In need of inspiration, we turned to John Tukey, who defined the term “exploratory data analysis.” (Tukey is also the father of fast fourier transforms, the term “bit,” boxplots, among others.) To highlight a few of his mantras [41]:

- “Three main strategies of data analysis are: 1. graphical presentation. 2. provision of flexibility in viewpoints and in facilities, 3. intensive search for parsimony and simplicity.”
- “Exploratory data analysis is actively incisive rather than passively descriptive, with real emphasis on the discovery of the unexpected.”
- “Exploratory data analysis does not need probability, significance or confidence”

And in leafing through Tukey’s volumes [42], it is interesting to note how many carefully hand-drawn figures there are and how enthusiastically Tukey extols the advantages of tracing paper. While tracing paper may not help us with the many thousands of genes Nahant Collection, the notion of finding the best medium for the job is useful. The approach we chose to take in Chapter 3 is to write a javascript visualization that allows a user to interact with the data and regression results. Not all regressions are sensible, and full genome alignments of bacteria and phage are not logical. So instead, the user is able to interactively chose which regression results to view and which genomes to view the results on. Brushing and zooming are also written into the Manhattan plots in order to display details about the particular regions of interest.

1.5 Goals of this thesis

The general goal of this proposal is to explore the genetic variations that determine phage-host interactions. In Chapter 2, we outline an interrogation of the selective advantages that a particular strategy, carrying tRNA, may convey to a T4-like Vibriophage, 2.275.O (348,911 bp, 18 tRNA spanning 13 amino acids). We show that host DNA and RNA degrade upon infection - particularly, host tRNA degradation baselines around 15 minutes into infection, while phage particles are only released at 60 minutes, implying that without further tRNA production, phage genes expressed late in the cycle may experience resource limitation during translation. All 18 phage tRNA are expressed, at levels slightly better adapted to phage codon usage, especially

that of the late genes, which may rely mostly on the phage tRNA pool for translation. Strikingly, the phage is very unlikely to pick up as diverse or more diverse an array of tRNA as what it currently carries. This suggests what appears to be a goal toward nearly self-sufficient translation as the host translational machinery degrades.

In Chapter 3, we turn to the dataset as a whole in order to infer mechanistic insights from the large scale sequencing and phenotyping efforts. Doing so comes with a few challenges: (1) While the diverse population structure of phage and hosts is an interesting feature of the data, it means that statistical independence does not apply. To address this, we screen for genes of interest using generalized least squares to correct for phylogenetic confounding. We find that this procedure allows us to pick out relevant signals, especially negative effects such as restriction modification systems and exclusionary prophage elements, which would otherwise be drowned out by spurious correlations resulting from statistically oversampled blooms of microbes. (2) Due to the observational nature of environmental sampling, we are not able to draw conclusive links between genetic elements and infection specificity. Instead, the Nahant Collection should be viewed as a resource for exploratory analyses that can inform the design of additional experiments. Thus, we've written an interactive visualization to facilitate the process of developing testable hypotheses concerning mechanisms of phage infection and host response.

Chapter 2

Selective advantages of bacteriophage tRNA

Joy Y. Yang¹, Wenwen Fang^{2,3}, Julia M. Brown⁴, Kathryn M. Kauffman⁵, Libusha Kelly⁶, David P. Bartel^{2,3}, Martin F. Polz⁵

¹Computational and Systems Biology Program, Massachusetts Institute of Technology, Cambridge, Massachusetts 02139, USA

²Howard Hughes Medical Institute and Whitehead Institute for Biomedical Research, Cambridge, Massachusetts 02142, USA

³Department of Biology, Massachusetts Institute of Technology, Cambridge, Massachusetts 02139, USA

⁴Bigelow Laboratory for Ocean Sciences, East Boothbay, Maine 04544, USA

⁵Department of Civil and Environmental Engineering, Massachusetts Institute of Technology, Cambridge, Massachusetts 02139, USA

⁶Department of Systems and Computational Biology, Albert Einstein College of Medicine, Bronx, New York 10461, USA

J.Y. carried out the computational analyses and the phage infection timecourse experiments. W.F. conducted tRNA sequencing and full transcriptome sequencing on the infection timecourse samples. J.M.B. performed initial computational analyses which inspired this work. K.M.K. isolated the bacteria and bacteriophage upon which this work was based and captured EM images of the phage. J.Y., W.F., D.P.B., L.K., and M.P. conceived of the project, designed the analyses, and wrote this manuscript. All authors contributed toward revisions and editing.

2.1 Abstract

Viruses are traditionally thought to be under selective pressure to maintain compact genomes and thus depend on host cell translational machinery for reproduction. However, some viruses encode abundant tRNA and other translation related genes, the presence of which is thought to optimize for the codon usage differences between the phage and host. In this paper, we outline a systematic interrogation of selective advantages that carrying tRNA may convey to a particular T4-like Vibriophage, 2.275.O (348,911 bp, 18 tRNAs spanning 13 amino acids), during infection of its host of isolation. We observe that host DNA and RNA degrade upon infection - particularly, host tRNA degrades and reaches a minimum around 15 minutes into infection, while phage particles are only released at 60 minutes, implying that without further tRNA production, phage genes expressed late in the cycle may experience resource limitation during translation. All 18 phage tRNA are expressed, at levels slightly better adapted to phage codon usage, especially that of the late genes, which may rely mostly on the phage tRNA pool for translation. Strikingly, the phage is very unlikely to pick up as diverse or more diverse an array of tRNA as what it currently carries ($p = 0.0016$). Taken together, our results support early findings [43] that the main driver behind phage tRNA acquisition is the pressure to sustain translation as the host machinery degrades, a process which results in a dynamically adapted codon usage strategy during the course of infection.

2.2 Significance

Bacteriophage are traditionally thought to be under selective pressure to maintain compact genomes constrained by capsid size. Therefore, for phage, translational machinery is thought to be better rented than owned and is considered a signature of cellular organisms [44–47]. However, the recent explosion in phage genome sequences

reveals a wide distribution in phage genome content and size [48], including “jumbo phage” that carry tRNA and other translation-associated genes. More diverse strategies must therefore be at play. Our results here point toward a tradeoff: although encoding translation-related components requires shuttling a larger phage genome, it also reduces dependence on host translational machinery, allowing the phage to be more aggressive in degrading and recycling the host genome and other resources required for replication.

2.3 Introduction

The question of why some bacteriophages encode their own tRNAs has been of interest since the late 1960s, when tRNAs were discovered to be carried by T4 [49, 50]. This finding counters the notion that bacteriophage should be under selective pressure to maintain compact genomes. Most phage simply make use of the hosts’ translational machinery, and thus tRNA genes and other translation-related genes are often considered a hallmark of cellular life [44–47]. Why then, do some phage carry tRNAs?

For the T4 phage, almost all of its eight tRNAs correspond to codons that it uses more frequently than its host [51]. Based on this example, it was proposed that bacteriophage typically carry tRNA in order to bias translation toward their own genes. Additionally, Cowe, et al. found evidence suggesting that the codon usage bias introduced by T4 tRNAs is especially pronounced toward its late genes [43]. Experimentally, tRNA mutants of T4 are still able to replicate and lyse their hosts, but show a moderate decrease in burst size under some experimental conditions [52].

However, for another broad host-range T4-like phage KVP40, which carries 25 tRNAs [53, 54], the signal for codon usage bias optimization by phage tRNAs is less clear [54]. In fact, this signal may be an artifact because bacterial tRNA levels are

often highly optimized for their codon utilization [55, 56], and codon usage tends to be very species-specific [57, 58]. Hence even phage that do not carry tRNAs commonly have noticeably different codon usage distributions than that of their hosts. It therefore remains an open question whether codon bias optimization is a strong enough driving force for phage to carry tRNA genes. Other correlations have been described of, for example, larger phage carrying more tRNAs, and lytic phage being more likely to carry tRNA than temperate phage [59]. And through a process of elimination, Delesalle, et al. [60] hypothesized that tRNAs help to sustain growth during infection or to expand host range of the phage.

Because of these competing hypotheses, we systematically explored the selective advantages that carrying tRNA might confer to a particular phage, 2.275.O [NCBI:txid1881285]. To verify whether the codon usage bias hypothesis may be plausible, we conducted preliminary genomic analyses to verify that a codon usage difference exists between the phage and host. Next, because alternative uses for tRNAs exist - such as being convenient sites for recombination - we checked for signatures of posttranscriptional tRNA modifications in the sequencing data and found that the phage sequences were indeed recognized as tRNA and therefore are likely to participate in translation. We returned to assess the codon usage optimization hypothesis, and found that while the evidence suggests that there could be some amount of optimization, this did not appear to be the most important factor at play. Instead, we found that the infection phenotype is all-destructive in that within approximately the first 15 minutes of infection, the host genome was degraded, as was the host transcriptome. There is, therefore, little host RNA left to optimize codon usage bias against. Rather, because the host tRNAs were degrading as well, the phage presumably supplies its own translational machinery in order to sustain its reproduction cycle. Finally, we show that the main factor optimized for by the phage tRNA is the diversity of the tRNA array, which allows the large phage to sustain a longer replication cycle amid

the decaying pool of host resources that result from the lytic infection cycle. This illustrates a pressure that may select for larger phage: because large phage must degrade host machinery for parts, bringing its own machinery allows it to gain a competitive edge, which selects for even larger phage.

2.4 Results

2.4.1 Genomic analysis of phage and host reveals differences in genomic codon usage patterns

Phage 2.275.O is part of the Nahant Collection, an extensive collection of Vibriophage previously described by Kauffman et al. [28, 29], and is notable for a few reasons: at 348,911 bp, it is among the largest known bacteriophage (Figure 2-1); it is capable of infecting hosts from two different species, *Vibrio cyclitrophicus* and *V. lentus*; and its genome encodes for 18 tRNAs that correspond to 13 amino acids, as well as another seven other tRNA-like sequences with putative introns (Figure 2-2A). To test whether the codon usage hypothesis is plausible, we first conducted preliminary analyses to verify that a codon usage difference between the phage and host exists. To this end, we applied multidimensional scaling (Figure 2-3a) and multinomial discriminant analysis (Figure 2-3b) to the codon usage for each gene from the genomes of the phage and its host of isolation. We observed that there is, in fact, a codon usage difference between the two organisms, allowing us to next ask, do the phage tRNA bias translation in the direction of this difference? Previously, tRNA copy number in the genomes of phage and their hosts was used to assess whether phage tRNAs may optimize codon usage differences [59]. And in examining the odds ratio for each codon in the phage vs. host genome (Figure 2-2b), the codons that can be recognized by an anticodon from a host tRNA (according to extended wobble rules summarized by dos Reis, et al. [61–63]) appears to be more commonly used by host genes than by phage genes. On

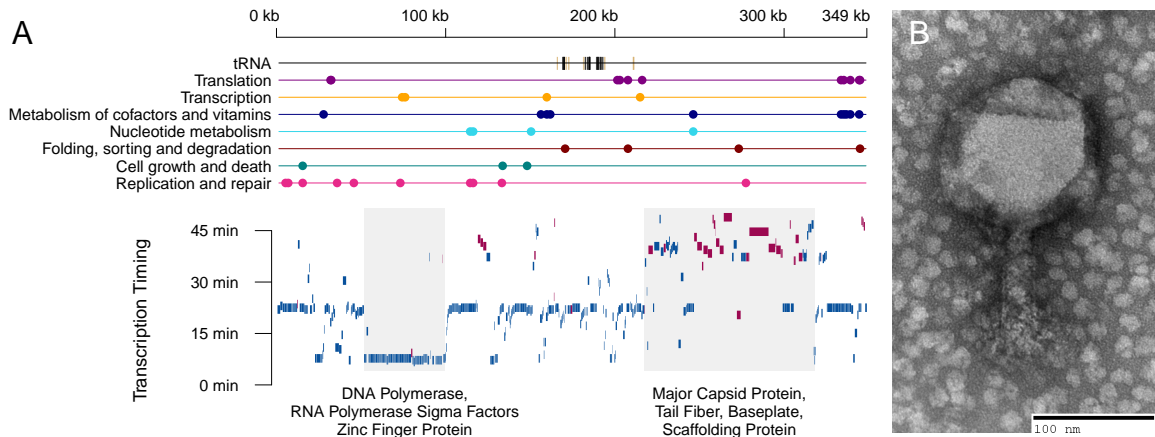


Figure 2-1: Phage 2.275.O carries 18 tRNA genes and is a large phage in both capsid size (120 nm) and genome size (348,911 bp). (A) The x-axis of the genome summary is genome position, the tracts above in color indicate hits to kegg annotated genes. The y-axis of the timing plot below depicts time to reach half the maximum expression of that gene. Blue bars indicate genes on the positive strand, and red bars indicate genes on the negative strand. This summary gives an estimate as to what the transcriptional units may be. Similarly to T4, early genes tend to be polymerases and sigma factors, while late genes tend to be structural proteins. (B) An electron microscopy image of phage 2.275.O is shown.

the other hand, codons that can be recognized by both phage and host tRNAs span the range of usage preferences. Instead of selectively acquiring tRNAs that are more beneficial to it than its host, it appears the phage seeks to acquire diverse tRNAs, but places lower priority on those that benefit mainly its host. However, this analysis does not account for RNA modifications (which can often be found at the wobble base); and furthermore, tRNA expression level may be more relevant information for assessing any translational bias that may be introduced. We therefore performed tRNA sequencing on an infection timecourse, sampled at 15-minute intervals, in order to track the phage tRNA expression levels throughout the infection cycle.

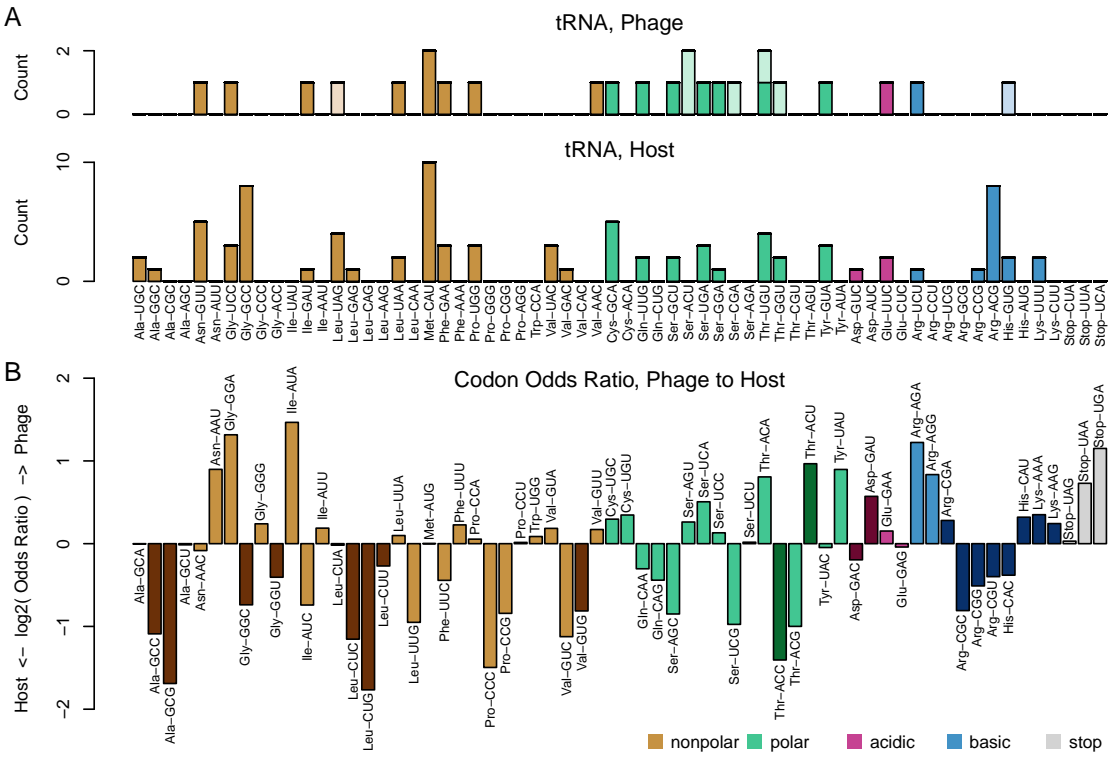


Figure 2-2: Analysis of the phage and host genome supports the codon usage hypothesis. (A) tRNA content in the genomes of the phage and host. Less saturated bars indicate putative tRNA with introns. (B) Differences between the codon usages of phage and host. Darkened bars indicate codons that cannot be recognized by phage tRNA, given the wobble rules summarized by dos Reis, et al.

2.4.2 tRNA sequencing suggests that phage tRNA actively participate in translation

The presence of many tRNA genes in the 2.275.O genome suggests that (at least some of) the tRNAs do indeed participate in translation. However, this assumption should still be tested, as there are non-canonical uses for tRNAs, such as serving as convenient sites of integration for phage and integrative conjugative elements [64–66] or serving as primer binding sites (more pertinent to RNA viruses) [67, 68].

Based on data from tRNA sequencing, we are able to verify that phage tRNA are expressed during the infection cycle; and furthermore, we can infer post-transcriptional modifications on the phage tRNA transcripts using the sequencing data, which indicates

that the phage tRNA are likely involved in translation. For example, in tRNA, the CCA tail is required for amino acid attachment as well as for successful interaction with the ribosome, and synthesis of the CCA tail is thought to be a step in tRNA quality control [69–71]. We observed that the tails of the five phage tRNA whose genomic sequences do not end in CCA (Cys-GCA ends in CTA, Gly-TCC ends in CTA, Ile-GAT ends in CAA, Leu-TAA ends in CCG, and Tyr-GTA ends in CAA), are modified into CCA upon transcription. On the other hand, the genomic sequences of all host tRNA end with a CCA tail. And while the host carries a CCA modification protein in its genome (Genbank locus tag NVP2275O_348); the phage carries its own CCA modification protein as well. Hence, the phage tRNA appear to be processed such that they can participate in translation.

We are additionally able to infer putative addition of similar base modifications on the phage and host tRNAs. In our tRNA sequencing protocol, we used the group II intron reverse transcriptase TGIRT [72], which can read through RNA modifications but may leave DNA base substitution signatures. For example, in comparing one of the phage CAU tRNAs (Genbank genome location: 182648-18272) with a host CAU tRNA (Genbank locus tag: BCV12_11325), both are modified with 4-thiouridine on the 8th base, 3-(3-amino-3-carboxypropyl)uridine on the 47th base, and, importantly, 2-lysidine on the 34th base, putatively changing them to AUA-recognizing isoleucine tRNA [73]. Other similar putative modifications can be observed between phage tRNA and their host analogs, for example, 5-carboxymethylaminomethyl-2-thiouridine on base 34 of Glutamine tRNA, 1-methylguanosine on base 37 of (most) Leucine tRNA. These similarities suggest that phage tRNAs may be recognized and processed by the same enzymes as corresponding host tRNAs.

It is of course possible that the phage tRNA additionally participate in other functions, and in fact, seven intron-containing tRNA-like sequences, while not recognized by tRNAscan-SE [74], are recognized by another tRNA caller, Aragorn [75]. These

sequences are only expressed at as low as 0.003 times (as in the case of threonine tRNA) to 0.2 times (as in the case of serine tRNA) the abundance of an isoacceptor phage tRNA without an intron. Although a small fraction of the reads did appear to be spliced as called, many did not, and the aligned anticodon loop was fairly heterogeneous for these species. In addition, many of these sequences do not end in CCA and did not appear to receive CCA tails. These intron-containing tRNA-like sequences may serve non-canonical functions, and so were therefore not used beyond the initial preliminary analyses.

2.4.3 Codon usage bias is present but not pronounced

Having found evidence supporting the idea that the 18 phage tRNAs without introns likely participate in translation, we then turned to testing the most common hypothesis as to why phage carry tRNA - to increase the translational efficiency of their own genes over that of their hosts' [51, 52, 59, 76]. For each gene, we calculated a value representing the efficiency with which it can be translated by the phage tRNA pool, relative to the efficiency with which it can be translated by the host tRNA pool (see Materials and Methods), for simplicity, we will refer to this value as the "slant" of a gene. We observed that the slant of the phage genes was slightly more in the direction of the phage tRNA pool than was the slant of the host genes (Figure 2-3C); however, this effect was weak compared to a more optimal axis of discrimination, which is defined by the average gene codon usage for each organism (Figure 2-3B). The statistical significance of this small effect (KS-test: $p < 2.2\text{e-}16$) seems unreasonable; and in fact, we must re-evaluate this test under the context of the problem at hand - specifically, we already know that a codon usage bias exists between the host and phage genes, and we also know that the host tRNA are closely matched to the host codon usage (Figure 2-3A). Therefore, almost any randomly chosen set of tRNA will betray a codon usage difference between the phage and host genes. It is simply then a

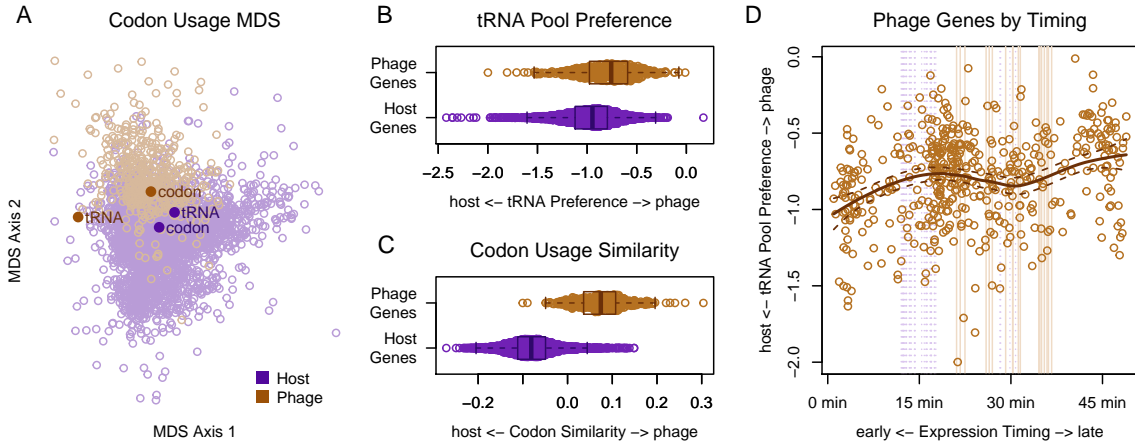


Figure 2-3: Codon usage bias introduced by the phage tRNA pool is more pronounced in late genes than early genes. (A) A multidimensional scaling plot of phage and host proteins using Shannon-Jensen Divergence of the codon distributions shows that a codon usage difference exists between phage and host. Points representing the codon recognition capacities of the tRNA pool for each organism are overlaid. Points representing the average codon usage for each organism are also overlaid. In (B), the x-axis shows the “slant” for each gene, or the preference for the phage tRNA pool vs. the host tRNA pool. (Zero signifies ambivalence.) While a statistically significant difference in the slant of phage and host genes exists, this axis is by no means optimized. A more optimal axis is shown in (C), which is defined by the mean codon usage for host and phage. (D) The slant toward the phage tRNA pool is slightly higher for late genes than for early genes. Here, the timing depicted along the x-axis is the center of mass of RNA expression for the first round of infection. Note that this is different from the expression timing described in figure 1. The center of mass in this plot also gives a sense of how quickly the RNA transcript is degraded, while the time to half maximum expression shown in figure 1 mainly summarizes transcription timing.

coin flip as to whether the difference is in the direction of the host tRNA pool or the phage tRNA pool.

A better question to ask then, is whether the slant values for phage vs. host genes are different given the known difference in codon usage for the two organisms. Conditioning appropriately, the probability of seeing as high or a higher difference in slant between the phage proteins and host proteins in the direction of the phage tRNA pool was approximately 0.08. (See Materials and Methods for details of this

calculation) This probability is suggestive, but we cannot be confident that codon usage bias optimization has been the main factor driving tRNA acquisition.

2.4.4 Host genomic DNA and RNA transcripts are degraded

Perhaps the signal for codon usage optimization was low because codon usage optimization mainly targets a subset of the phage genes, in particular the late genes, as is the case for T4 [43]. Codon usage optimization toward the late genes might be advantageous for a few reasons: (1) mRNAs from the earliest genes might already be undergoing translation and degradation as the phage tRNAs are transcribed, and therefore must utilize mainly the host tRNA pool; and (2) the host tRNA pool might degrade, in which case, translation, during the late stages of infection might heavily rely on phage tRNA.

Some evidence in the literature supports the latter hypothesis. During T4 infection of *E. coli*, degradation of host DNA is initiated by Endo II and Endo IV [54], in part to help supply the nucleotide pool for phage replication. This comes with a consequence: although tRNAs tend to be more stable than other RNAs [77], they can undergo rapid degradation under stress conditions [78, 79]. In fact, during T4 infection, *E. coli* uses nucleases to deplete its own lysine tRNA, dialing down translation, seemingly in defense. While, as a “rebuttal,” T4 RNA ligase is able to repair damaged tRNA [80], the evidence for this all-destructive infection phenotype suggests that supplying translational components might help the phage to fill the growing gaps in host machinery and thereby prolong the replication period.

To test whether phage 2.275.O infection is similarly all-destructive, we used qPCR to check whether host DNA was degraded upon infection. We found that the genomic copy number of the host genes probed for (GroEL and CTP Synthetase) dropped by approximately 80% within the first 15 minutes of infection (Figure 2-4A). These levels climb again at 60-90 minutes, likely due to regrowth of uninfected host cells. These

dynamics would be expected with a multiplicity of infection (MOI) of approximately 1.6, assuming Poisson infection probabilities. (Although we had targeted a higher MOI of ~8, the actual MOI might have been lower due to inefficiencies in phage-host encounters.) Because the host genome is degraded, tRNA can no longer be produced from the host genome, and if host tRNA are degraded as well, tRNA might become a limiting resource for translation during the late stages of infection. When examining the tRNA expression from transcriptome sequencing data, we found that the host tRNA were indeed degraded rapidly, reaching a minimum value around 15 minutes (the climb after 15 minutes is likely due to regrowth of uninfected cells), whereas phage tRNA were continually produced (Figure 2-4B). In contrast, phage particles were produced only 60 minutes into the infection (Figure 2-4A). These observations supported the hypothesis that, as the host tRNA pool is degraded, the phage tRNA allow translation to be sustained; this may especially benefit the late genes, which do not reach half their maximum expression until 40–45 minutes into the infection (Figure 2-1).

Having found that the host genome and transcriptome (including the tRNA) were indeed degraded during infection, we next utilized the full transcriptome sequencing data to quantify 2.275.O gene expression timing in order to assess whether late genes, which have a greater necessity for relying on phage translational machinery, were more adapted to the phage tRNA pool than early genes. We did in fact observe that the slant of the late phage genes was further in the direction of the phage tRNA pool than the slant of the early genes (Figure 2-3d). However, the absolute slant of even the late genes was closer toward the host tRNA pool than the phage tRNA pool, implying that while suggestive, codon usage bias optimization might not be the driving force for phage acquisition of tRNAs.

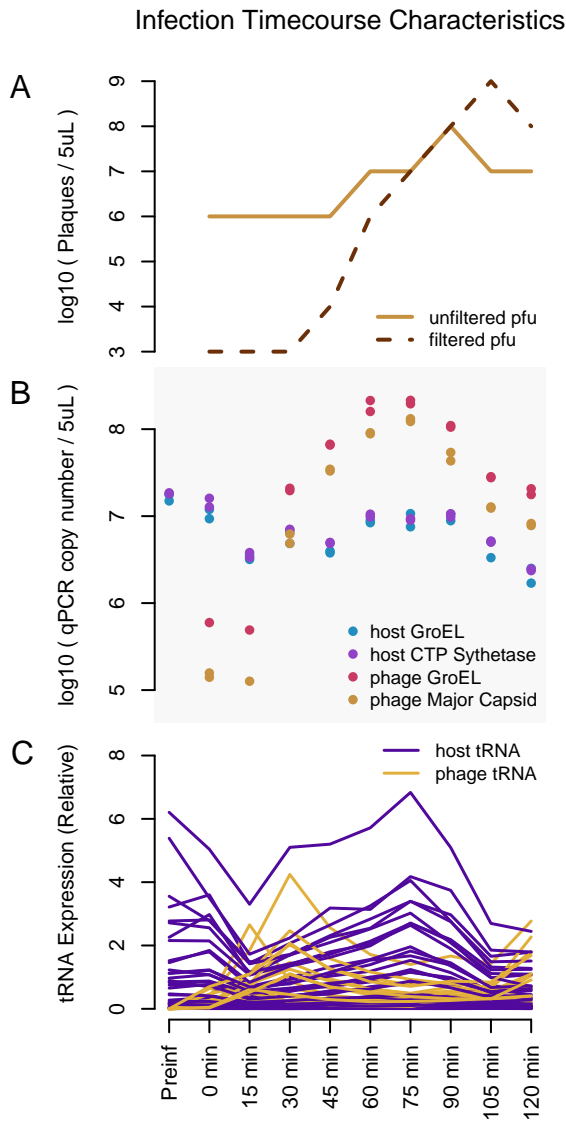


Figure 2-4: 2.275.O infection is aggressively lytic. (A) Phage burst occurs around 60 minutes into infection. (B) QPCR results show that the host genome is degraded rapidly upon infection. (C) RNA sequencing results show that host tRNA (and generally, most host RNA, with the exception of stress response genes) are degraded upon infection as well. In contrast, phage tRNA rapidly increase, supplementing the degrading pool of host tRNA. Here, the reads are normalized to a firefly luciferase spike-in for each sample, as opposed to the total read count per sample.

2.4.5 Prolonging the replication period amidst host cell shut-down

If the phage tRNAs optimize for the ability to sustain translation in the absence of the host tRNAs, we would expect the phage to carry as diverse an array of tRNA as possible. In fact, it is striking that the 18 phage tRNAs without introns each represent different anticodons (there are two CAU anticodons, however, one of these is likely modified by 2-lysidine, making it an AUA-recognizing Leucine as opposed to an AUG-recognizing methionine, please refer to the github for details about modification calling). And in simulating draws of tRNA from the host genome, we find that the tRNA carried by 2.275.O is more diverse in anticodons encoded than would be expected at random (Figure 2-5A, $p=0.0016$). This observation was even more striking, when considering that neighboring tRNAs within the host genome generally have very low diversity, as they are likely the result of gene duplication events, and tend to code for the same amino acid (Figure 2-5A). This indicates that picking up as diverse an array of tRNAs as observed in the 2.275.O genome was not a matter of a few simple recombination events, but many. Thus, the diversity of this tRNA array appears to be under high selective pressure.

And what of the tRNAs that the phage does not carry? We found that the host expresses of many of these tRNAs more highly than the tRNAs with phage analogs (Figure 2-5B). Assuming similar rates of degradation for each tRNA, the more highly expressed tRNAs may persist longer during infection, thereby reducing the selective pressure for the phage to acquire its own copies. The tRNAs without phage analogs that are expressed lowly by the host recognize codons that are used very infrequently by the phage. These two types of tRNA may confer less of a selective advantage to the phage than the tRNA already present in the phage, implying that for these tRNAs the phage has reduced its dependence on their codons rather than acquire its own copies of the tRNAs. Taken together, the observations presented in this paper imply that

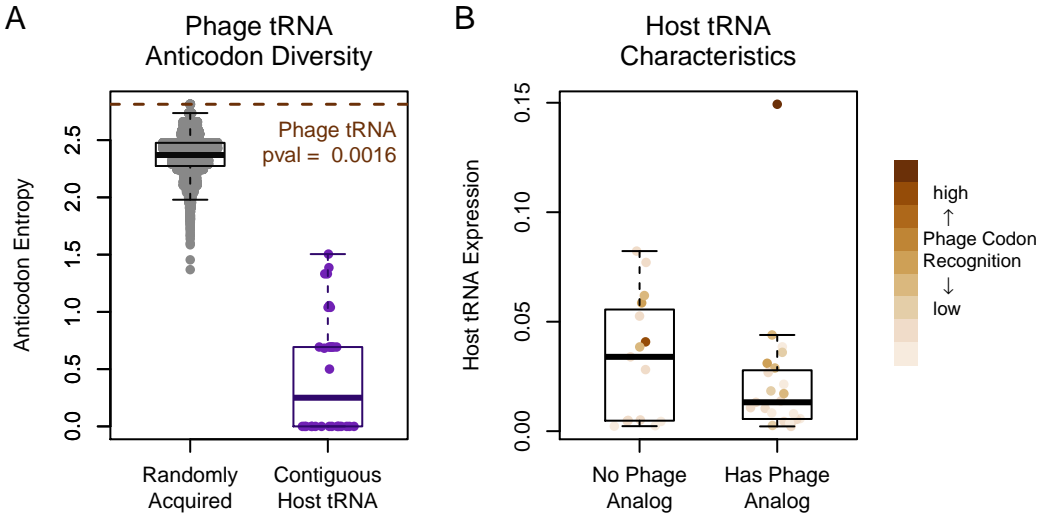


Figure 2-5: The main function of tRNA carried by the phage is likely to supplement the degrading pool of host tRNA. (A) The diversity of the phage tRNA array appears to be under selection, and is likely the result of multiple recombination events. Based on simulation results, the probability of selecting, uniformly at random from the host genome, a tRNA array that is able to encode as many anticodons as that carried by the phage is 0.0016, indicating that tRNA array diversity is under selection. In addition, contiguous stretches of tRNA in the host genome, which are typically thought to be the result of duplication events, encode very lowly diverse anticodons. The phage's tRNA collection, therefore, appears to be the result of multiple acquisition and selection events. (B) Of the tRNA not carried by the phage, most are very highly expressed by the host, and others correspond to codons not very highly used by the phage genome.

the primary function for phage tRNAs is to supplement degrading host translational machinery, which results from an all-destructive lytic infection phenotype.

2.5 Discussion

Our results indicate that the main role of the phage 2.275.O tRNAs is to support translation of this large lytic phage as the host cell shuts down. Upon 2.275.O infection, host genomic DNA is degraded, as are mRNA transcripts. Degradation reaches a baseline around 15 minutes; however, phage particles are only released around 60

minutes after the onset of the infection, implying that without phage tRNA production, late genes might experience resource limitation during translation. Although the tRNA array of phage 2.275.O does not appear to optimize tRNA/codon usage bias toward its genes on the whole, we do observe that the codon usage of the phage genes expressed late during the infection are more in the direction of the phage tRNA pool than that of the early genes. Additionally, the diversity of the phage tRNA array appears to be optimized, implying that the main selective force at play is a drive toward self-sufficiency in the wake of host degradation.

This simple line of logic unifies many observations previously made in the literature, either through deep interrogations of the T4 infection cycle or broad analyses of tRNA-carrying phage: First, the presence of many tRNAs is more often found in genomes of lytic phage than those of temperate phage [59]. Aggressively lytic phage often degrade the host genome as the phage can then use the nucleotides to increase its burst size. But because translation is required for phage particle production, these phage presumably benefit from shuttling their own translation machinery by extending the replication period beyond the time at which the host resources are depleted.

A second observation is that phage tRNAs appear to optimize codon usage bias toward phage genes and away from host genes [51]. According to our findings, tRNAs absent from the phage correspond to those that tend to be highly expressed in the host, and tRNAs highly expressed in the host correspond to codons that are most commonly used by the host, or are most biased toward the host. This back door correlation may explain a large part of the observed codon usage bias effect. Moreover, once the phage acquire tRNA, an adaptive feedback loop can form between the phage genome codon usage and the tRNA array that it carries. This feedback loop explains a third observation, which is that codon usage bias is more pronounced in late phage genes than in the early genes [43, 81, 82]. Early mRNAs require use of host tRNAs, as the bulk of phage tRNAs are still in the process of being transcribed and processed,

whereas late mRNAs are expected to be more dependent on the phage tRNAs, as the bulk of the host tRNA might be degraded later in the infection.

And finally, a fourth observation is that phage with tRNAs generally have larger genomes than those without [59]. For phage with large genomes, it is more important to degrade the host genome to free up nucleotides, leading again to the quandry presented by the first point. In addition, larger phage might require longer periods of replication and more resources for supporting translation in the wake of degrading host tRNA. The longer the infection persists past host resource degradation, the stronger the selective pressure for phage to encode their own machinery, which in turn selects for larger phage.

Using this lens, it is interesting to compare 2.275.O against its foil in the same phage sampling collection, the Autolykiviridae [29]. In contrast with this 349kb phage, Autolykiviridae carry a particularly small, streamlined genome, at only 10kb. With such small genomes, there may be less selective pressure to free up the nucleotide pool. In fact, Autolykiviridae do not degrade the host genome. The infection cycle of these viruses can last on the order of weeks, and with only 20 genes in its genome, having no known translation supporting functions, they must rely entirely on the host translation machinery. Although a whole spectrum of strategies might co-exist, we can see here two extreme, contrasting strategies.

This type of phage infection might have convenient applications for studying tRNA regulation. Although translation is fundamental to all of life, many aspects are still unknown. For example, while some tRNA modifications have been shown to be necessary for correct folding, synthetase recognition, degradation, and translation regulation [83], the functions of most modifications are unknown [84]. Many recent findings about tRNA are conducted in systems in which a cellular stress response involving tRNA can be triggered [84]. Lytic phage infection offers a similar convenience in that it can be synchronized through a one-step-growth experiment [21]. Because of

this, tRNA can be “tracked” from the newly synthesized nascent form to processed intermediates and degraded products. In fact, this can be seen in our tRNA sequencing timecourse. Exciting new technologies for probing translation now exist, such as ribosomal footprint profiling [85], tRNA-ribo-seq [86], etc. Work in combining these techniques with phage growth experiments may be a promising future direction for uncovering further insights into tRNA processing and use in translation.

2.6 Materials and Methods

Code and data for the analyses described here are available on Github ([polzlab](#) and [kellylab](#)) in the form of an R [87] package. A more high-level set of vignettes are available for the purpose of walking through the data and analysis thought process; and a more low-level set of vignettes is also available that dive into the weeds of the implementation details for those who are interested analyses of similar data. Raw sequencing reads are available on the NCBI Sequenced Reads Archive under BioProject numbers PRJNA524872 (tRNA-seq) and PRJNA524877 (full transcriptome RNA-seq).

2.6.1 Exploratory genome-based codon usage bias analysis

In order to assess the plausibility of the codon usage bias hypothesis, we conducted a preliminary analysis of the phage and host genomes. The tRNA carried by each organism was called using tRNAscan-SE [74]. The multidimensional scaling analysis uses Shannon-Jensen divergence between codon distributions for each protein as the distance metric. The odds ratio for each codon is defined as

$$\frac{P(\text{codon} \mid \text{org} = \text{phage}) / (1 - P(\text{codon} \mid \text{org} = \text{phage}))}{P(\text{codon} \mid \text{org} = \text{host}) / (1 - P(\text{codon} \mid \text{org} = \text{host}))}.$$

2.6.2 tRNA Sequencing Timecourse

In order to explore the shift in tRNA abundance throughout the course of infection, we conducted a one-step-growth experiment and collected samples at 15 minute intervals. Cells from the same culture were split in two (control vs. infection) then centrifuged to pellets. The control sample was resuspended in 200 μ L of Difco 2216 Marine Broth, and the infection sample was resuspended in 150 μ L 2216 and 50 μ L of phage lysate. The samples were left to sit for 5 minutes to allow for adsorption of the phage, then diluted to a volume of 15 mL in order to deter further infection. This total volume was split in 5, one sample from each set was immediately centrifuged and flash frozen as a “time 0” sample, and the rest were placed on a shaker, then centrifuged down and flash frozen at 15 minute intervals. 500 μ L aliquots were taken from each sample prior to centrifugation to be plated as a spot check of phage concentration.

2.6.3 RNA Sequencing Timecourse

To further hone in on particular genes that the codon usage bias may favor, a second phage growth experiment was collected for full-transcriptome RNA sequencing. In this experiment, an aliquot of a culture was centrifuged and flash frozen as a preinfection timepoint, the remainder of the culture was then centrifuged to a pellet then resuspended with 400 μ L of a phage lysate. The samples were left to sit for 5 minutes to allow for adsorption of the phage, then diluted to a total volume of 45 mL in order to deter further infection. This total volume was split into 9 samples of 5 mL each, to be taken in 15 minute intervals from time 0 to 120 minutes. The sampling procedure involved flash freezing 3 pellets spun down from 1.5 μ L aliquots of each sample, then immediately doing serial dilutions of unfiltered and filtered viruses to assess phage growth and stage of infection.

2.6.4 Total RNA extraction

Total RNA from the infection time series (flash-frozen pellets) was extracted by the hot phenol method. Briefly, cell pellets were resuspended in TE (10 mM Tris pH 7.0, 1 mM EDTA) and treated with 0.5 mg/ml lysozyme at room temperature for 5 minutes. Then NaOAc (100 mM final concentration) and SDS (1% final concentration) were added, followed by an equal volume of acid phenol:chloroform pH 4.5 (ThermoFisher). The mixture was shaken at 65°C for 10 minutes using a thermomixer, and centrifuged at 20000 x g for 5 minutes. The upper phase was washed by chloroform and centrifuged at 20000 x g for 5 minutes. The phenol/chloroform extraction was repeated once, and the upper phase was precipitated with isopropanol and 300 mM NaOAc. Precipitated RNA was washed with 75% ethanol, air dried and resuspended in water.

2.6.5 High-throughput sequencing of tRNAs

tRNAs were gel purified from total RNA on a 10% urea polyacrylamide gel (size selected between 70 and 100 nt). Gel pieces were macerated and soaked in 0.3 M NaCl overnight with rotation at 4°C for elution. tRNAs were precipitated with isopropanol using linear acrylamide as the carrier. RNA pellets were resuspended in 100 mM Tris-Cl pH 9.5 and incubated at 37°C for 1.5 hours for deacylation. After deacylation RNA was purified using Oligo Clean & Concentrator (Zymo Research) and eluted in 10 mM Tris pH 8.0. Purified RNA was ligated to a 3' preadenylated adapter AppNNNNAGATCGGAA-GAGCACACGTCT/iBiodT/iBiodT/3ddC/ (final concentration 10 uM) using RNL2 truncated KQ (NEB) with 10% PEG8000 at room temperature overnight. After ligation RNA was purified using the MinElute PCR Purification kit (Qiagen) and reverse transcribed using TGIRTTM-III enzyme (InGex) under manufacturer's instructions. Briefly, RNA was incubated with an RT primer AGACGTGTGCTCTCCGATCT (0.1 μ M final concentration) and RT buffer at 85°C for 5 minutes, and cooled to 25°C at 0.1°C per second. DTT and TGIRTTM-III were added and the mixture was incubated

at room temperature for 30 minutes. dNTPs were added and the reaction was incubated at 60°C for 30 minutes. RNA was hydrolyzed by NaOH, neutralized by HCl and purified using MinElute PCR purification kit. cDNA was ligated to a preadenylated DNA adapter AppNNNNGATCGTCGGACTGTAGAACTCTGA/3ddC/ (preadenylated by 5' DNA adenylation kit (NEB)) using thermostable 5' App DNA/RNA ligase (NEB) following manufacturer's protocol (ligated at 65°C for 5 hours and heated inactivated at 90°C for 3 minutes). cDNA was purified using MinElute PCR purification kit, and amplified using KAPA HiFi HotStart PCR kit (Roche). PCR primers were AATGATAACGGCGACCACCGAGATCTACACGTTCAGAGTTC-TACAGTCCGACGATC and CAAGCAGAAGACGGCATACGAGATBBBBBBGT-GACTGGAGTTCAGACGTGTGCTCTCCGATCT (BBBBBB stands for barcode sequence). PCR products were size selected between 150 nt and 260 nt using Pippin Prep (Sage Science), and sequenced on an Illumina HiSeq under 100 bp by 100 bp paired-end mode.

2.6.6 Full transcriptome RNA-seq

For quantitative RNA-seq, 1.5 ng Firefly luciferase mRNA and 0.015 ng of Renilla luciferase mRNA was added to each cell pellet before hot phenol extraction. As each sample was derived from the same infection batch, which was distributed in equal volumes, these two luciferase mRNA spike-ins are proportional to the starting quantity of infected cells. Total RNA was treated by TURBO DNase (ThermoFisher) according to manufacture's protocol and purified using RNA Clean & Concentrator kit (Zymo Research). mRNA was isolated using the Illumina Ribozero prokaryote kit (gram positive and negative, Illumina) and was prepared into libraries using the Kapa Hyperprep kit (Roche) following manufacturer's protocols. Libraries were sequenced on an Illumina HiSeq under 40 bp single-end mode.

2.6.7 Calling modifications on tRNA sequencing data

For the dual purposes of 1. assessing whether the phage tRNA are, indeed, functional tRNA that participate in translation and 2. more accurately assigning wobble base affinities, RNA modifications were called based on reverse transcriptase substitutions. First, a reference alignment of phage and host tRNA was made. LocaRNA [88], which accounts for RNA secondary structure, was used to make a first-pass multiple alignment. Phage tRNA called with introns often aligned poorly, and so the alignments were fixed using the putative secondary structures provided by Aragorn. The variable loops were aligned separately using MUSCLE [89], then stitched back into the tRNA alignment. Next, *E. coli* tRNA from the modomics database [90, 91] were aligned to this reference in order to identify what types of post-transcriptional modifications may be present. Reads from tRNA sequencing were then aligned to this reference using the affine gap penalty method “gotoh” provided by the *align.seqs()* function in mothur, version 1.34.4 [92], with the following scoring: match=2, mismatch=0, gapopen=-5, gapextend=-1. Phage and host tRNA are sufficiently different such that reads can be mapped back to the originating organism. And finally, the base distribution at each position was then used to fit a model for how modifications correspond to “missequenced” reads (as many of these are likely the result of base substitutions inserted by the reverse transcriptase upon encountering a modified base).

2.6.8 Calculating phage RNA expression timing

Instead of classifying phage genes into distinct categories of expression timing, continuous scales were defined. Because the host RNA expression level climbs until 75 minutes, this is taken to be the timepoint before the second round of infections begin. In order to get a sense of transcription and degradation for the purposes of the analyses presented in Figure 2-3, the phage RNA expression timing was then defined as the center of mass of the expression levels over time. However, for the purposes of visually

identifying what may be transcriptional units within the genome (Figure 2-1), another measure of expression timing - the time taken to reach half the maximum level of expression - was defined.

2.6.9 Assessing Genome Degradation

Two genes were selected for qPCR to assess whether the host genome is degraded upon infection: GroEL (Genbank locus tag BCV12_01410, primers: CAATG-GATCTTAAGCGCGGC and CAGAGATAACCGTACCGCCC) and CTP synthetase (Genbank locus tag BCV12_03025, primers: CTTGGCGATCGTGGTGGT and TTTCTAATTGCCCGCGCTG). The phage genes, GroEL (Genbank locus tag NVP2275O_355, primers: CTTGAAGACATGGGCGCAC and AACGAC-TAGGGTTGCAAGCA) and the Major Capsid Protein (Genbank locus tag NVP2275O_445, primers: TGAAGGTGTTATGGGTCGCC and ATACGGGCAGTA-GAACGCAG), was also assayed for contrast. Each sample was prepared using the Kapa SYBER Fast kit according to the manufacturer's instructions.

2.6.10 Codon Usage Bias Analysis

In order to assess whether the phage tRNA pool may introduce translational bias toward its own genes, a summary statistic for each gene that represents the efficiency with which it can be translated by the phage tRNA pool, relative to the efficiency with which it can be translated by the host tRNA pool was calculated. This value, referred to as the “slant” of a gene is calculated as follows:

The codon usage preference of a tRNA pool must first be calculated. Here, it is

defined as the probability of a codon being bound given the tRNA pool:

$$\begin{aligned}
P(\text{codon}|\text{pool} = \text{host}) &= \sum_x P(\text{codon}, \text{tRNA} = x|\text{pool} = \text{host}) \\
&= \sum_x P(\text{codon}|\text{tRNA} = x, \text{pool} = \text{host})P(\text{tRNA} = x|\text{pool} = \text{host}) \\
&= \sum_x P(\text{codon}|\text{tRNA} = x)P(\text{tRNA} = x|\text{pool} = \text{host})
\end{aligned}$$

$P(\text{tRNA} = x|\text{pool} = \text{host})$ is defined as the read abundances from tRNA sequencing, normalized to each organism. $P(\text{codon}|\text{tRNA} = x)$ is defined according to revised wobble rules noted by Murphy, et al. [62, 63, 93], accounting for wobble base modifications inferred through tRNA sequencing results.

These two points define a path that the codon distribution for each protein can, essentially, be projected upon in order to calculate a tRNA pool preference for each protein. Specifically, the slant for a given gene with codon counts y , is calculated as the log likelihood ratio of observing the codons from that gene given the coding capacity of the phage tRNA pool vs. that of the host tRNA pool (divided by the number of codons, for comparability among proteins):

$$\begin{aligned}
\frac{1}{n}\Lambda(y) &= \frac{1}{n} \log \left(\frac{\frac{n!}{y_1! \dots y_k!} p_1^{y_1} \dots p_k^{y_k}}{\frac{n!}{y_1! \dots y_k!} h_1^{y_1} \dots h_k^{y_k}} \right) \\
&= \frac{1}{n} \sum_{\text{codons } c} y_c \log \frac{p_c}{h_c}
\end{aligned}$$

where $p_c = P(\text{codon} = c|\text{pool} = \text{host})$ and $h_c = P(\text{codon} = c|\text{pool} = \text{phage})$. The slant is 0 if the two multinomial probabilities are equal, which can be interpreted intuitively as the gene having equal efficiencies of coding by the pool of phage tRNA and the pool of host tRNA. A nice property of this calculation is that if y is exactly np (if the codon usage of a gene matches exactly the coding efficiency of the phage tRNA pool), then the slant is $KL(p||h)$, or the Kullback-Leibler divergence between p and h . And if y is exactly nh (if the codon usage preference of a gene matches

exactly the coding efficiency of the host tRNA pool), then the slant is $-KL(h||p)$, or the negative Kullback-Leibler divergence between h and p . However, it is possible for the slant to be less than $-KL(h||p)$ if the codon distribution for a given protein is even further away from the coding efficiency of the phage tRNA pool than that of the host tRNA pool. And likewise, the slant can be greater than $KL(p||h)$ if the codon distribution for a given protein is further away from the coding efficiency of the host tRNA pool than that of the phage tRNA pool.

2.6.11 Assessing statistical significance of codon usage bias

A one-sided Kolmogorov-Smirnov test was used to assess the difference in distributions of slant values for phage genes vs. slant values for host genes. This resulted in a suspiciously low p-value (less than 1e-22), which was taken as a signal that the null model used may not have been fair in the context of this problem, and more relevant assumptions should be specified. In this case, we must keep in mind that we already know from preliminary analyses that the distributions of codon usage between phage and host genes is different (Figures 2C and 4B), so any randomly chosen vector of phage tRNA expression is likely to betray this difference.

Instead, it is more appropriate to ask whether the slant values for phage genes vs. the slant values for host genes are different conditioning on the known codon usage distribution of the two organisms. This was done using the following resampling scheme: First, 18 tRNA (the number of phage tRNA) are randomly sampled with replacement from the host genome, then a random expression vector for these 18 tRNA was generated by normalizing exponentially distributed random variables. This expression vector was used as a random phage tRNA expression vector. Then, based on this random phage tRNA expression vector and the known host tRNA expression vector, slant values were calculated for phage and host genes, and a one-sided KS-test was conducted on these slant values. This procedure was replicated 200 times, forming

the null distribution against which the original result was compared.

2.6.12 tRNA array diversity analysis

The diversity of the tRNA pools was defined as the Shannon entropy of the amino acids encoded by the tRNA for each organism. The simulated randomly acquired diversity depicted in Figure 2-5 was calculated by sampling 18 tRNA (the number of tRNA in the phage genome) with replacement from the host genome.

2.7 Acknowledgements

We thank Uttam RajBhandary for pouring over the tRNA structures and for insights about relevant literature. We would additionally thank Jan-Christian Hütter for thoughtful discussion and comments about the analysis methods. J. Y. Yang was supported by the Department of Energy Computational Science Graduate Fellowship Program of the Office of Science and National Nuclear Security Administration in the Department of Energy under contract DE-FG02-97ER25308.

Chapter 3

Interactive visualization of high dimensional genomic data underlying bipartite graph structure in virus-host interactions

Joy Y. Yang¹, Kathryn M. Kauffman², Martin F. Polz², Libusha Kelly³

¹Computational and Systems Biology Program, Massachusetts Institute of Technology, Cambridge, Massachusetts 02139, USA

²Department of Civil and Environmental Engineering, Massachusetts Institute of Technology, Cambridge, Massachusetts 02139, USA

³Department of Systems and Computational Biology, Albert Einstein College of Medicine, Bronx, New York 10461, USA

J.Y. carried out the computational analyses and wrote the javascript visualization. K.M.K. isolated the bacteria and bacteriophage upon which this work was based. J.Y., K.M.K., L.K., and M.P. conceived of the project, designed the analyses, and wrote this manuscript.

3.1 Abstract

In this paper, we discuss methods for exploring, through interactive visualizations, possible genetic bases for successful phage host infections. The dataset we are working with consists of a binary infection matrix, or a bipartite graph, with 243 bacteria (or “hosts”) and 241 bacteriophage (or “phage,” which are viruses that infect bacteria), as well as genome sequences of all bacteria and all phage. The genomes of the bacteria can be simplified to binary predictor variables indicating the presence/absence of 10,000 protein clusters; and likewise, the genomes of the phage can be represented by 1,000 protein clusters. The questions we ultimately would like to address are - Which host proteins permit or inhibit infection by a particular phage? And which phage proteins promote or are detrimental for infection of a particular host? In most cases, we are unable to definitively identify the exact mechanism of infection or defense; however, we are sometimes able to, from a whole genome of 4000 proteins, narrow in on two or three regions of interest, in order to design future experiments targeting these promising regions. So, the questions we will instead address here are - What additional explorations/experiments do we need in order to answer the initial questions? And what further questions can this dataset inform? Bipartite graphs are common to many fields (for example, medicine - medication and cancer types - and advertising - products and users); and current technology allows us to collect more complex and larger amounts of data about each node on the graph, (referring to the same examples, transcriptomes of cancers and the mass spectrometry data of medications, or user profiles and product metadata and reviews). While this work focuses on a particular instance in the Nahant Collection, it addresses the need for tools that facilitate intuitive exploration of signals in high dimensional data on bipartite interaction networks. This visualization can currently be accessed at the following address: http://www.mit.edu/~yangjy/infection_explorer/

3.2 Introduction

In referring to observational data, Colin Mallows says “science (including statistics) is an iterative process.” [94] This is especially pertinent to the dataset discussed here. The “Nahant Collection” [28–30] is the largest genomically-characterized virus-host bipartite network available (Figure 3-1). This collection includes 243 bacterial hosts representing 19 well-characterized, ecologically-differentiated host species [31, 32], and 241 unique viruses representing 18 phylogenetically distinct groups, and 4 morphotypes. The sequenced genomes of the host can be summarized into 10,000 gene clusters, and the genomes of the phage can be summarized into 1000 gene clusters.

The diversity of this dataset presents an opportunity for asking broad ecological questions; however in trying to pin down the molecular mechanisms of infection, the correlation structure as well as the dimensionality means we are faced with many issues of confounding/non-identifiability. In a vast ocean of microbes, sampling just the right organisms with the precise combination of genetic profiles necessary to make a conclusive, causal link is highly improbable. Still, we are able to identify subsets of candidate proteins that may define the structure of the bipartite infection network. Honing in on the precise mechanisms may still require additional experiments. The ultimate goal of the interactive visualization we present here is to facilitate the process of formulating testable hypotheses about biological mechanisms based on large-scale sequencing data.

This chapter is structured as follows:

1. We introduce the biological context for the data.
2. Using a guided walkthrough approach we provide an example of how an experimentalist might interact with the visualization to generate hypotheses prioritizing the investigation of specific proteins or genomic regions for functional studies.
3. We discuss the reasoning behind the statistics used to summarize the data in

the visualization, and how it helps to prioritize relevant signals over spurious correlations

4. Because this visualization is a means of doing exploratory data analysis, we discuss additional analyses, models, and methods for approaching this data.

3.3 The biological context

Study of the interactions between viruses and their hosts over the past century has been the foundation for revealing the rules of the “Central Dogma” that defines the nature and directionality of information flow in cellular systems as well as the discovery of proteins that have been transformative for research, medicine, and bioengineering , including restriction enzymes, Hfr conjugation, transposon mutagenesis, and CRISPR-Cas [13]. There is therefore great interest in identifying additional mechanisms that make up the genomic underpinnings of virus-host interactions. Analyses of growing viral genome databases have revealed that the total number of phage protein clusters has been growing with each sequenced phage genome, without signs of saturation [95], and on average approximately 70% of predicted proteins in phage genomes are of unknown function [11]. There is thus a major need for tools that can guide the prioritization of protein candidates for experimental functional studies. To address this need, we present a tool for exploratory data analysis to aide in the identification of candidate proteins for experimental study in the context of the Nahant Collection. The fine-scale phylogenetic resolution of this dataset offers the opportunity to identify mechanistic underpinnings of the observed interactions and to experimentally validate the roles of specific proteins in these interactions.

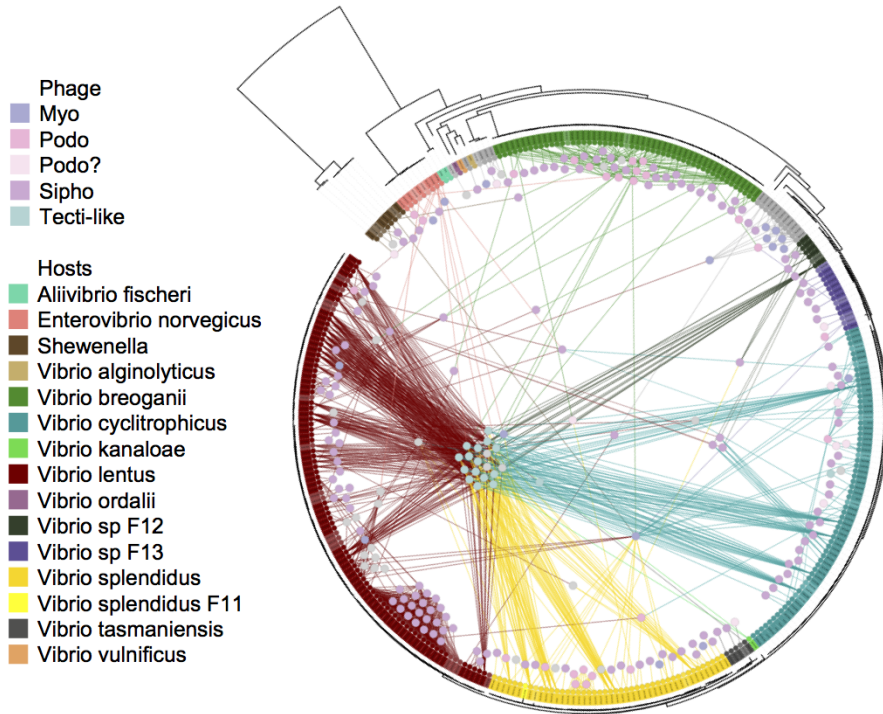


Figure 3-1: Depicted here is the bipartite graph representation of the infection data. The hosts (arranged along the leaves of the circular tree) hail from ecologically differentiated populations; the phage (nodes within the circle) are also genetically and morphologically diverse.

3.4 A guided walkthrough of the visualization

A problem that phage researchers will commonly seek to address is to, upon selecting a phage of interest, identify proteins in hosts that are either positively or negatively associated with infection. Positive associations may be suggestive of proteins that permit infection, for example, membrane receptors on hosts that phage can latch onto, and negative associations may be suggestive of proteins that inhibit infection, for example, restriction modification systems that digest the phage genome once it is injected into the host cell.

The visualization has three main “div”s, or containers, tiled vertically. On first navigating to the page, only the first div 1, the phage-host infection matrix, is loaded. We start by selecting a particular phage from the infection matrix whose infection

profile will be matched against host proteins in order to identify host proteins that are either positively associated with (may permit) or negatively associated with (may inhibit) infection. Then a host genome can be selected on which to display the negative log of the regression p-values to create, in essence, a linkage map [96]. (A more detailed discussion of how these values are calculated will be presented in the following section of this paper.) To illustrate the logic of the flow described, we walk through an example where we would like to identify host proteins that may inhibit a particular phage infection. Because the screenshots here only convey a rough sense of interaction with the data, we encourage the reader to follow the example on the site: http://www.mit.edu/~yangjy/infection_explorer/

3.4.1 Div 1: Selecting a phage for finding host proteins that may allow or protect against its infection

The infection matrix (Figure 3-2) is displayed immediate upon navigating to the visualization. Here a row (a phage) can be selected. Upon mouseover, a row is highlighted in order to emphasize the infection profile of that phage. In this example, we'll select phage 1.089.O. This particular phage is able to infect 3 closely related hosts that belong to a "microclade" of 5 very closely related *Vibrio lentus* bacteria but cannot infect the 2 other hosts in this clade. This leads us to wonder whether there may be signatures of defense genes in these two uninfected hosts that inhibit the infection.

3.4.2 Div 2: Selecting a host genome for identifying candidate proteins that inhibit infection

Upon clicking phage 1.089.O, the page scrolls down to the next div (Figure 3-3), which becomes populated with another matrix. Here, as with the infection matrix,

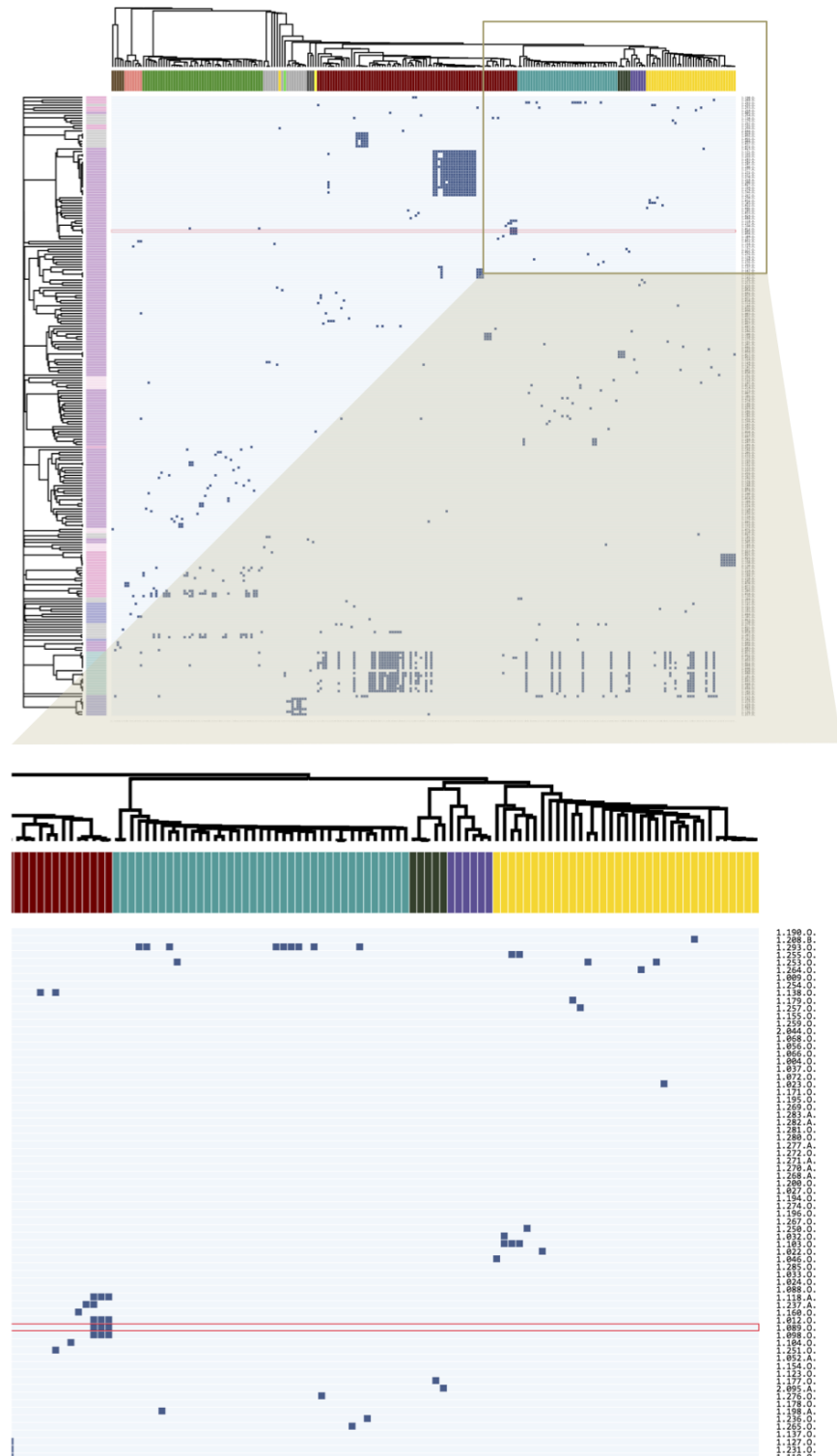


Figure 3-2: Div 1 infection matrix and zoom in. The working example of phage 1.089.O. is shown selected.

each column represents a host; but now, each row represents a host protein cluster. A cell in the matrix is filled if the host in that column carries the protein in that row. The host proteins are sorted by their p-values as determined by generalized least squares regression against the infection profile of phage 1.089.O. This technique is further described in the Methodological Notes section below. The colorbar on the left indicates the effect direction, blue for positive, and red for negative, making it easy for users to distinguish genes that enable infection from those that prevent infection. This plot summarizes the distribution of proteins among hosts in order to facilitate visual comparison of host protein profiles against the phage infection profile. From this plot, any host (column) can be selected. For this example, we'll select host 10N.261.52.C5 (referred to as "host A" from here). This host is one of the two within the "microclade" that cannot be infected by phage 1.089.O to examine any inhibitory features that may exist.

3.4.3 Div 3: Exploring the Manhattan plot to find candidate proteins that may allow or inhibit infection

On selecting host A, the page scrolls to the last div (Figure 3-4), which becomes populated with a genome diagram of the host. The x-axis is genome location, and the y-axis is the regression score. In the main canvas, the length of the boxes plotted are scaled according to the length of the genes, and in the brush region, each gene is plotted as a point at the gene midpoint. The brush region can be used to zoom in on a position of interest along the genome, and the scrolling up and down in the canvas region results in zooming in and out. These functionalities are adapted from Mike Bostock's S&P 500 Brush and Zoom example [97]. There appear to be three main regions in host A's genome where proteins highly associated with infection are co-localized. The effect direction in all three of these regions is negative, or appears to be protective against phage infection. This makes sense as we selected a bacterial

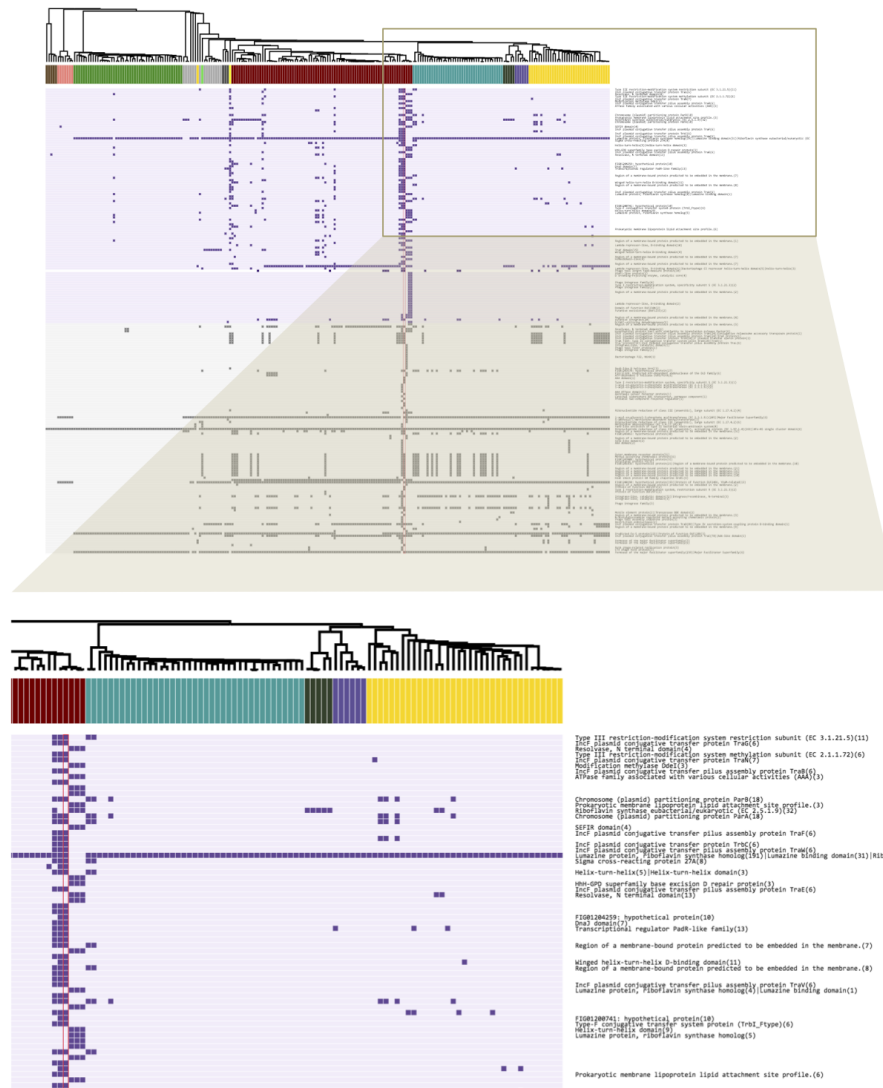


Figure 3-3: Div 2 gene summaries and zoom in. The working example of host host A is shown selected.

strain that is not infected by 1.089.O. In this way, we can rapidly identify phage genes that protect against infection.

The first region carries a phage tail assembly gene as well as a bacteriophage repressor gene, likely indicating a virus that has established latency in host A. Perhaps it now participates in host defense to protect from further infection. This is an ecological process known as “competitive exclusion” [98]. There does not appear to be a protein annotated clearly with a known defense function; however, a possible

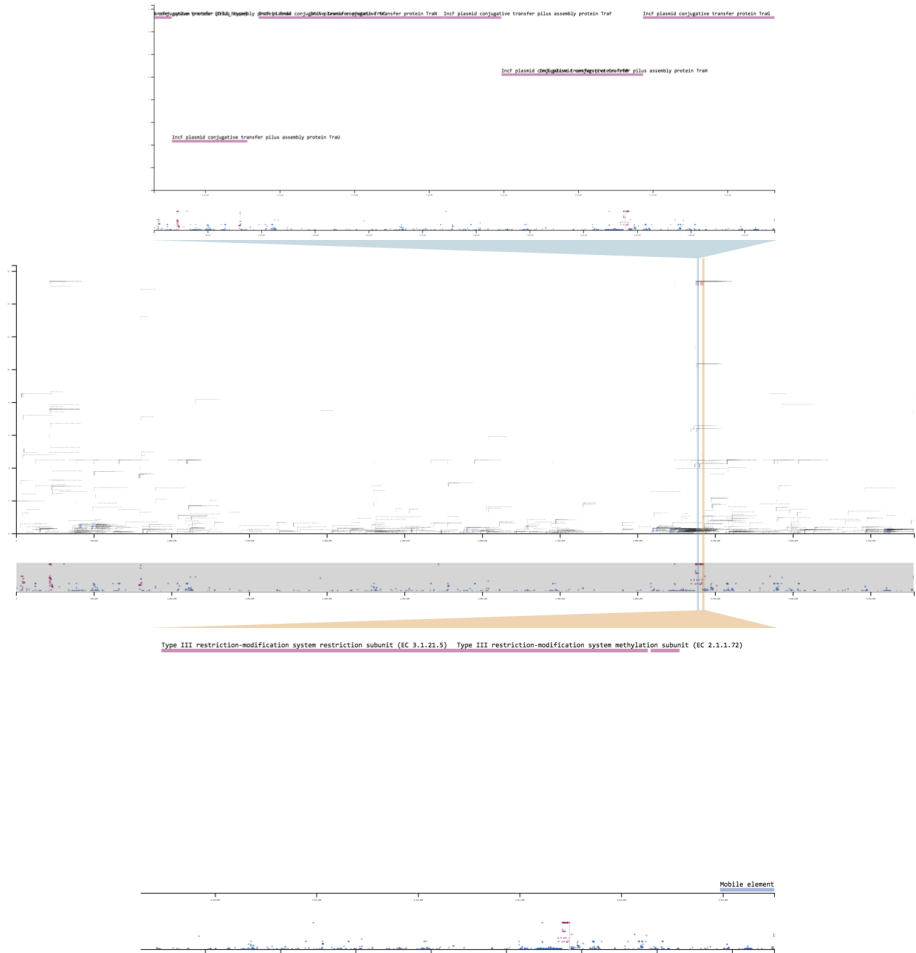


Figure 3-4: Div 3 and brush selection examples. The two zoomed-in views lie on region 3, the first shows the conjugative transfer element annotations, and the second shows the Type III restriction modification system genes.

inhibitory mechanism can simply be competition. If this phage, which is capable of latency, is able to replicate more quickly upon infection by phage 1.089.O, then it may be able to suppress the killing phenotype of 1.089.O.

The second region carries a phage tail tape measure protein and integrases. This region may be another virus, which was able to integrate itself in the host A genome. We do not observe a protein annotated with a defense function here either; however, again, we cannot rule out competition.

The last region is a mobile plasmid that comes equipped with genes that enable it

to induce its bacterial host to form a pilus and transfer the element to another cell. Additionally, this plasmid carries a Type III restriction modification system, which places markers on native DNA and recognizes/cuts up foreign unmarked DNA. This plasmid has likely picked up this defense system along the way, and now earns its keep in its host by defending the cell against invasion by foreign DNA.

Which of these hypotheses is/are true? Because the third region has an annotated defense system, we are more inclined to believe this as being the active agent of defense; however, it's worth noting that many of the proteins in all three regions are unannotated (have unknown functions). And because the protein profiles in these three regions are co-linear, we cannot rule out any of the regions as participating in defense, and it could be possible that they all participate to some degree. A more targeted experiment is needed to hone in on the precise region(s) involved in protecting this bacteria from infection. [Please see the following subsection on experiments for discussion of possible experiments that can be done.]

3.4.4 Backtracking to Div 2: Selecting a genome for identifying candidate proteins that permit infection

Next, we turn to an example that focuses on how to identify proteins in hosts that appear to permit infection by phage. Keeping phage 1.089.O as an example, let's return to div 2, and select the 10N.261.51.F9 ("host B") genome. Div 3 is wiped clean and replaced with a new genome diagram. We see here that the majority of proteins associated with infection are co-localized in a genomic region that seems to be associated with DNA modification and repair. While it's possible that this aids the bacteriophage infection process in some way, a more likely hypothesis is that this element is incompatible with one of the elements described in the previous section. For example, perhaps the repair mechanisms conferred by proteins in this region conflict with other remodelling mechanisms in the protective region(s) of host A, making the

genome susceptible to 1.089.O infection. The implication here is that while this region may not functionally make its bacterial host susceptible to infection, it may perhaps be indirectly allowing infection by excluding elements that exclude phage 1.089.O. This, however, is again only a hypothesis, and requires additional experiments to verify.

3.4.5 Designing experiments based on hypotheses suggested by this visualization

We wish to characterize the third region in host A, the plasmid carrying a conjugative transfer pathway, protects the host against infection by phage 1.089.O. We can, using genome recombineering strategies, attempt to delete the element from the host genome, or, because maintaining elements accessory to core cell functions comes at a fitness cost to the host, we can passage the host and look for daughter strains that may have lost the element.

If we are able to obtain a host with element 3 deleted, and it is susceptible to infection by 1.089.O, this suggests that element 3 was important for defense against the phage. We can further validate this genome region as being a defense element by inserting a synthetic version of element 3 into the deletion host and testing whether this new host is once again protected from infection.

We may also wish to test whether elements 1 and 2 participate in infection and can attempt to make combinatorial deletions.

To provide a contrasting example, let's say that we select phage 1.025.O, and set off to find proteins in its hosts that are permissive of infection. Because all of the hosts of this phage are extremely closely related, without a closely related host that is resistant to infection, it is incredibly difficult to hone in on a handful of promising targets, as we lack the appropriate data. Because these hosts are so closely related, and there are too many collinear candidates. Therefore, to accomplish this task we

may want to experimentally evolve the hosts until we find resistant strains. Then, from here, we can conduct additional statistical analyses, and continue to iterate between experiments and analyses.

3.5 Methodological notes

3.5.1 Regression results depicted

Our data cannot be considered to be independent and identically distributed. Bacteria and viruses in the ocean evolve, migrate, and share genes (like any other living organism), and so their genomes are correlated by nature. Each bacterial or viral strain’s population can boom or bust based on the environmental conditions, nutrients, and predators. Hence in taking a bucket of water from the ocean, the organisms in this bucket cannot be thought of as being statistically independent. Ignoring phylogenetic relationships can result in relevant signals being drowned out by spurious correlations.

To address this issue, we’ve employed phylogenetic generalized least squares [33]. This is equivalent to “whitening” in signal processing. The idea is to infer the covariance structure among the organisms, then “whiten out” the correlated errors by simply multiplying both the predictor and the response by the inverse square root of the covariance matrix.

$$Y = X\beta + \epsilon$$

$$\Sigma^{-1/2}Y = \Sigma^{-1/2}X\beta + \Sigma^{-1/2}\epsilon$$

$$\tilde{Y} = \widetilde{X}\beta + \tilde{\epsilon}$$

$$\begin{aligned} cov(\tilde{\epsilon}) &= \Sigma^{-\frac{1}{2}}\epsilon\epsilon'\Sigma^{-\frac{1}{2}}' \\ &= \Sigma^{-\frac{1}{2}}\Sigma\Sigma^{-\frac{1}{2}}' \\ &= I \end{aligned}$$

To illustrate the necessity of this correction with an example, Figure 3-5 contrasts associations identified by simple ordinary least squares (OLS) and phylogeny-corrected generalized least squares (GLS) regressions. Here, phage proteins are regressed against the phage infection profiles, as tested against one particular host. The most striking difference here are the negative effects identified by each method. OLS identifies genes that are present in one particularly clonal (or closely related/oversampled) group of phage that cannot infect the host of interest. As an analogy, this would be similar to identifying all variations present in a large family of 18 siblings as being protective against a genetic disease that is present in a member of a different family. While these genetic variations have been observed in 18 people, the people are all very closely related (are oversampled), so the effects of these variations are overestimated, as they are confounded by population structure. In contrast, GLS identifies genes that are present in strains closely related to the infective population that are not themselves infected. To continue with the analogy, this is similar to identifying a genetic variation present in the healthy twin of a patient as being protective against a disease. Even if this twin is the only observed subject with this variation, we may still feel justified in our suspicions, because the subjects are matched.

3.5.2 Implementation details

The visualization was written using javascript to assure accessibility for a wide audience. It relies heavily on the D3 library [99] as well as the many beautiful working examples from Mike Bostock.

An attempt to use the out-of-the-box Plotly-R function to display the infection matrix (~60,000 cells) was very slow. So because the matrices of phage-host infections, phage proteins, and host proteins are each sparse, in order to optimize speed and responsiveness, taking a leaf out of the book of coordinatewise sparse encodings, we display only the non-zero values of the matrices.

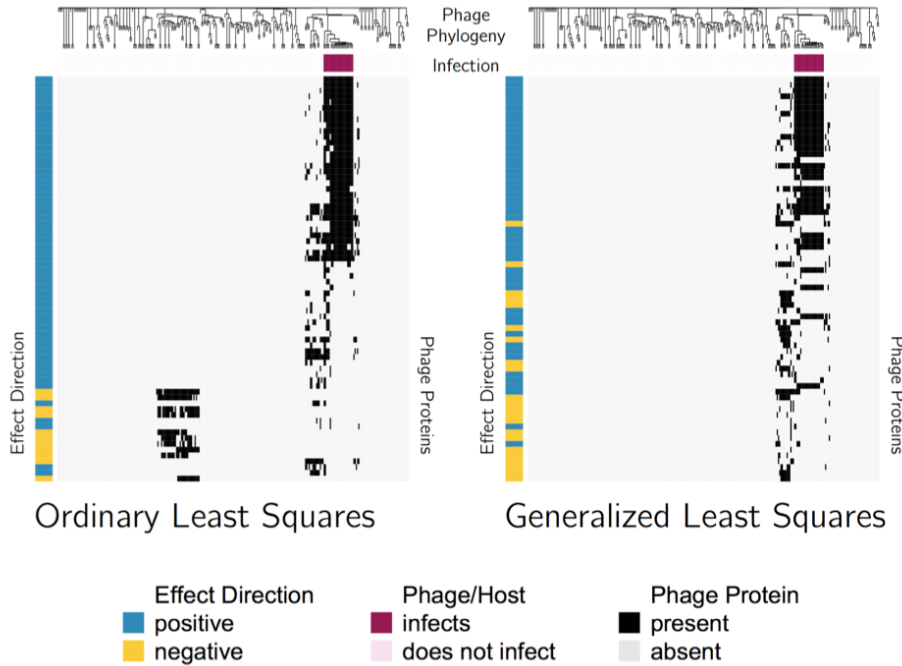


Figure 3-5: Profiles of the top 100 phage proteins found to be associated with ability to infect a particular *Vibrio lentus* host. The columns represent phage genomes, and are ordered according to phylogeny, as depicted by the dendrogram. The black lines immediately below the dendrogram indicate the strains of phage that were able to infect the host of interest. On the heat map, red indicates absence of the protein in a particular phage, while off-white indicates presence of the protein. The color bars on the left indicate whether the effect is positive (blue), or negative (orange).

And to further optimize responsiveness of the visualization, regression results are precomputed. And for purposes of providing a concise summary of the results as well as to keep the browser from having to load too much data, in div 2, only a subset of the results are displayed. The number of proteins displayed is $\max \{200, n_{holm}\}$, where n_{holm} is number of proteins selected by the Holm procedure for controlling familywise error rates. The Holm procedure was used as to allow us to set the number of tests. Proteins selected by the Holm procedure are plotted in a purple background, and the rest are plotted in a grey background.

The visualization code will be available on Github ([kellylab](#) and [polzlab](#)).

3.6 Discussion and future analyses

With a large dataset such as the Nahant Collection, it can be difficult to pin down a hypothesis, because there are too many candidate hypotheses to draw from. Which of these hypotheses do the data suggest may be the most promising? What data are relevant for addressing these hypotheses? Which experiments must be done/are feasible?

We have present a simple technique for using interactive graphics to enable intuitive exploration of the high dimensional genomic data associated with this bipartite graph. We hope that it will have some utility for beginning to address these questions.

A more holistic model should capture the generally lock-and-key nature of infection specificities due to protein interactions (for example, a specific methylase may evade a specific restriction modification system). And, instead of whitening the correlated errors, we could employ a multivariate model, which accounts for population structure through conditioning on all other genes.

Chapter 4

Conclusion

Because phage-host studies are generally aimed at identifying many phage that infect a clonal group of hosts, or many hosts that are infected by a small set of phage; up until now, there is perhaps only one dataset [100] that encompasses both polyclonal phage and host populations. The data is not accompanied by any form of molecular information, and so it is limited in its ability to provide insight into the precise mechanisms from which the infection structure arose. The Nahant Collection [28–30] is very unique in being a complete cross test accompanied with sequenced genomes, from which we can derive mechanistic hypotheses; as well as archived samples, with which we can test these hypotheses.

In chapter 2 of this thesis, we focused in on a specific phage in the Nahant Collection, 2.275.O, to characterize the pressures that may select for phage that shuttle their own translational machinery. We were able to conclude that while encoding translation-related components requires shuttling a larger phage genome, it also reduces dependence on host translational machinery, allowing the phage to be more aggressive in degrading and recycling the host genome and other resources required for replication.

This investigation illuminated many other paths that we believe could be fascinating

for future exploration. For example, from TGIRT substitutions, we called base modifications, assuming a multinomial distribution of base counts. However, there is a layer of complexity that we were not able to unroll - the distribution could have been a mixture of nascent tRNA and modified species. And in fact, in a tangential exploration examining the unique tRNA reads, we observed a succession pattern in the tRNA species during the course of infection. One question arising from this observation is a methodological one: is it possible to deconvolute the mixture of base substitutions from the mixture of tRNA species by incorporating data from, for example, mass spectroscopy (a gold standard for identifying chemical compounds) or nanopore direct RNA sequencing (this technique has recently been demonstrated [101] and there is some excitement about the potential for direct detection of nucleotide modifications)? If so, we would be able to paint a clearer picture of exactly which tRNA species are present during various stages of the infection. This has applications beyond bacteriophage, as there is currently an ongoing line of research into the role of tRNA through “adaptive translation” during various forms of stress response. Another question that arises is along the same train of thought as “adaptive translation.” Do the different species of the same tRNA have different roles? Are some species activated or inactivated by the modifications that are present? Exciting new technologies for probing translation now exist, such as ribosomal footprint profiling [85], tRNA-ribo-seq [86], charge-seq [102], etc. Work in combining these techniques with phage growth experiments may be a promising future direction for uncovering further insights into translation.

Another tangential analysis we conducted was to examine the host expression profile throughout infection. While essentially the entire host transcriptome is degraded, we do observe three main outlier groups. It would be interesting to conduct additional trials in order to determine variation around these expression characteristics. And next, it may be of interest to do a closer exploration of the function and structure

of these transcripts. For example, one group of outliers consists of transcripts that appear to be degraded more quickly than the average transcript. What makes them susceptible? Are they specifically targetted by the phage for degradation? Another group of outliers consists of transcripts that initially increase in abundance, and then are rapidly degraded. These tend to be stress response genes. Do these genes participate in tuning down phage infection? If they are knocked out, does this result in a more successful infection phenotype (perhaps an increase in burst size or decrease in latent period)? If this experiment is repeated in the same host with different phage, could different stress response pathways be triggered?

In chapter 3, we developed a systematic approach for uncovering genomic features that underlie phage-host interactions. We found that correcting for phylogenetic relationships allows us to pick out relevant signals that would otherwise be drowned out by spurious correlations resulting from statistically oversampled blooms of microbes. Using these results, we wrote an interative javascript visualization to facilitate the process of developing testable hypotheses concerning the mechanisms of phage infection and host response. From the visualization, we are able to identify, in the hosts, mobile genetic elements containing restriction modification systems that may defend against infection, as well as membrane protein modifications that may serve as phage attachment sites.

This analysis was not, by any means, the most obvious path. There were many somewhat promising routes that we wandered down but could find no obvious means for inferring biological insight through. For example, initially we sought to predict the matrix of infections by using the genetic data. One problem that we encountered was that a reasonable model should capture the generally lock-and-key nature of infection specificities due to protein interactions. For example, a specific methylase may evade a specific restriction modification system. However, with 1000 phage protein clusters and 10,000 host protein clusters, this meant we had in total, 10 million possible

interaction terms. So there was also a conundrum about whether it was necessary to encode a $60,000 \times 10,000,000$ matrix of predictors (60,000 being approximately 241 x 243, the dimensions of the infection matrix). Ultimately we were able to utilize a trick called alternating minimization, which is elaborated further in the appendix. Another technique we employed was to conduct an initial step of screening, then using the most promising protein profiles for the final stage of prediction. However, both methods suffered from the same drawback in that the results lacked interpretability. We were able to see some promising results through examining the outer products of the decomposed matrix of interaction coefficients, and this may be a promising direction for future exploration.

Then, of course, because the goal of the visualization we presented in chapter 3 was for the purpose of generating testable hypotheses, there are many hypotheses suggested by this visualization that we hope may eventually be tested. For example infection by phage 1.293.O is very positively associated with the presence of a pyruvyl polysaccharide transferase protein. Could this be a membrane protein modification that serves as an attachment site for the virus? If so, deleting the gene from a host or inserting the gene into a non-host should be able to change the microbes' infection susceptibility. Or, a couple of proteins strongly negatively associated with infection by 1.159.O, 1.028.O, and 1.219.O are annotated as participating in programmed cell death. Could this be a "protect your neighbors" host defense? If so, these genes should be seen to be expressed early in the infection. And finally, there are numerous prophage-like islands and conjugative transfer elements, often associated with various forms of restriction modification systems that are sometimes positively and sometimes negatively associated with infection. This leads us to believe that there may be a network of competitive exclusion (and potentially, cooperation) among these elements. This could be a particularly tricky hypothesis to test, as it may involve making a carefully crafted combinatorial library of various mobile elements.

Work on phage-host interactions from the last century has lead to the discovery of important insights into the central dogma as well as the development of impactful technologies such as restriction enzymes, Hfr conjugation, transposon mutagenesis, and CRISPR-Cas [13]. Still, on average approximately 70% of open reading frames in a phage are unannotated hypothetical proteins [11]. We are excited to see what future research may unfold.

Appendix A

Predicting Phage-Host Interactions Using Alternating Minimization

Joy Y. Yang¹, Libusha Kelly², Martin F. Polz³, Philippe Rigollet⁴

¹Computational and Systems Biology Program, Massachusetts Institute of Technology, Cambridge, Massachusetts 02139, USA

²Department of Systems and Computational Biology, Albert Einstein College of Medicine, Bronx, New York 10461, USA

³Department of Civil and Environmental Engineering, Massachusetts Institute of Technology, Cambridge, Massachusetts 02139, USA

⁴Department of Mathematics, Massachusetts Institute of Technology, Cambridge, Massachusetts 02139, USA

J.Y. carried out the analyses under the guidance of L.K., M.P., and P.R. P.R. conceived of the methodology for applying alternating minimization to this problem.

Note: The following analysis was done without the use of sparse matrices, partially as a first pass, and partially due to the need to separately rescale the matrices V and H (the virus protein matrix and the host protein matrix). However, using sparse matrix encodings would even further reduce memory requirements, and a clever application of the Sherman-Woodbury-Morrison formula should allow us to compute an equivalent solution as that having rescaled V and H accordingly.

A.1 Abstract

In order to address memory constraints, we have applied alternating minimization to a particular formulation of regularized logistic regression. Here, the model predicts edges on a bipartite graph where the number of predictor variables associated with each node is greater than the total number of nodes in the graph.

More specifically, we have a binary infection matrix with 243 bacteria (or “hosts”) and 241 bacteriophage (or “phage,” which are viruses that infect bacteria), as well as genome sequences of all bacteria and all phage. The genomes of the bacteria can be simplified to binary predictor variables indicating the presence/absence of 10,000 protein clusters; and likewise, the genomes of the phage can be represented by 1,000 protein clusters.

And as infection specificities involve interacting factors between organisms, a more realistic model requires using interaction terms between phage and host proteins. This means 10,000,000 possible interaction terms for the 58,000 observations. With centered and scaled predictors, this amounts to approximately 4.7 TB. Alternating minimization allows us to reduce the memory requirements to around 14 GB.

A.2 Introduction

Work on phage-host interactions from the last century has lead to the discovery of important insights into the central dogma as well as the development of impactful technologies such as restriction enzymes, Hfr conjugation, transposon mutagenesis, and CRISPR-Cas [13]. Still, analysis of phage genomes has revealed that the number of phage orthologous groups (protein clusters) has been growing with each sequenced phage, without signs of saturation [95]. On average approximately 70% of open reading frames in a phage are unannotated hypothetical proteins (predicted proteins with unknown function) [11]. This vast unknown may hold exciting prospects for future research. The Polz Lab maintains the Nahant Collection [28], which consists of 243 *Vibrio* strains challenged by 241 unique phage, all with sequenced genomes. This is the largest phylogenetically-resolved host range cross test available to date. These host strains match to 19 well-characterized populations that have been shown to be coexisting but ecologically differentiated. For example, *Enterovibrio norvegicus* are primarily free-living, *Vibrio cyclitrophicus* are large-particle specialists, *V. tasmaniensis* and *V. splendidus* are generalists, and *V. breoganii* are algal-degradation specialists and form biofilms [31, 32]. The phage fall into around 18 phylogenetically distinct groups; have diverse infection strategies, with both broad and narrow host-range phage; and have distinct morphologies, with representatives from nontailed (*Tectiviridae*), and tailed (*Podoviridae*, *Myoviridae*, and *Siphoviridae*) morphotypes.

This is a rich dataset that offers the opportunity to glean mechanistic insights from sequencing data. Our ultimate goal is to generate hypotheses about which proteins may be involved in the infection process. Traditional GWAS-like (genome wide association) methods involve running multiple regressions of the response variable against each predictor variable. The interpretation of each coefficient in this technique only captures the covariance of the response variable with each predictor. We are interested in using a multivariate model that regresses the response variable against all

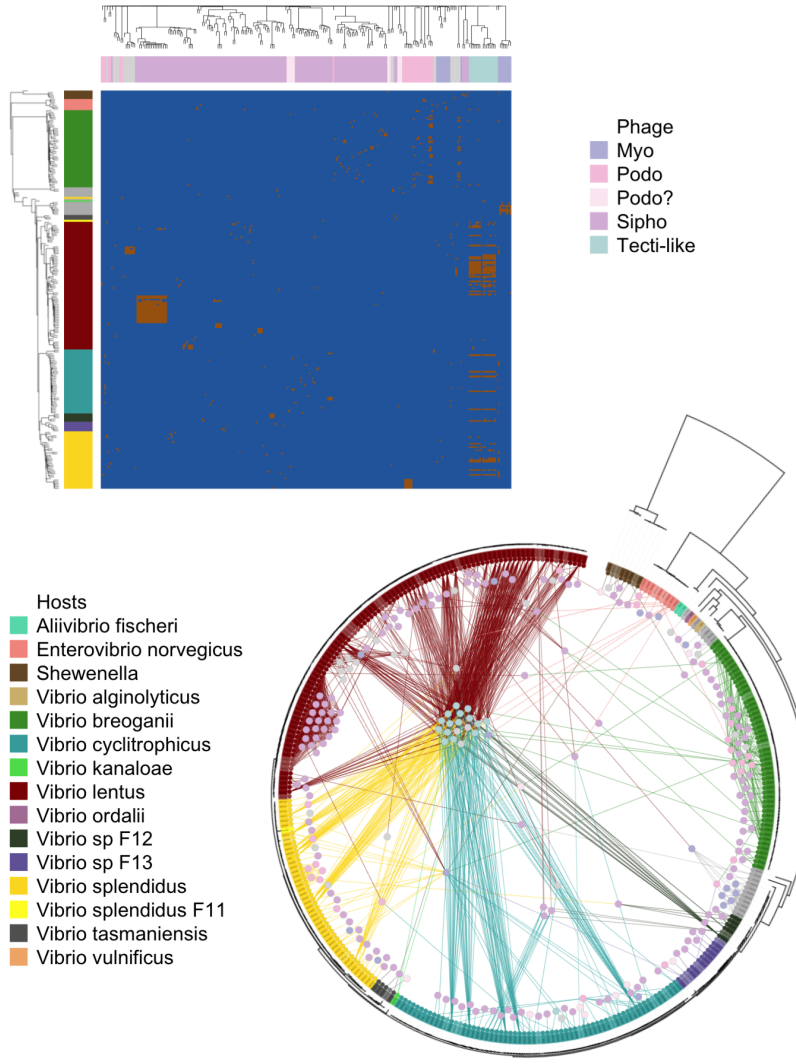


Figure A-1: Depicted here are two representations of the infection data. One in matrix form, and the other as a bipartite graph. The hosts hail from ecologically differentiated populations; the phage are also genetically and morphologically diverse.

predictor variables. Here, the interpretation of the coefficients captures the covariance of the response variable with each predictor conditioned on the other predictors. The multivariate model also allow us to address the problem from the infection prediction perspective.

However, the challenge is that, as infection specificities involve interacting factors between organisms (for example, a specific methylase from a phage may evade only a specific restriction modification system from a host), the model should include

interaction terms between phage proteins and host proteins. With approximately 1000 distinct phage gene clusters and 10,000 distinct bacterial gene clusters, there are 10,000,000 possible interaction terms for the 58,000 observations. This 58,000 x 10,000,000 interaction matrix is roughly 4.7 TB.

A.3 Methodology

To model the infection data based on the phage and host genomes, we use logistic regression:

$$vec(Y) \sim Bern(\mu)$$

$$\text{logit}(vec(\mu)) = \beta_0 + X^v \beta_1 + X^h \beta_2 + X^{vh} \beta_3$$

Here, Y is a n_v (number of phage) by n_h (number of hosts) matrix of 0/1 values that indicate whether a given phage is able to infect a given host. Here, it is vectorized in order to facilitate the regression. X^v is a $n_h * n_v$ by p_v (number of phage proteins) matrix. It can broadly be interpreted as a matrix of predictors representing virus proteins. More precisely, each column X_i^v is $\text{vec}(V_i \otimes 1_{nh})$, where V is a n_v by p_v matrix of phage proteins, and \otimes is the kronecker product. Kronecker products of two vectors are simply vectorized outer products; this notation greatly simplifies matrix representations mentioned later in this paper [103]. Similarly, X^h is a $n_h * n_v$ by p_h matrix of host proteins, which can broadly be interpreted as a matrix of predictors representing host proteins. Each column X_i^h is $\text{vec}(H_i \otimes 1_{nv})$, H is a n_h by p_h matrix of host proteins. And finally, X_{vh} is a $n_h * n_v$ by $p_h * p_v$ matrix of phage-host interaction terms $\text{vec}(V_i \otimes H_j)$.

Note that this regression can also be written as

$$Y \sim \text{Bern}(\mu)$$

$$\text{logit}(\mu) = VMH'$$

Where M is a p_v by p_h matrix of regression coefficients. To be precise, here, the columns of V and H are augmented by a vector of 1s to represent the lower order terms and intercept. As before, in order to solve for M , it is necessary to compute a matrix of predictors $H \otimes V$, which is approximately of size 58,000 x 10,000,000 ($n_v \times n_h \times p_v \times p_h$). If M is decomposed into AB' , we now have

$$\text{logit}(\mu) = VAB'H'$$

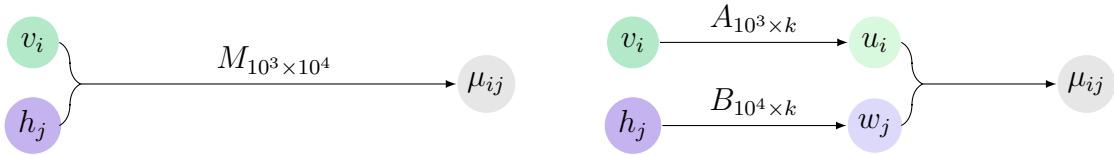
Where A is p_v by k and B is p_h by k , k being the rank of the matrix M . We can constrain k to a low value and apply alternating minimization to make this regression problem more feasible. In alternating minimization, the matrix in question, here our matrix of coefficients M , is written in bilinear form, here AB' . A low rank assumption is made, then the alternating steps are solving for A while holding B fixed, and solving for B while holding A fixed. This process is then iterated until convergence.

A particularly notable application of low rank matrix completion was in the winning solution of the Netflix Challenge [104–106]. A nice parallelism to our problem exists in this challenge of drawing edges between users and movies. However our problem additionally comes informed with predictors which would be similar to having detailed demographic information about the users and detailed genre and casting information about the movies. Therefore, continuing with the analogy, the matrix to be completed in our problem is not the users by movies matrix, but rather the matrix of coefficients describing the interactions of demographic and genre.

A question arises: is the low-rank assumption fair for our problem/data? Because

proteins often act as part of a pathway (for example, there can be multiple proteins acting as part of a restriction modification system), vectors of coefficients may be highly correlated, and so the low rank assumption is justified.

To detail the application of alternating minimization to our logistic regression model, in order to solve for A, it is necessary to compute a matrix of predictors $BH \otimes V$, which is of size $58,000 \times 1,000 \times k$ (for $k=3$, this is roughly 1.4 GB). And to solve for B, it is necessary to compute a matrix of predictors $H \otimes VA$, which is of size $58,000 \times 10,000,000 \times k$ (for $k=3$, this is roughly 14 GB). For low k , this is a much less expensive problem to solve in terms of memory. A visual schematic emphasizing the difference between the two methods is depicted below.



Solve for	Predictors	Size	Memory
M	$H \otimes V$	$5.8e4 \times 1e7$	4.7 TB
A	$HB \otimes V$	$5.8e4 \times 3e3$	1.4 GB
B	$H \otimes VA$	$5.8e4 \times 3e4$	14 GB

A.4 Implementation and tuning

The dataset was first trimmed down to a more manageable subset of 60 phage proteins and 112 host proteins by performing a first round of lasso with only phage proteins as predictors, then another round of lasso with only host proteins as predictors. To avoid reimplementing regularized logistic regression, the *glmnet* package in R was used. In this smaller problem, the summary table of expected memory usage is as follows:

Solve for	Predictors	Size	Memory
M	$H \otimes V$	$5.8e4 \times 6893$	3.2 GB
A	$HB \otimes V$	$5.8e4 \times 183$	85 MB
B	$H \otimes VA$	$5.8e4 \times 336$	156 MB

A.4.1 Initialization

On a subset of 60 phage and 112 host proteins, M can be computed directly. A smart way to initialize the matrices A and B would then be to take the singular value decomposition of M. This initialization was used as a first step in implementing alternating minimization, because starting with values that should be much closer to optimal than random would eliminate initialization as a possible source of failure in implementation.

Because the goal is to use alternating minimization as a means for working with the entire dataset, which we currently cannot do because of memory constraints, ideally, we would like to not need to directly solve for M. The question is then, would random initialization perform just as well? It turns out that random initialization converges at the same rate as SVD initialization (Figure A-2, and reaches the similar likelihoods. This bodes well for generalizing the method to the full dataset.

A.4.2 Scaling A and B

Because $VAB'H'$ is the inner product of $A'V'$ and $B'H'$, if each predictor variable in V and H are centered and A and B are scaled appropriately, A and B effectively project the phage and the host, respectively, into a k dimensional space, where the angle between phage and host that interact are low (or the correlation is high). Therefore, if k is constrained to 2 or 3, $A'V'$ and $B'H'$ can also be used for dimensionality reduction and visualization purposes.

This geometric interpretation is somewhat thrown off by the included intercept

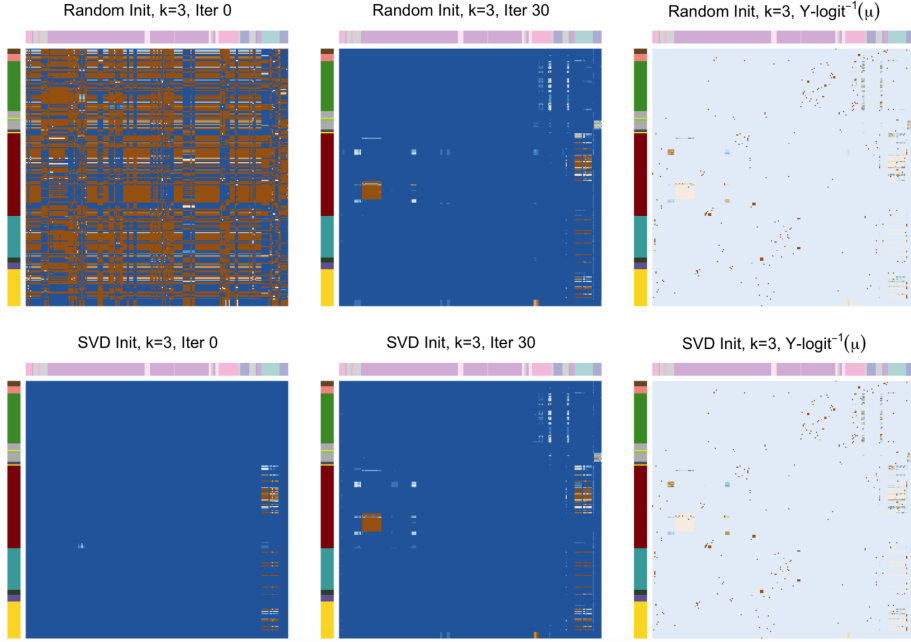


Figure A-2: Initializing A and B randomly performs comparably to initializing with the SVD of M , indicating that random initialization could still be a reasonable strategy when working with the entire dataset.

variables in V and H , which centering would render ineffectual. However, empirically, for solutions of A and B which are orthogonalized after each iteration, the first dimension always represents the intercept term. With the offset removed from the remaining dimensions, the geometric interpretation is again recovered. (Figure A-3)

In a sense then, this is similar to canonical correlation analysis [107], in which a rotation matrix is chosen for a multivariate set of predictor variables and another rotation matrix is chosen for a multivariate set of response variables in order to maximize the correlation, or minimize the angle, between corresponding rows of predictors and their responses in the first k dimensions. To make this more concrete, a commonly used real-world example is relating multivariate genomic data (each patient has many genomic variation, or colloquially, mutation) to multivariate health metrics (each patient is also associated with records of height, bmi, disease status, etc.). The difference is that there isn't a one-to-one relationship between hosts and phage. It's possible for a host to be susceptible to many phage, and it's possible for a phage to

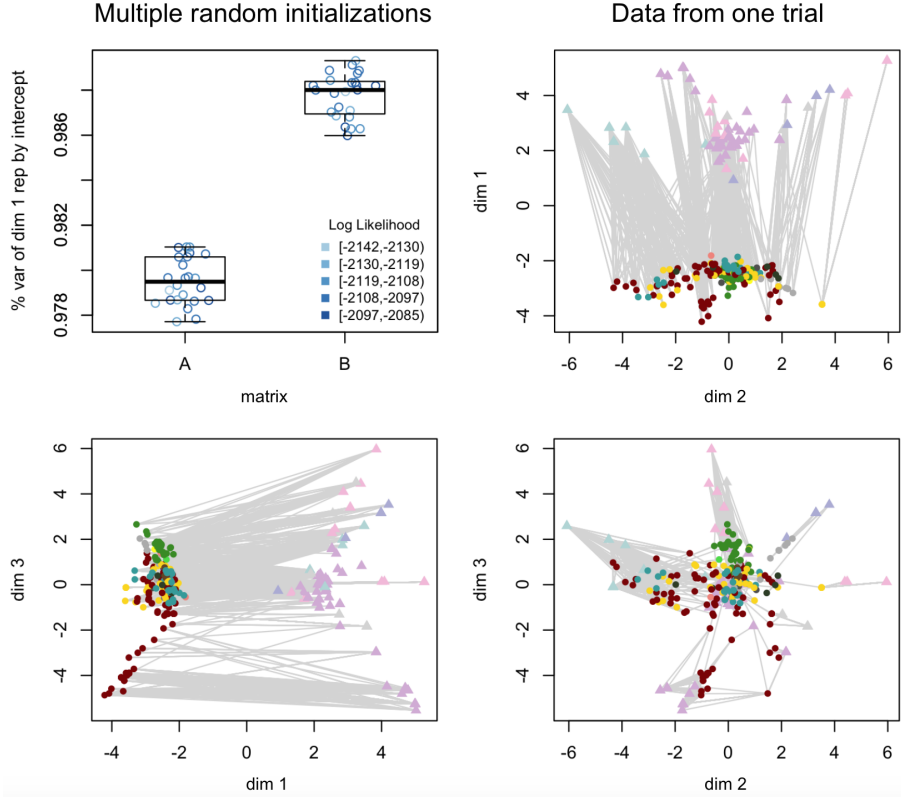


Figure A-3: When the rank of the coefficient matrices is set to 3, A and B project the phage and host genomes into a 3D space. The first dimension empirically always corresponds to the intercept. Proximity of phage and hosts in the second and third dimensions roughly corresponds to the success of infection. In this figure, the colorscheme is the same as that from before, and to emphasize the difference in organism type, phage are plotted as triangles while hosts are plotted as circles.

be able to infect many hosts.

A.5 Performance engineering results

All analyses in this paper were performed using the R programming language [108]. In order to assess whether these back-of-the-envelope memory calculations hold, we profiled the code using *Rprof()*, a sampling profiler, *Rprofmem()*, which records memory usage each time memory is allocated, and *gc()*, which reports memory usage whenever it is called.

A.5.1 Memory

Snapshots at each step of the algorithm taken using `gc()` shows that memory usage increases every time the predictors for B are calculated, and memory usage drops when predictors for A are calculated, as they overwrite those for B. The change in memory usage corresponds quite well with the calculated 70 MB difference in the sizes of A and B.

Storing the values of A and B at each iteration takes up a negligible amount of memory, as the matrices are only approximately 1.5 and 2.6 KB respectively. For the full dataset, they would be 24 KB and 240 KB, but still trivial, especially compared to the size of the predictor matrices.

To address the concern that memory usage may fluctuate between the intentionally sampled timepoints, more detailed sampling was conducted using `Rprof()` and `Rprofmem()`. Results from `Rprofmem()` show that three successive memory allocation events of the same size are made when the predictor matrices are calculated, hinting that they may be duplicated during parameter fitting. And indeed, `Rprof()` shows that the maximum amount of memory used at any time is three times the size of the largest matrix (the predictor matrix for B). While this factor of three duplication still allows us to fit to the entire dataset using $k \leq 3$, additional optimization of memory usage through implementing stochastic gradient descent will be required.

A.5.2 Runtime

The amount of wall time used to solve for the entire matrix is roughly equivalent to performing 6 or 7 iterations of alternating minimization. At this point, the log likelihood is within a threshold of 0.001 times the magnitude of the log likelihood from the last iteration. This is a reasonable stopping point, and so for this trimmed dataset at a rank set to 3, there is very little time trade-off for the increased efficiency of memory usage. The trade-off, however, comes in the modeling.

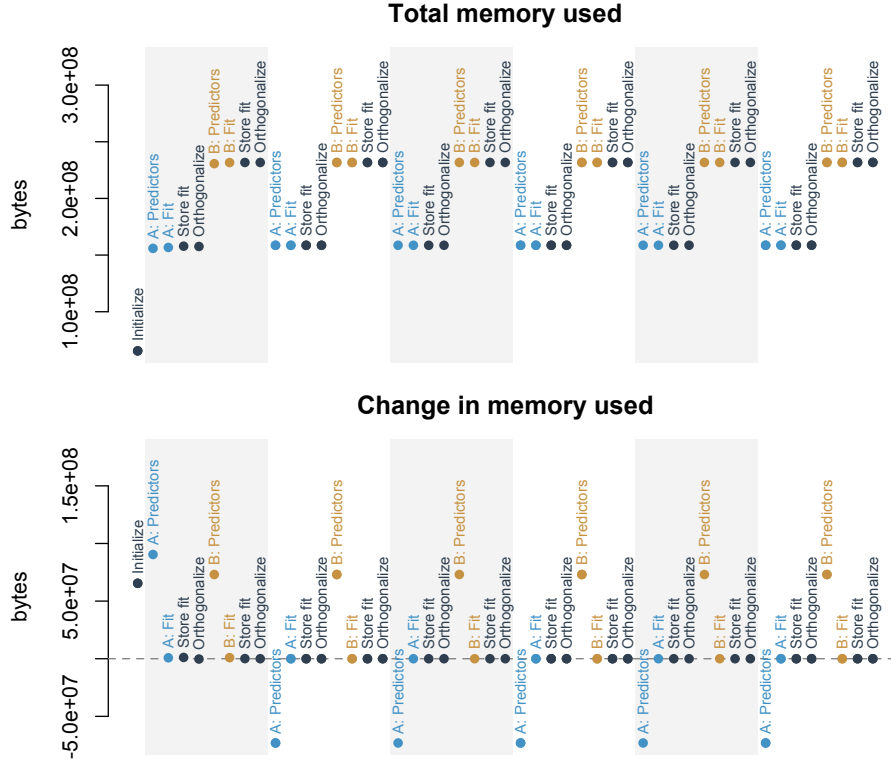


Figure A-4: Blue points highlight operations performed in order to solve for A, the matrix of phage protein coefficients, and tan points highlight operations performed in order to solve for B, the matrix of host protein coefficients. Alternating grey and white backgrounds demarcate successive iterations. Snapshots at each step of the algorithm shows that memory usage increases every time the predictors for B are calculated, and memory usage drops when predictors for A are calculated, as they overwrite those for B.

A.5.3 Correspondence with the original model

It is comforting to see in figure A-6 that the correlation between parameters from fitting M directly and parameters from computing AB' after alternating minimization climbs with each iteration of the algorithm. However, the correlation only reaches 0.38 (when excluding the intercept term), and the log likelihood only reaches -2100 (whereas the log likelihood solving for M directly is -1460). This isn't too surprising, given that for this analysis, the rank has been set to 3.

Inspection of the eigenvalues from singular value decomposition in the third panel

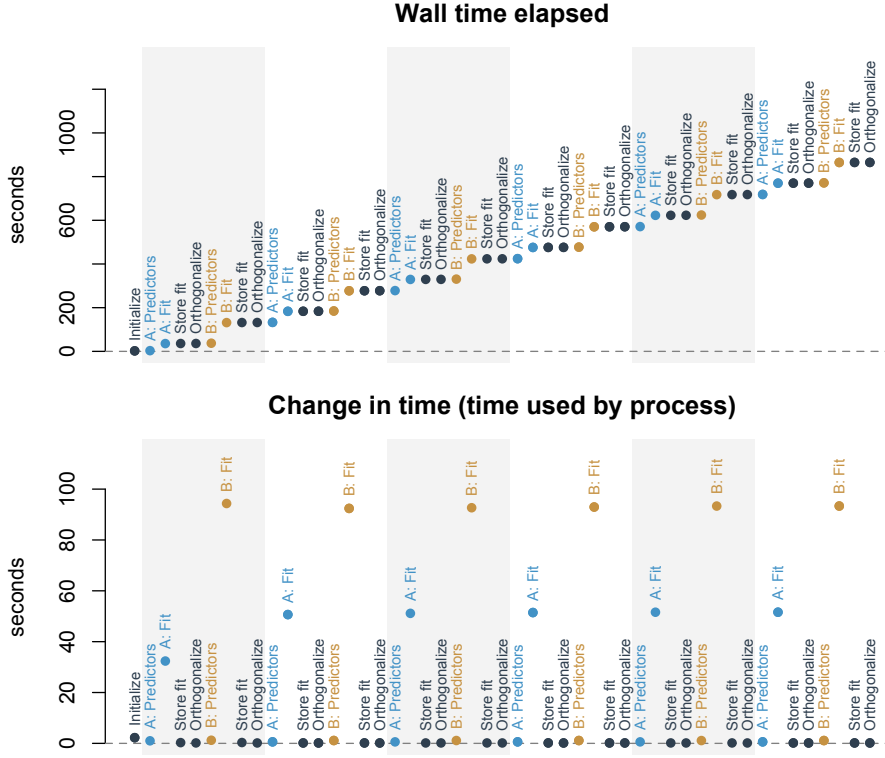


Figure A-5: Because parameter optimization involves searching in a high-dimensional space, the steps of solving for A and B are inevitably the rate-limiting steps of the method. Directly fitting the matrix M takes 1352 seconds (22 minutes) on the same machine.

of figure A-6 can give us a hint as to what a more realistic value of k should be. However, it is still difficult to interpolate to the full dataset, as the procedure for picking predictors to form the smaller dataset selects variables with high explanatory power. In general, even in the problem of matrix completion, it is not well understood how k should be set. This is a question for future exploration.

A.6 Additional directions for exploration

This implementation of alternating minimization is only the first step in the analysis of the Nahant Collection. Matrices in R have been traditionally constrained to having less than 2^{31} entries, and for $k > 3$, unfortunately, $58,000 \times 10,000 * k$ surpasses 2^{31} .

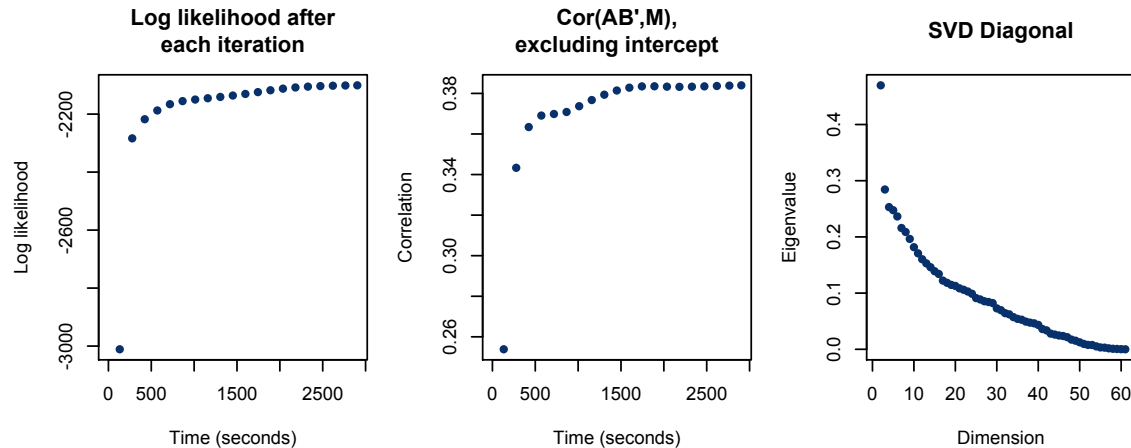


Figure A-6: In the first two plots here, the log likelihood and correlation with M (excluding the intercept term, the intercept term is so low in magnitude and so consistent with fitting that including it bumps up the correlation to around 0.97) are plotted for each iteration. Initial values are left off from these plots, since, because the parameters are randomly initialized, the log likelihood starts at $-\infty$ and the correlation starts close to 0. The eigenvalues from singular value decomposition of the coefficient matrix M when solving for M directly is shown in the third plot. The first dimension is left off, since it is a value large in magnitude, corresponding to the intercept.

While the most recent release of R allows larger matrices, many packages, including *glmnet*, do not yet support this new data structure. So in order to work with k larger than 3, we will need to reimplement elastic net regression.

Additionally, because living organisms can intuitively be placed on a tree, there naturally exists correlation among the bacteria and among the phage. This means that the data is not independently and identically distributed. Our next step is to account for this in order to, as much as possible, avoid identifying spurious associations.

Furthermore, because $p \gg n$ the interpretability of parameter estimates is often given up as a hopeless task. Many traditional statisticians will steer away from these types of problems, and in the “machine learning” community, the focus is instead on predictive accuracy. A philosophical question also exists in whether it may, in fact, be ill-advised to seek interpretation or draw any type of inferences whatsoever from this type of data. To address this concern, we turn to Tukey, “Danger only

comes from mathematical optimizing when the results are taken too seriously... It is understood that such optimum problems are unrealistically oversimplified, that they offer *guidance*, not the *answer*" We cannot claim that our analysis will be able to root the precise cause of each infection event. Rather, we would simply like to generate testable hypotheses concerning infection mechanisms.

Key to interpretation of parameter estimates is quantifying their uncertainty, and alternating minimization adds another layer of complication in that the original parameters of interest are now vector products of parameters we have solved for. However, taking a bayesian approach may help with this problem, as deriving the probability distribution of sums and products of other quantities with known distributions is straightforward.

Appendix B

Reasoning Through Games of Chance - Statistics for Play

Joy Y. Yang¹, Joseph Elsherbini²

¹Computational and Systems Biology Program, Massachusetts Institute of Technology, Cambridge, Massachusetts 02139, USA

³Microbiology Graduate Program, Massachusetts Institute of Technology, Cambridge, Massachusetts 02139, USA

J.Y. and J.E. designed the curriculum, taught the class, and wrote this paper.

This paper was originally accepted as a contributed paper to ICOTS10; however, due to scheduling conflicts, neither author was able to attend and present the paper.

B.1 Abstract

We present a case study of a best attempt at creating a fun and approachable after school statistics curriculum for grades 7-12. Our goal was to use interactive games to provide intuition into a broad range of problems that can be tackled with statistical thinking, as opposed to teaching a comprehensive statistics immersion program. For example, we reviewed distributions by carrying out Fisher’s hypergeometric taste testing experiment; introduced game theory by holding an iterated prisoners’ dilemma tournament; and “because danger only comes from mathematical optimizing when the results are taken too seriously” (Tukey [109]), ended with correlation/causation critical thinking puzzles. Additionally, we will discuss lessons learned from attempting to synthesize many activity based learning and context-driven statistical education tools that have arisen from conferences such as ICOTS.

B.2 Introduction

We’ve designed a six-session summer weekend curriculum consisting of games, in the spirit of Box’s paper helicopter experiments, [110] that seeks to elicit the context of need under which various statistical analyses were developed/are employed. In this paper, we will first introduce the setting under which we’ve taught this class, then comment on our experience of designing and running the class, and finally discuss the arguments for teaching in this manner by summarizing the viewpoints of seasoned statisticians who have thought deeply about activity-based and context-driven statistical education.

Our materials for this class are available at <http://mit.edu/reasoningchance/>

B.3 MIT HSSP

MIT Summer HSSP (this acronym has no expanded meaning) is a 6-week 7-12th grade program that runs on Sunday afternoons. Students can register for multiple classes, and MIT-affiliates (undergraduates, graduate students, or alumni) can apply to teach a class of any topic. The MIT Educational Studies Program (ESP) handles the logistics of doing outreach at local schools, recruiting teachers, selecting classes, and reserving classrooms. During 2017, around 1500 students enrolled, and 44 different classes were offered over a wide range of topics: swing dancing, complex analysis, adulting 101; etc. MIT ESP encourages students to leave the classroom if they find that they are not enjoying the material.

Under this program, we piloted a probability/statistics teaser series called “Reasoning through games of chance.” The afterschool program format meant that our lesson plans could not be a regimented, comprehensive overview of statistics. Instead, we indulged in prioritizing fun and intuition, with the aim of encouraging students to think about where, in their lives, chance and data play a role, and how they can use probability and statistics to explore their environment.

B.4 Class Setup

While we did not require programming as a prerequisite and did not plan to teach students how to code, we wanted students to realize that statistics is deeply intertwined with computing, as eloquently expressed by [111]. To this end, we requested the use of laptops and were given access to 12 chromebooks. The class size was then limited to 24 students so that each group of 2 students could work with one chromebook. Each chromebook was associated with a google classroom account to facilitate distribution of activities and interaction among groups.

We also prepared short code snippets on Rfiddle (<http://www.r-fiddle.org/>) to

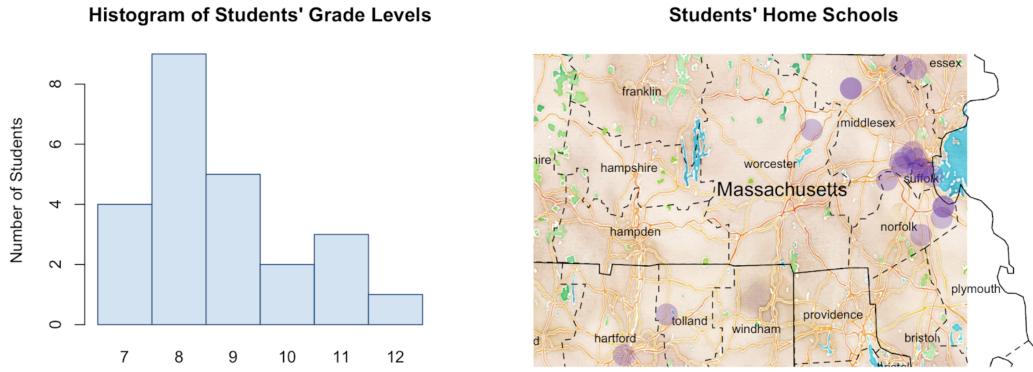


Figure B-1: This map omits two students, one from Maine, another from Illinois.

demonstrate basic functions and simulations. Because saving fiddles creates urls with different version numbers, we could update the fiddles live and ask students to follow along by navigating to newer versions. Students were also encouraged to continue playing with the code on their own time.

The students were from a wide range of different schools and grades. This sounds challenging; however, we believe it worked to our advantage. Each class was almost entirely activity based. So while in theory, our goal was to teach using guiding questions, in reality, the students taught each other. In general, we tried to encourage as much discussion as possible and aimed to maintain an atmosphere of organized chaos. And while the precise class structure varied from week to week, the scaffolding we used for planning was somewhat consistent: we started with an ice-breaker, followed with drill exercises, and ended with an experiment, or “game.”

To provide an example, we will use class 2: distributions and hypothesis testing. The learning goal was to expose students to the concept of a “null model,” and encourage them to consider what a null outcome should look like.

The icebreaker (~10-20 min) was often only tangentially related to the main topic. Because there are many ways of approaching the same problem, and problems can often be reduced to each other, these tangents allowed us to point out subtle connections among topics. Our icebreaker in class 2 was a classification problem. Pairs

of students were given 12 labeled images that fell into two categories, for example, chessboards from either early in the game or late in a game. Students were then asked to come up with rules that categorized their images. For instance, a rule might be “the image is from (early/late) in the game if the number of pawns on the board is (less than/equal-to/greater than) c.” After the students designed a set of rules, we then gave them 4 additional images to test how well their rules did.

For the drill exercises (~20-40 min), we typically asked students to number off into groups of four, then work out the answers together on board space marked for each group. Because the icebreakers were usually very open ended, and the games focused on having fun, these more structured exercises were intended to hone in on the relevant concepts of the week. Using boards helped promote interaction within the groups and allowed us, as the teachers, to easily identify and brainstorm with groups that looked stuck. The drill exercises in class 2 aimed to reinforce concept of distributions. There were two parts: In part one, students answered various questions about heights of Lilliputians by reading a histogram, and were then asked how likely it was Gulliver was a Lilliputian. In part two, students were given sequences of coin-flips and guided through deducing the geometric distribution by calculating probabilities for runs of heads and tails. They then used this information to determine which sequences were from real coin flips and which were faked by the instructors. Half of the groups worked on part one and the other half on part two. After everyone had finished, the groups swapped boards to discussed/corrected another group’s work.

Finally, the goals for the games (~30-40 min) were to demonstrate that statistical thinking is fun and to provide an example of how students can apply probability and statistics in their own lives. In class 2, the game was a taste testing experiment. We had three different tests: skittles vs. m&ms, coke vs. pepsi, and different colors of vegetable chips. Students worked in groups of three to administer the tests and record the results in a linked spreadsheet. We then briefly talked about the hypergeometric



Figure B-2: When asked to summarize the sheep in their herd, one group responded with pictorial summaries.

distribution as a null and showed the students the distribution of their cell counts compared to the null. Students were then asked to explain what the visualizations meant and whether we had evidence that people could discriminate between the different foods.

B.5 Reflection and Outlook

Statistical thinking is a necessary companion of the scientific process; or if we dare to go as far as Stigler, statistics is “a unified logic of empirical science.” A corollary to this, as stated poignantly by Rebecca Nugent in her JSM 2017 talk [112], is that “statistics does not belong to statisticians, statistical questions are present in every field, from physics, to chemistry, to history.” So in an attempt to attract as diverse a group of students as possible, we required no pre-requisites, marked the difficulty for our class to be 1 (on the scale of 1-4, 1 being the lowest), and welcomed students from the entire range of 7-12 grade. Still, there’s quite a bit of selection bias present in a group of students who come to MIT on weekends in the summer. When asked what their favorite subject were, most of our students said math, and only one student said English. Our students were incredibly supportive. They were eager to have fun and quick to come up with entirely unexpected responses. We designed the activities to focus on intuition, and did not attempt to be mathematically rigorous. We did

attempt to teach the Bayes class using probability notation, and our students became uncharacteristically frustrated. We had not built up the intuition before introducing the symbols, and so the symbols carried no meaning. To the final question of a worksheet (“what are some ways that you can increase the accuracy of the test?”), one student responded, “math, solve your own problems.” We found this humorous but also alarming. This student had come in with math as her favorite subject, and we had a responsibility for encouraging her mathematical curiosity, or at the very least, for not discouraging her. So after class we sent out new explanation based on intuition. We also reworked the lesson plan to no longer use probability notation. This new lesson plan was tested on November 18-19, and seemed to be received with greater success. However, the class sizes were also smaller, so there may have been some amount of confounding.

Focusing on intuition has a twofold advantage: as [113] pointed out, in democratizing statistics we should “avoid the ‘professional’s fallacy’ of imagining that our first courses are a step in the training of statisticians.” For students who do not choose to continue on with statistics, it is the big picture ideas, and not the fine-grained details that will leave a lasting impression. And for students who do decide to pursue statistics, again quoting [114], “most of our students would better master theory after some acquaintance with practice.”

Gudmund Iversen explains from his experience: “Those students who have had my Statistical Thinking course early (freshmen, sophomores) are having a ball with mathematical statistics as juniors or seniors. Others struggle more because they get bogged down by probability theory and mathematical niceties like moment generating functions, and they have a harder time seeing what statistics is all about. This points to a need to hear statistics twice before it makes sense, and we cannot lose the connection to real data.” [115] Our hope was that by placing emphasis on simply having fun, we could plant a seed to mark a spot that students may conceivably want

to revisit, sooner rather than later.

One advantage we had during HSSP is that we had a returning group of students over the course of six weeks, so we were able to refer back to examples from previous classes. However, we realize that running examples can create barriers to entry, and many after-school programs may not have the luxury of continuity. So in order to increase the accessibility and versatility of this set of lesson plans, we've also adapted three of the classes from this series for SPLASH, another MIT ESP program with a one-weekend-only format, held, this year, November 18-19.

While we do not have enough space here to discuss SPLASH in detail, interestingly, we had a very different audience. Only about 10% of our students said Math was their favorite subject, and one student made a seemingly outlandish comment about hating the coordinate system when he first learned about it. When asked to elaborate, he said, “In school they have you draw this Cartesian grid, and then plot things like lines on it, but it seemed pretty pointless. Then, I realized that you can actually graph food or baseball statistics, and I became a lot more interested. I’m not really bad at math, but most of the times it just seems really pointless and boring to me, because they don’t tell you what you can use it for.” Behind each statistical method, there are many fascinating stories about how it is used. Playfully invoking these contexts makes statistics relatable [116–118], and we are excited about the prospect of using this thought process to design additional afterschool lesson plans that are accessible at the jr. high/high school level.

B.6 Acknowledgements

We’d like to thank to Max Shen and Hayley Gadol for co-teaching. We also owe so many thanks to Luke Miratrix for activity ideas and feedback on the agendas for most of our lesson plans as well as this paper. Our curriculum benefitted greatly

from activities developed previously by others. [119–121] An interest in context-based education came from many dinner-table conversations among friends (Leanne Fan, Charlie Shi, Matt Nickell, and Kelly Vitzhum) that evolved into writing an education grant. While we did not receive the grant, this concept has become a mild obsession for each of us in our respective fields. And finally, we'd like Libusha Kelly for her thoughtful comments on this paper.

References

1. Brillinger DR (2002) John W. Tukey: his life and professional contributions. *The Annals of Statistics* 30:1535–1575. doi: [10.1214/aos/1043351246](https://doi.org/10.1214/aos/1043351246)
2. Bergh O, Børshem KY, Bratbak G, Heldal M (1989) High abundance of viruses found in aquatic environments. *Nature* 340:467–8. doi: [10.1038/340467a0](https://doi.org/10.1038/340467a0)
3. (2015) The North Sea Abloom : Image of the Day.
4. Wilson WH, Tarran GA, Schroeder D, et al. (2002) Isolation of viruses responsible for the demise of an *Emiliania huxleyi* bloom in the English Channel.
5. Schroeder DC, Oke J, Hall M, et al. (2003) Virus succession observed during an *Emiliania huxleyi* bloom. *Applied and environmental microbiology* 69:2484–90.
6. Hyman P, Abedon ST (2010) Chapter 7 – Bacteriophage Host Range and Bacterial Resistance. In: *Advances in applied microbiology*. pp 217–248
7. Fuhrman JA (1999) Marine viruses and their biogeochemical and ecological effects. *Nature* 399:541–8. doi: [10.1038/21119](https://doi.org/10.1038/21119)
8. Wilhelm S, Brigden S, Suttle C (2002) A Dilution Technique For The Direct Measurement Of Viral Production: A Comparison In Stratified And Tidally Mixed Coastal Waters. *Microbial Ecology* 43:168–173. doi: [10.1007/s00248-001-1021-9](https://doi.org/10.1007/s00248-001-1021-9)
9. Hendrix RW (2003) Bacteriophage genomics. *Current Opinion in Microbiology* 6:506–511. doi: [10.1016/J.MIB.2003.09.004](https://doi.org/10.1016/J.MIB.2003.09.004)
10. Hendrix RW, Smith MC, Burns RN, et al. (1999) Evolutionary relationships among diverse bacteriophages and prophages: all the world's a phage. *Proceedings of the National Academy of Sciences of the United States of America* 96:2192–7.
11. González V, Lozano L, Bustos P, Santamaría RI (2015) Genomic Tools for the Study of Azospirillum and Other Plant Growth-Promoting Rhizobacteria. In: *Handbook for azospirillum*. Springer International Publishing, Cham, pp 83–97
12. Griffiths AJF (2000) An introduction to genetic analysis. 860.
13. Salmond GPC, Fineran PC (2015) A century of the phage: past, present and

- future. *Nature Reviews Microbiology* 13:777–786. doi: [10.1038/nrmicro3564](https://doi.org/10.1038/nrmicro3564)
14. Maloy S Insights from Phage.
 15. Luria SE, Delbrück M (1943) Mutations of Bacteria from Virus Sensitivity to Virus Resistance. *Genetics* 28:
 16. Hershey AD, Chase M (1952) Independent functions of viral protein and nucleic acid in growth of bacteriophage. *The Journal of general physiology* 36:39–56.
 17. Benzer S Fine Structure of a Genetic Region in Bacteriophage. 41:344–354. doi: [10.2307/89013](https://doi.org/10.2307/89013)
 18. Benzer S On the Topology of the Genetic Fine Structure. 45:1607–1620. doi: [10.2307/90127](https://doi.org/10.2307/90127)
 19. Crick FHC, Barnett L, Brenner S, Watts-Tobin RJ (1961) General Nature of the Genetic Code for Proteins. *Nature* 192:1227–1232. doi: [10.1038/1921227a0](https://doi.org/10.1038/1921227a0)
 20. Summers WC How Bacteriophage Came to Be Used by the Phage Group. 26:255–267. doi: [10.2307/4331263](https://doi.org/10.2307/4331263)
 21. Ellis EL, Delbrück M (1939) The Growth of Bacteriophage. *The Journal of general physiology* 22:365–84.
 22. Boland PJ (1984) A Biographical Glimpse of William Sealy Gosset. *The American Statistician* 38:179–183. doi: [10.1080/00031305.1984.10483195](https://doi.org/10.1080/00031305.1984.10483195)
 23. Clarke RD (1946) An application of the Poisson distribution. *Journal of the Institute of Actuaries* 72:481–481. doi: [10.1017/S0020268100035435](https://doi.org/10.1017/S0020268100035435)
 24. DNA Sequencing Costs: Data - National Human Genome Research Institute (NHGRI).
 25. Pesant S, Not F, Picheral M, et al. (2015) Open science resources for the discovery and analysis of Tara Oceans data. *Scientific Data* 2:150023. doi: [10.1038/sdata.2015.23](https://doi.org/10.1038/sdata.2015.23)
 26. Brum JR, Ignacio-Espinoza JC, Roux S, et al. (2015) Patterns and ecological drivers of ocean viral communities. *Science (New York, NY)* 348:1261498. doi: [10.1126/science.1261498](https://doi.org/10.1126/science.1261498)
 27. Pope WH, Bowman CA, Russell DA, et al. (2015) Whole genome comparison of a large collection of mycobacteriophages reveals a continuum of phage genetic diversity. *eLife*. doi: [10.7554/eLife.06416](https://doi.org/10.7554/eLife.06416)
 28. Kauffman AKM (2014) Demographics of lytic viral infection of coastal ocean vibrio.
 29. Kauffman KM, Hussain FA, Yang J, et al. (2018) A major lineage of non-tailed dsDNA viruses as unrecognized killers of marine bacteria. *Nature* 554:118–122. doi:

[10.1038/nature25474](https://doi.org/10.1038/nature25474)

30. Kauffman KM, Brown JM, Sharma RS, et al. (2018) Viruses of the Nahant Collection, characterization of 251 marine Vibrionaceae viruses. *Scientific Data* 5:180114. doi: [10.1038/sdata.2018.114](https://doi.org/10.1038/sdata.2018.114)
31. Hunt DE, David LA, Gevers D, et al. (2008) Resource partitioning and sympatric differentiation among closely related bacterioplankton. *Science (New York, NY)* 320:1081–5. doi: [10.1126/science.1157890](https://doi.org/10.1126/science.1157890)
32. Preheim SP, Boucher Y, Wildschutte H, et al. (2011) Metapopulation structure of Vibrionaceae among coastal marine invertebrates. *Environmental Microbiology* 13:265–275. doi: [10.1111/j.1462-2920.2010.02328.x](https://doi.org/10.1111/j.1462-2920.2010.02328.x)
33. Stone GN, Nee S, Felsenstein J (2011) Controlling for non-independence in comparative analysis of patterns across populations within species. *Philosophical transactions of the Royal Society of London Series B, Biological sciences* 366:1410–24. doi: [10.1098/rstb.2010.0311](https://doi.org/10.1098/rstb.2010.0311)
34. Felsenstein J (2008) Comparative methods with sampling error and within-species variation: contrasts revisited and revised. *The American naturalist* 171:713–25. doi: [10.1086/587525](https://doi.org/10.1086/587525)
35. Cheverud J (1985) The quantitative assessment of phylogenetic constraints in comparative analyses: sexual dimorphism in body weight among primates.
36. Price AL, Patterson NJ, Plenge RM, et al. (2006) Principal components analysis corrects for stratification in genome-wide association studies. *Nature Genetics* 38:904–909. doi: [10.1038/ng1847](https://doi.org/10.1038/ng1847)
37. Pagel M (1997) Inferring evolutionary processes from phylogenies. *Zoologica Scripta* 26:331–348. doi: [10.1111/j.1463-6409.1997.tb00423.x](https://doi.org/10.1111/j.1463-6409.1997.tb00423.x)
38. Hadfield J MCMCglmm Course Notes.
39. Hadfield JD, Nakagawa S (2010) General quantitative genetic methods for comparative biology: phylogenies, taxonomies and multi-trait models for continuous and categorical characters. *Journal of evolutionary biology* 23:494–508. doi: [10.1111/j.1420-9101.2009.01915.x](https://doi.org/10.1111/j.1420-9101.2009.01915.x)
40. Hadfield JD (2010) MCMC Methods for Multi-Response Generalized Linear Mixed Models: The MCMCglmm R Package.
41. Brillinger DR Data Analysis, Exploratory. International encyclopedia of political science. doi: [10.4135/9781412959636.n128](https://doi.org/10.4135/9781412959636.n128)
42. Tukey JW(W (1977) Exploratory data analysis. 688.
43. Cowe E, Sharp PM (1991) Molecular evolution of bacteriophages: Discrete patterns of codon usage in T4 genes are related to the time of gene expression. *Journal of*

Molecular Evolution 33:13–22. doi: [10.1007/BF02100191](https://doi.org/10.1007/BF02100191)

44. La Scola B, Audic S, Robert C, et al. (2003) A giant virus in amoebae. *science-sciencemag.org* 299:2033.
45. Raoult D, Audic S, Robert C, et al. (2004) The 1.2-megabase genome sequence of Mimivirus. *Science (New York, NY)* 306:1344–50. doi: [10.1126/science.1101485](https://doi.org/10.1126/science.1101485)
46. Abergel C, Legendre M, Claverie J-M (2015) The rapidly expanding universe of giant viruses: Mimivirus, Pandoravirus, Pithovirus and Mollivirus. *FEMS Microbiology Reviews* 39:779–796. doi: [10.1093/femsre/fuv037](https://doi.org/10.1093/femsre/fuv037)
47. Schulz F, Yutin N, Ivanova NN, et al. (2017) Giant viruses with an expanded complement of translation system components. *Science (New York, NY)* 356:82–85. doi: [10.1126/science.aal4657](https://doi.org/10.1126/science.aal4657)
48. Hatfull GF (2008) Bacteriophage genomics. *Current opinion in microbiology* 11:447–53. doi: [10.1016/j.mib.2008.09.004](https://doi.org/10.1016/j.mib.2008.09.004)
49. Daniel V, Sarid S, Littauer U (1968) Amino acid acceptor activity of bacteriophage T4 transfer RNA. *FEBS Letters* 2:39–41. doi: [10.1016/0014-5793\(68\)80095-X](https://doi.org/10.1016/0014-5793(68)80095-X)
50. Weiss SB, Hsu WT, Foft JW, Scherberg NH (1968) Transfer RNA coded by the T4 bacteriophage genome. *Proceedings of the National Academy of Sciences of the United States of America* 61:114–21.
51. Scherberg NH, Weiss SB (1972) T4 transfer RNAs: codon recognition and translational properties. *Proceedings of the National Academy of Sciences of the United States of America* 69:1114–8. doi: [10.1073/PNAS.69.5.1114](https://doi.org/10.1073/PNAS.69.5.1114)
52. Wilson JH (1973) Function of the bacteriophage T4 transfer RNA's. *Journal of Molecular Biology* 74:753–757. doi: [10.1016/0022-2836\(73\)90065-X](https://doi.org/10.1016/0022-2836(73)90065-X)
53. Matsuzaki S, Tanaka S, Koga T, Kawata T (1992) A Broad-Host-Range Vibriophage, KVP40, Isolated from Sea Water. *Microbiology and Immunology* 36:93–97. doi: [10.1111/j.1348-0421.1992.tb01645.x](https://doi.org/10.1111/j.1348-0421.1992.tb01645.x)
54. Miller ES, Heidelberg JF, Eisen JA, et al. (2003) Complete genome sequence of the broad-host-range vibriophage KVP40: comparative genomics of a T4-related bacteriophage. *Journal of bacteriology* 185:5220–33.
55. Ikemura T (1981) Correlation between the abundance of Escherichia coli transfer RNAs and the occurrence of the respective codons in its protein genes: A proposal for a synonymous codon choice that is optimal for the E. coli translational system. *Journal of Molecular Biology* 151:389–409. doi: [10.1016/0022-2836\(81\)90003-6](https://doi.org/10.1016/0022-2836(81)90003-6)
56. Sharp PM, Emery LR, Zeng K (2010) Forces that influence the evolution of codon bias. *Philosophical transactions of the Royal Society of London Series B, Biological sciences* 365:1203–12. doi: [10.1098/rstb.2009.0305](https://doi.org/10.1098/rstb.2009.0305)
57. Grantham R, Gautier C, Gouy M, et al. (1980) Codon catalog usage and the

- genome hypothesis. *Nucleic acids research* 8:r49–r62.
58. Botzman M, Margalit H (2011) Variation in global codon usage bias among prokaryotic organisms is associated with their lifestyles. *Genome biology* 12:R109. doi: [10.1186/gb-2011-12-10-r109](https://doi.org/10.1186/gb-2011-12-10-r109)
 59. Bailly-Bechet M, Vergassola M, Rocha E (2007) Causes for the intriguing presence of tRNAs in phages. *Genome research* 17:1486–95. doi: [10.1101/gr.6649807](https://doi.org/10.1101/gr.6649807)
 60. Delesalle VA, Tanke NT, Vill AC, Krukonis GP (2016) Testing hypotheses for the presence of tRNA genes in mycobacteriophage genomes. *Bacteriophage* 6:e1219441. doi: [10.1080/21597081.2016.1219441](https://doi.org/10.1080/21597081.2016.1219441)
 61. Reis M dos, Savva R, Wernisch L (2004) Solving the riddle of codon usage preferences: a test for translational selection. *Nucleic acids research* 32:5036–44. doi: [10.1093/nar/gkh834](https://doi.org/10.1093/nar/gkh834)
 62. Watanabe K, Osawa S (1995) tRNA sequences and variation in the genetic code. In: Söll D, Rajbhandary U (eds) *tRNA: Structure, biosynthesis, and function*. ASM Press, Washington, DC, pp 225–250
 63. Yokoyama S, Nishimura S (1995) Modified nucleosides and codon recognition. In: Söll D, RajBhandary UL (eds) *tRNA: Structure, biosynthesis, and function*. ASM Press, Washington, DC, pp 207–223
 64. Reiter WD, Palm P, Yeats S (1989) Transfer RNA genes frequently serve as integration sites for prokaryotic genetic elements. *Nucleic acids research* 17:1907–14.
 65. Williams KP (2002) Integration sites for genetic elements in prokaryotic tRNA and tmRNA genes: sublocation preference of integrase subfamilies. *Nucleic acids research* 30:866–75.
 66. Johnson CM, Grossman AD (2015) Integrative and Conjugative Elements (ICEs): What They Do and How They Work. *Annual review of genetics* 49:577–601. doi: [10.1146/annurev-genet-112414-055018](https://doi.org/10.1146/annurev-genet-112414-055018)
 67. Marquet R, Isel C, Ehresmann C, Ehresmann B (1995) tRNAs as primer of reverse transcriptases. *Biochimie* 77:113–124. doi: [10.1016/0300-9084\(96\)88114-4](https://doi.org/10.1016/0300-9084(96)88114-4)
 68. Kleiman L (2002) tRNALys3: The Primer tRNA for Reverse Transcription in HIV-1. *IUBMB Life (International Union of Biochemistry and Molecular Biology: Life)* 53:107–114. doi: [10.1080/15216540211469](https://doi.org/10.1080/15216540211469)
 69. Hou Y-M (2010) CCA addition to tRNA: implications for tRNA quality control. *IUBMB life* 62:251–60. doi: [10.1002/iub.301](https://doi.org/10.1002/iub.301)
 70. Korostelev A, Trakhanov S, Laurberg M, Noller HF (2006) Crystal Structure of a 70S Ribosome-tRNA Complex Reveals Functional Interactions and Rearrangements.

Cell 126:1065–1077. doi: [10.1016/j.cell.2006.08.032](https://doi.org/10.1016/j.cell.2006.08.032)

71. Dupasquier M, Kim S, Halkidis K, et al. (2008) tRNA integrity is a prerequisite for rapid CCA addition: implication for quality control. *Journal of molecular biology* 379:579–88. doi: [10.1016/j.jmb.2008.04.005](https://doi.org/10.1016/j.jmb.2008.04.005)
72. Clark WC, Evans ME, Dominissini D, et al. (2016) tRNA base methylation identification and quantification via high-throughput sequencing. *RNA* 22:1771–1784. doi: [10.1261/rna.056531.116](https://doi.org/10.1261/rna.056531.116)
73. Harada F, Nishimura S (1974) Purification and characterization of AUA specific isoleucine transfer ribonucleic acid from Escherichia coli B. *Biochemistry* 13:300–307. doi: [10.1021/bi00699a011](https://doi.org/10.1021/bi00699a011)
74. Lowe TM, Eddy SR (1997) tRNAscan-SE: a program for improved detection of transfer RNA genes in genomic sequence. *Nucleic acids research* 25:955–64.
75. Laslett D, Canback B (2004) ARAGORN, a program to detect tRNA genes and tmRNA genes in nucleotide sequences. *Nucleic acids research* 32:11–6. doi: [10.1093/nar/gkh152](https://doi.org/10.1093/nar/gkh152)
76. Enav H, Béjà O, Mandel-Gutfreund Y (2012) Cyanophage tRNAs may have a role in cross-infectivity of oceanic Prochlorococcus and Synechococcus hosts. *The ISME journal* 6:619–28. doi: [10.1038/ismej.2011.146](https://doi.org/10.1038/ismej.2011.146)
77. Davis BD, Luger SM, Tai PC (1986) Role of ribosome degradation in the death of starved Escherichia coli cells. *Journal of bacteriology* 166:439–45.
78. Zhong J, Xiao C, Gu W, et al. (2015) Transfer RNAs Mediate the Rapid Adaptation of Escherichia coli to Oxidative Stress. *PLOS Genetics* 11:e1005302. doi: [10.1371/journal.pgen.1005302](https://doi.org/10.1371/journal.pgen.1005302)
79. Svenningsen SL, Kongstad M, Stenum TS, et al. (2017) Transfer RNA is highly unstable during early amino acid starvation in Escherichia coli. *Nucleic acids research* 45:793–804. doi: [10.1093/nar/gkw1169](https://doi.org/10.1093/nar/gkw1169)
80. Amitsur M, Levitz R, Kaufmann G (1987) Bacteriophage T4 anticodon nuclease, polynucleotide kinase and RNA ligase reprocess the host lysine tRNA. *The EMBO journal* 6:2499–503.
81. Kunisawa T (1992) Synonymous codon preferences in bacteriophage T4: a distinctive use of transfer RNAs from T4 and from its host Escherichia coli. *Journal of theoretical biology* 159:287–98.
82. Kunisawa T, Kanaya S, Kutter E (1998) Comparison of synonymous codon distribution patterns of bacteriophage and host genomes. *DNA research : an international journal for rapid publication of reports on genes and genomes* 5:319–26.
83. Lorenz C, Lünse CE, Mörl M (2017) tRNA Modifications: Impact on Structure

- and Thermal Adaptation. *Biomolecules*. doi: [10.3390/biom7020035](https://doi.org/10.3390/biom7020035)
84. Kirchner S, Ignatova Z (2015) Emerging roles of tRNA in adaptive translation, signalling dynamics and disease. *Nature Reviews Genetics* 16:98–112. doi: [10.1038/nrg3861](https://doi.org/10.1038/nrg3861)
 85. Ingolia NT, Ghaemmaghami S, Newman JRS, Weissman JS (2009) Genome-Wide Analysis in Vivo of Translation with Nucleotide Resolution Using Ribosome Profiling. *Science* 324:218–223. doi: [10.1126/science.1168978](https://doi.org/10.1126/science.1168978)
 86. Chen C-W, Tanaka M (2018) Genome-wide Translation Profiling by Ribosome-Bound tRNA Capture. *Cell Reports* 23:608–621. doi: [10.1016/j.celrep.2018.03.035](https://doi.org/10.1016/j.celrep.2018.03.035)
 87. R Core Team (2018) R: A language and environment for statistical computing. R Foundation for Statistical Computing, Vienna, Austria
 88. Will S, Reiche K, Hofacker IL, et al. (2007) Inferring Noncoding RNA Families and Classes by Means of Genome-Scale Structure-Based Clustering. *PLoS Computational Biology* 3:e65. doi: [10.1371/journal.pcbi.0030065](https://doi.org/10.1371/journal.pcbi.0030065)
 89. Edgar RC (2004) MUSCLE: multiple sequence alignment with high accuracy and high throughput. *Nucleic acids research* 32:1792–7. doi: [10.1093/nar/gkh340](https://doi.org/10.1093/nar/gkh340)
 90. Dunin-Horkawicz S, Czerwoniec A, Gajda MJ, et al. (2006) MODOMICS: a database of RNA modification pathways. *Nucleic Acids Research* 34:D145–D149. doi: [10.1093/nar/gkj084](https://doi.org/10.1093/nar/gkj084)
 91. Boccaletto P, Machnicka MA, Purta E, et al. (2018) MODOMICS: a database of RNA modification pathways. 2017 update. *Nucleic Acids Research* 46:D303–D307. doi: [10.1093/nar/gkx1030](https://doi.org/10.1093/nar/gkx1030)
 92. Schloss PD, Westcott SL, Ryabin T, et al. (2009) Introducing mothur: open-source, platform-independent, community-supported software for describing and comparing microbial communities. *Applied and environmental microbiology* 75:7537–41. doi: [10.1128/AEM.01541-09](https://doi.org/10.1128/AEM.01541-09)
 93. Murphy FV, Ramakrishnan V (2004) Structure of a purine-purine wobble base pair in the decoding center of the ribosome. *Nature Structural & Molecular Biology* 11:1251–1252. doi: [10.1038/nsmb866](https://doi.org/10.1038/nsmb866)
 94. Mallows C (1998) The Zeroth Problem. *The American Statistician* 52:1–9. doi: [10.1080/00031305.1998.10480528](https://doi.org/10.1080/00031305.1998.10480528)
 95. Kristensen DM, Waller AS, Yamada T, et al. (2013) Orthologous Gene Clusters and Taxon Signature Genes for Viruses of Prokaryotes. *Journal of Bacteriology* 195:941–950. doi: [10.1128/JB.01801-12](https://doi.org/10.1128/JB.01801-12)
 96. Lander ES, Botstein D (1989) Mapping mendelian factors underlying quantitative

- traits using RFLP linkage maps. *Genetics* 121:185–99.
97. Bostock M Brush and Zoom - bl.ocks.org.
 98. HARDIN G (1960) The competitive exclusion principle. *Science* (New York, NY) 131:1292–7. doi: [10.1126/SCIENCE.131.3409.1292](https://doi.org/10.1126/SCIENCE.131.3409.1292)
 99. Bostock M, Ogievetsky V, Heer J (2011) D³ Data-Driven Documents. *IEEE Transactions on Visualization and Computer Graphics* 17:2301–2309. doi: [10.1109/TVCG.2011.185](https://doi.org/10.1109/TVCG.2011.185)
 100. Moebus K, Nattkemper H (1981) Bacteriophage sensitivity patterns among bacteria isolated from marine waters. *Helgoländer Meeresuntersuchungen* 34:375–385. doi: [10.1007/BF02074130](https://doi.org/10.1007/BF02074130)
 101. Garalde DR, Snell EA, Jachimowicz D, et al. (2018) Highly parallel direct RNA sequencing on an array of nanopores. *Nature Methods* 15:201–206. doi: [10.1038/nmeth.4577](https://doi.org/10.1038/nmeth.4577)
 102. Evans ME, Clark WC, Zheng G, Pan T (2017) Determination of tRNA aminoacylation levels by high-throughput sequencing. *Nucleic acids research* 45:e133. doi: [10.1093/nar/gkx514](https://doi.org/10.1093/nar/gkx514)
 103. Mardia KV, Kent JT(T, Bibby JM(M (1979) Multivariate analysis. 521.
 104. Jain P, Netrapalli P, Sanghavi S (2012) Low-rank Matrix Completion using Alternating Minimization.
 105. Koren Y (2009) The BellKor Solution to the Netflix Grand Prize.
 106. Koren Y, Bell R, Volinsky C (2009) MATRIX FACTORIZATION TECHNIQUES FOR RECOMMENDER SYSTEMS. IEEE COmputer Society
 107. Hotelling H (1936) Relations Between Two Sets of Variates. *Biometrika* 28:321. doi: [10.2307/2333955](https://doi.org/10.2307/2333955)
 108. R Core Team (2016) R: A language and environment for statistical computing. R Foundation for Statistical Computing, Vienna, Austria
 109. Tukey JW (1962) The future of data analysis. *The annals of mathematical statistics* 33:1–67.
 110. Box GE (1992) Teaching engineers experimental design with a paper helicopter. *Quality Engineering*
 111. Nolan D, Temple Lang D (2010) Integrating computing and data technologies into the statistics curricula. *Proceedings of the eighth international conference on teaching statistics*
 112. Nugent R (2017) Lessons Learned in Transitioning from “Intro to Statistics” to

“Reasoning with Data.” Joint statistical meetings

113. Moore DS (1997) New pedagogy and new content: The case of statistics. International statistical review 65:123–137.
114. Moore DS (1992) Teaching statistics as a respectable subject. Statistics for the twenty-first century 14–25.
115. Cobb G (1992) Teaching statistics. Heeding the call for change: Suggestions for curricular action 22:3–43.
116. Davies N, Barnett V, Marriott J, Authority C (2010) One hundred years of progress—Teaching statistics 1910–2010: What have we learned? Part i: It’s not mathematics but real data in context. Data and context in statistics education: Towards an evidence-based society. proceedings of the eighth international conference on teaching statistics (icots8)
117. Dierdorp A, Bakker A, Van Maanen J, Eijkelhof H (2010) Educational versions of authentic practices as contexts to teach statistical modeling.
118. Franklin C, Kader G, Mewborn DS, et al. (2005) A curriculum framework for preK-12 statistics education. American Statistical Association Board of Directors for Endorsement
119. Garfield J (1993) Teaching statistics using small-group cooperative learning. Journal of Statistics Education
120. Gelman A, Nolan D (2017) Teaching statistics: A bag of tricks. Oxford University Press
121. Kaufman C (2010) Stat 131: Statistical Computing. UC Berkeley